Application of Nature Inspired Metaheuristic Computation for Automatic Generation Control of Multi Source Interconnected Power System

By

Amil Daraz

Reg. No. 108-FET/PHDEE/S16

A dissertation submitted to I.I.U. in partial fulfillment of the requirements for the degree of

DOCTOR OF PHILOSOPHY

Department of Electrical Engineering
Faculty of Engineering and Technology
INTERNATIONAL ISLAMIC UNIVERSITY
ISLAMABAD
2021

DEDICATED TO

My Teachers,

Parents,

Wife,

Brothers and Sister

ABSTRACT

A power system is typically built from the interconnection of various complex electrical networks comprising of electrical generation, transmission, and distribution systems. A balanced power system is comprised of two components; active and reactive power. The active power is responsible for Automatic Generation Control (AGC) or Load Frequency Control (LFC) while the reactive power is called Automatic Voltage Regulator (AVR). For reliable and quality power supply AGC plays an important role to sustain the exchange of power between the control areas via tie-lines and retain the frequency at a predetermined value.

A properly designed power system must be able to support the customer demands at all times, taking into account the load variation. In order to maintain the system frequency and tie-line power at their scheduled values, a proper design of the controller and its parameter tuning is a dire need of the AGC system. Therefore, in this research study, a PID controller and its modified structure known as the I-PD controller are successfully applied for two areas interconnected power system comprised of reheat thermal unit, hydropower generation, and gas power unit with the linear power system. A more recent powerful meta-heuristic algorithm known as Fitness Dependent Optimizer (FDO) is applied for the optimization of proposed controller parameters. The proposed technique is further applied to a more practical model of the power system by taking into account physical constraints such as Boiler dynamic (BD), Time Delay (TD), Generation Rate Constraint (GRC), and Governor Dead Band (GDB).

Further, Fractional Order PID controller and their modified form FOI-PD controller are designed and implemented for two areas interconnected deregulated power system. The two areas interconnected power system is comprised of reheat thermal, gas, hydro, and wind power unit incorporated with Redox Flow Battery (RFB) and Thyristor Controlled Series Compensator (TCSC) including non-linearities such as GRC, GDB, TD, and BD. The parameters of the proposed controller are optimized with an improved –Fitness Dependent Optimizer (I-FDO) algorithm. Finally, the robustness of the proposed controller is verified by changing the system parameters and load conditions within a range of $\pm$ 25%. The supremacy of FDO based FOPID and FOI-PD controllers proposed in this work clearly demonstrates the capability of these controllers to tackle the AGC problem effectively with oscillation-free and quick response.

LIST OF PUBLICATIONS

[1]. **A. Daraz**, S. A. Malik, H. Mokhlis, I. U. Haq, F. Zafar and N. N. Mansor, "Improved-Fitness Dependent Optimizer Based FOI-PD Controller for Automatic Generation Control of Multi-Source Interconnected Power System in Deregulated Environment," in IEEE Access, vol. 8, pp. 197757-17775, 2020, doi: 10.1109/ACCESS.2020.3033983. **(SCI-Expended)**

[2]. **A. Daraz**, S. A. Malik, H. Mokhlis, I. U. Haq, G. F. Laghari and N. N. Mansor, "Fitness Dependent Optimizer-Based Automatic Generation Control of Multi-Source Interconnected Power System With Non-Linearities," in IEEE Access, vol. 8, pp. 100989-101003, 2020, doi: 10.1109/ACCESS.2020.2998127**. (SCI-Expended)**

[3]. **Daraz A**, Malik SA, Haq IU, Khan KB, Laghari GF, Zafar F (2020) Modified PID controller for automatic generation control of multi-source interconnected power system using fitness dependent optimizer algorithm. PLoS ONE 15(11): e0242428. https://doi.org/10.1371/journal.pone.0242428. **(SCI-Expended)**

[4]. **A. Daraz**, S. A. Malik and A. ul Haq, "Review of Automatic Generation Control For Multi-Source Interconnected Power System Under Deregulated Environment," 2018 International Conference on Power Generation Systems and Renewable Energy Technologies (PGSRET), Islamabad, Pakistan, 2018, pp. 1-5, doi: 10.1109/PGSRET.2018.8685994.

[5]. **A. Daraz**, S. A. Malik, T. Saleem and S. Bhati (2017). Ziegler Nichols Based Integral Proportional Controller for Superheated Steam Temperature Control System. International Journal of Electrical, Computer, Energetic, Electronic and Communication Engineering. 11(5): 516-520.

ACKNOWLEDGEMENTS

In the name of Allah (Subhanahu Wa Ta'ala), who is the most gracious and the merciful. I would like to thank Allah for giving me the strength and patience to complete this research work. Peace and blessings of Allah be upon His last Prophet Muhammad (Sallulah-o-Alaihihe-Wassalam) and all his Sahaba (Razi-Allah-o-Anhu) who dedicated their lives for Dawah and spread of Knowledge.

I am truly grateful to my supervisor Dr. Suheel Abdullah Malik whose inspiration, ideas and efforts make it possible for me to complete my higher studies. He has been a role model for me and many others in teaching, research and other aspects of life. I would also like to thank my mentor Prof. Hazlie Mokhlis who always supported me to learn and spread knowledge. His supplications gave me a lot of strength.

I offer my sincere thanks to my colleagues Engr. Khan Bahader khan, Dr.Tahir Saleem, Engr. Athar Waseem, Engr. Ahmad saleem, Engr. Ghulam Farid, Mr. Farhan Zafar for their never-ending support and fruitful and healthy research discussions. I would like to acknowledge the support of the Prime Minister Fee Reimbursement Scheme (PMFRS), Pakistan for providing me a full fee waiver during the Ph.D. studies. I am also thankful to HEC to give me a scholarship for the International Research Initiative Program (IRSIP) for six months at the University of Malaya (UM) Malaysia.

I am grateful to my father, mother, brothers, and sister for their love and support throughout my life. I am also very thankful to my wife for her patience, encouragement, and prayers during every single stage of my Ph.D. degree.

(Amil Daraz)

Table of Contents

LIST OF FIGURES

LIST OF ABBREVIATIONS

AGC	Automatic Generation Control
LFC	Load Frequency Control
PID	Proportional Integral Derivative
I-PD	Integral- Proportional Derivative
ACE	Area Control Error
IPS	Interconnected Power System
FO	Fractional Order
FDO	Fitness Dependent Optimizer
I-FDO	Improved –Fitness Dependent Optimizer
TLBO	Teaching Learning based Optimization
PSO	Particle Swarm Optimization
FA	Firefly Algorithm
GRC	Generation Rate Constraint
GDB	Governor Deed Band
GDZ	Governor Deed Zone
BD	Boiler Dynamic
TD	Time Delay
DPM	Disco Participation Matrix
ITSE	Integral Time Square Error
ISE	Integral Square Error
ITAE	Integral Time Absolute Error
IAE	Integral Absolute Error
DISCOs	Distribution Companies

GENCOs	Generation Companies
VIU	Vertically Integrated Utility
ISO	Independent System Operator
PBT	Poolco Based Transaction
BBT	Bilateral Based Transaction
CVBT	Contract Violation Based Transaction
FACTS	Flexible Alternating Current Transmission System
RFB	Redox Flow Battery
TCSC	Thyristor Controlled Series Compensator
CES	Capacitive Energy Storage
DPS	Deregulated Power System
APF	Area Participation Factor
UPFC	Unified Power Flow Controller
TF	Transfer Function
FF	Fitness Function
CPF	Contract Participation Factor
SLP	Step Load Perturbation

LIST OF SYMBOLS

A list of commonly used symbols in this dissertation are given below.

ΔF_i Change in Frequency of i-th area

ΔP_{tie} Change in Tie-line Power

β Bias Constant

R_{th} Thermal Droop Constant

R_h Hydral Droop Constant

R_g Gas Droop Constant

R_w Wind Droop Constant

F_w Fitness Weight

α Weight Factor

γ Random Number

T_{12} Synchronization Coefficient

K_{ps} Gain constant of power system

T_{Ps} The time constant of the power system

T_g Governor constant

T_t Turbine constant

T_{rh} Reheat thermal constant

K_1, K_3 Boiler constant of Boiler Dynamic

Chapter 1. Introduction

This chapter presents a brief description of the Automatic Generation Control (AGC) of a two-area network system. A brief overview of the traditional and deregulated power system is also discussed. Finally, thesis contributions, statement of the problem, objectives, and organization of the thesis are provided.

1.1 Introduction

The power system is typically built from the interconnection of various complex electrical networks comprising of electrical generation, transmission, and distribution systems. Due to an increase in power demand, power systems operate as a wide Interconnected Power System (IPS) [1], [2], [3]. The benefit of IPS is to provide power supply from one area to other areas in case of deficiency in the power generation unit. All interconnected power system areas link via tie-lines. An appropriate power system must be able to support customer demands at all times, taking into account the load variation. A balanced power system comprises of two components; reactive and active power. The active power is responsible for AGC or Load Frequency Control (LFC) while the reactive power is called Automatic Voltage Regulator (AVR) [4], [5].

AGC is referred to as auxiliary service in a power network consisting of a primary and secondary control loop. The primary loop can control the small variation in frequency by the natural response of the governor while the secondary loop control uses a controller to regulate frequency at nominal values. The LFC in each network area monitors the tie-line power exchange and frequency of the system. The linear configuration of tie-line power and frequency is called Area Control Error (ACE) which computes error and is

allocated to the controller. For reliable and quality power supply AGC plays a vital role in balancing the output power of a generator considering the change in load pattern, regulating the frequency of IPS, and keeping the tie-line power, at the desired values [6], [7], [8].

Modern power systems are now turning from a conventional controlled environment to a dynamic deregulated environment to increase competition and supply efficient, cost-effective, and quality electricity. Without altering the fundamental basic power systems in these new restructured power systems, Ideas, the planning, and organizational infrastructure elements must be updated. In the conventional power sector, Transmission Companies (TRANSCOs), Distribution Companies (DISCOs) and Generation Companies (GENCOs) are controlled by a single body that delivered power at a regulated tariff, known as Vertically Integrated Utility (VIU). However, development in power industries has changed the structure of VIU into a deregulated scenario in which GENCOs, TRANCOs and DISCOs are owned by separate entities and they function independently in a competitive electricity market. Each company has the authority to contract others in the same or different control areas [9], [10], [11]. Regulations that govern all the electricity transactions and auxiliary services such as automatic generation control taken by the GENCOs and DISCOs are usually handled by a body known as Independent System Operator (ISO) [12], [13].

1.2 The control scheme in the AGC system

A variety of control functions are involved in the execution of AGC schemes. These control tasks are applied by the primary and supplementary AGC loops as depicted in Fig 1.1. The primary AGC loop is responsible for controlling the speed of the generator while supplementary AGC loops control the net interchange, real power of output, and frequency

[14], [15]. It contains a feedback mechanism that injects a signal into the speed governor. The supplementary control loop provides feedback through ACE, and incremental change adds feedback via an appropriate controller to the primary loop [16], [17], [18].

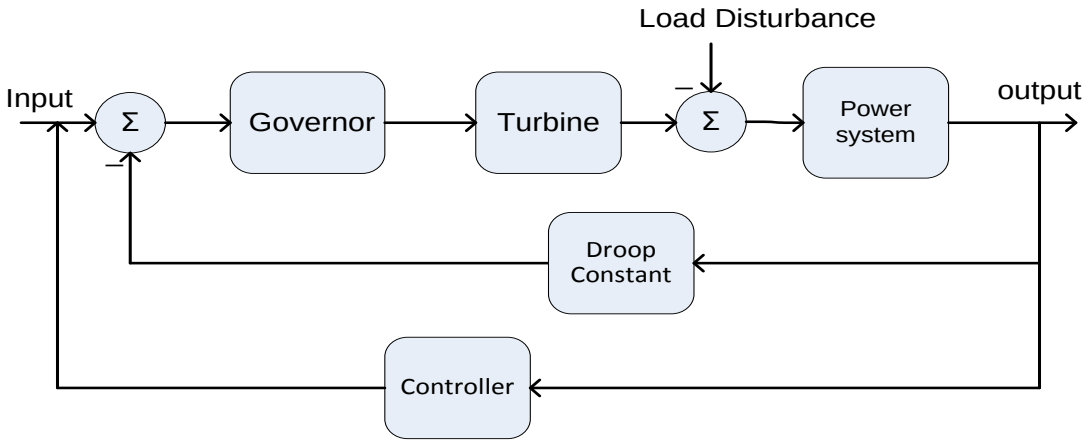

Figure 1.1 Control loops of the AGC system [17].

1.3 Statement of the Problem

In recent years a lot of studies have been conducted for AGC of power system networks and still, research is continued in this direction due to the importance of the problem and emerging modern power systems. Although various controllers have been used for controlling the frequency in AGC, however multi-area interconnected diverse generation unit power network system in a deregulated environment with various non-linearities such as Governor Dead Zone/Band (GDZ/GDB), Boiler Dynamics (BD), Generation Rate Constraint (GRC), and Time Delay (TD) has not been explored much. Therefore, in this research work, a modified model of the multi-area IPS with diverse power generation units including reheat thermal, hydropower, gas, and wind power unit with various non-linearities like GRC, BD, GDZ, and TD, incorporated in the power system has been deduced.

A glance at the literature reveals that numerous different classical and modern controllers have been employed for AGC of multi-area with diverse generation units. In this study, the PID controller and their modified structure known as the I-PD controller has been tested on the proposed modified model with various nonlinearities and diverse power generation units. Further, FOPID and FOI-PD controllers have been explored on the modified multi-area IPS with a diverse generation unit in a deregulated scenario.

In recent years, nature-inspired metaheuristic optimization algorithms have received tremendous attention from researchers and these techniques have been employed to deal with a variety of optimization problems in engineering. These techniques have also been used for the tuning of controller parameters. In this research study, some recently proposed nature-inspired metaheuristic algorithms like Fitness Dependent Optimizer (FDO) and Improved-Fitness Dependent Optimizer (I-FDO) algorithms have been explored. Besides, different performance indices such as Integral Square Error (ISE), Integral Absolute Error (IAE), Integral Time multiplied Square Error (ITSE) and Integral Time-weighted Error (ITAE) will be evaluated for a comprehensive comparative analysis of AGC of two areas IPS.

1.4 Motivation and Objectives of Research

Competition in power system networks around the world has been introduced based on the idea that it would increase manufacturing productivity and reduce electrical energy prices for all customers. Researchers across the globe are trying to propose a variety of techniques for the AGC system to preserve the frequency of the system and tie-line power at their prescribed values during regular service and even during minor disturbances. Various control approaches such as classical, modern control, and intelligent

techniques have been used and implemented from time to time in the design of AGC regulators. However, there is potential to investigate traditional and deregulated power systems to address such critical issues systematically. Based on the aforementioned discussion, the following are the main objectives of the research.

1. To develop a model for a multi-area IPS with diverse generation units including thermal, wind, hydro, and gas power unit.
2. To deduce a mathematical model of AGC incorporating various non-linearities like GRC, GDB, TD and BD.
3. Implementation and design of controllers such as I-PD controller, PID controller, fractional order PID controller, and fractional order I-PD controller.
4. Optimization of controller parameters using nature-inspired metaheuristic algorithms like FDO and I-FDO algorithms.
5. Comprehensive comparative analysis among various controllers using various performance indices like ITSE, ISE, ITAE, and IAE.

1.5 Organization of the Dissertation

The dissertation is presented in six chapters. The chapter-wise description of the study is presented in the below paragraphs.

Chapter 1: A brief introduction of the AGC problem in an interconnected power unit is presented. The AGC problem under the traditional and deregulated power system is discussed. Further, the motivation behind the presented work, problem statement and objectives are described.

Chapter 2: This chapter presents a detailed literature review of the AGC problem of various power networks. The literature survey has been conducted regarding a single area power system, multi-source generations with the linear and non-linear power system, deregulated power system, and impact of energy storage and FACTS devices on the AGC system.

Chapter 3: This chapter concerns with the designing and implementation of the I-PD and PID controller for the AGC problem of two areas IPS. The proposed controllers are tested on two areas with thermal reheat unit, gas unit, and collectively all the generation sources. Further, Fitness Dependent Optimizer (FDO) approach has been employed to tune the gains of the suggested controllers.

Chapter 4: It deals with the AGC problem of two area multi-source IPS considering various non-linearities including BD, TD, GRC, and GDZ. The efficacy of the proposed controller is first employed for two areas diverse generation units with two non-linearities i.e. GRC and GDZ and then the same power system is extended with multiple non-linearities.

Chapter 5: This chapter presents an Improved- Fitness Dependent Optimizer (I-FDO) algorithm for the optimization of a modified FOPID controller known as the FOI-PD algorithm for the AGC problem of two area multi-generation IPS. Two-area multi-generation system comprised of thermal reheat, gas, wind and hydro generation unit integrated with multiple non-linearities including GRC, GDZ, TD, and BD. Further, the performance of the system is enhanced by incorporating Redox Flow Battery (RBF) and Thyristor Controlled Series Compensator (TCSC) with a tie-line.

Chapter 6: This includes a review of the main contributions made from the analysis work discussed in the dissertation. The scope of future AGC work on multi-area interconnected traditional and deregulated power systems is also discussed.

Chapter 2. Literature Review

The power system is typically built from the interconnection of various complex electrical networks comprising of electrical generation, transmission, and distribution systems. Due to an increase in power demand, power systems operate as a wide Interconnected Power System (IPS). The elementary purpose of AGC is to deliver the desired amount of power within satisfactory quality to entire users. The system will be stable when there is an equilibrium between generated power and the consumer's load. Since, the consumer's load normally changes, the active power drawn from the generator increases which reduces the speed of a generator or turbine due to variation in frequency. In literature, different control approaches have been reported for the AGC model which is described in the below sections.

2.1 Single-Area Power System

A power system that is composed of only one area is called as single-area power systems. Initially, most of the work regarding the load frequency control problem has been performed in a single area network. For instance, the authors in [19], [20] considered a single area network of hydropower generation and reheat thermal power respectively. Ramakrishna and Bhatti in [21] proposed a Proportional Integral (PI) controller for AGC of a single area with diverse generation systems including hydro, thermal, and gas generation unit. The proposed controller is tuned by employing the Genetic Algorithm (GA). Integral Square Error (ISE) and Integral Time-weighted Absolute Error (ITAE) are used as performance criteria to achieve the optimal gains of the controllers. The authors also considered the performance of the AGC system with a single generation and multiple generation units and conclude that the transient response of the system changed with each

generation unit. The response of single-area load frequency models with a multi-unit generation like gas, hydro, and thermal units are given in reference [22], [23], [24].

2.2 Multi-Source with Linear Power System

The multi-source power unit consists of various generation like wind, thermal, reheat thermal, hydro, diesel, nuclear, etc. The modern power system comprises of numerous network areas that are connected to transmission lines via tie-lines. AGC plays a key role to sustain the exchange of power between the control regions via tie-lines and retain the frequency at a predetermined value. In this regard, different works have been described in the literature.

Authors in [25] have employed the PID controller for AGC of the different test models. The Quasi Oppositional based Grey Wolf Optimization (QOGWO) technique is used for the tuning of the proposed controller. Initially, two areas of the thermal and hydro unit are considered for the AGC problem. The authors extend the two areas model to four area models to explore the efficacy of the proposed approach. The results obtained from the QOGWO based PID controller show better performance compared to GWO and another intelligent method including fuzzy logic and Artificial Neural Networks (ANN).

Authors in [26] proposed a fuzzy-based Fractional Order (FO) PID controller optimized with Ant Lion Optimizer (ALO). The two areas with multi-source generation including wind, hydro, and thermal reheat units are considered in area-1 and diesel, hydro and thermal reheat units in area-2 are considered for the AGC system. The preeminence of the proposed approach is acknowledged by associating the results with PID, fuzzy-based PID, and FOPID controllers.

Mohanty et al. [27] have used the Differential Evolution (DE) method for the tuning of controller parameters considering two area LFC systems. Various controllers including Integral (I), PI, and PID are developed and implemented for the LFC of a single area and two areas with an HVDC/AC power unit. The response of the same power model was improved in [28] by employing a fuzzy-based PID (FPID) controller optimized with Local Unimodal Sampling (LUS) hybrid with Teaching Learning Based Optimization (TLBO) algorithm. The efficacy of the proposed approach is validated by comparing it with other methods including TLBO, DE, and LUS –DE. Authors in [29] have analyzed Two Degree of Freedom (2-DOF) FOPID controller by employing the Firefly Algorithm (FA) for AGC of two area multi-generation power networks. Besides, FA's convergence properties are compared with other well-known optimization approaches, such as Artificial Bee Colony (ABC), PSO and Bacteria Foraging Optimization (BFO) approach, to demonstrate their efficacy.

Verrasamy et al in [30] presented the LFC problem of two areas interconnected system integrated with renewable and conventional power sources. The stability analysis was evaluated using the Hankle models order reduction methodology in the non-linear hybrid power network. Besides, the cascaded PI-PD controller is applied to assess the performance of the AGC system. The parameters of the proposed controller are tuned with PSO-Grey Wolf Optimization (GWO) techniques. The performance of the PI-PD controller was compared to other conventional controllers and the efficacy of this method was deliberate for different cases of the hybrid power system model. Fathy et al. [13] considered the Adaptive Neuro-Fuzzy Inference System (ANFIS) for LFC integrated with

renewable energy resources. The proposed controller was trained with Ant lion Optimization (ALO) algorithm.

2.3 Multi-Source Power System with Non-Linearities

In literature, various nonlinearities such as GRC, GDB, TD, and BD have been incorporated by numerous researchers to make the power system more realistic. For instance, Puja Dash et al in [31] have used the PI-PD controller for AGC of four area networks with reheat single source and Generation Rate Constraint (GRC). The proposed controller has been tuned by employing a metaheuristic Flower Pollination Algorithm (FPA). Further, the proposed controller has been compared with other traditional controllers including PI, I and PID controllers, and conclude that the proposed approach performs superior as compared to other controllers.

Erdin Sahin in [32] developed a feedback controller with high differential order for LFC of multi-area power system considering GDB and GRC. The gains of the proposed controller are optimized with PSO using the performance criteria of an Integral Time-weighted Absolute Error (ITAE). Erdin compared the results yielded from the proposed techniques with some other approaches reported in the literature and determine that the proposed approach achieved better dynamic response and robustness.

Gonggui et al. [33] have used a fuzzy-based PID controller by employing an Improved – Ant Colony Optimization (I-ACO) algorithm. Initially, the authors considered the LFC problem of two areas with single-source generation. Further, they extended a two-area system with multi-source generation including thermal reheat and hydro unit incorporating with Governor Dead Zone (GDZ) linearity. Shiva et al. [34] discuss the AGC problem of interconnected system consideration with GRC. PID controller is used with

filtering effects for three areas optimized with Quasi Oppositional Harmony Search (QOHS) algorithm. The proposed algorithm shows superior transient response compared to the Imperialist Competitive Algorithm (ICA) is stated in the literature. Yogendra Arya in [35] has suggested Cascaded Fuzzy Fractional-Order Proportional-Integral (CFFOPI) with a FOPID controller for three areas with reheat single-source power generation of the AGC problem. The Imperialist Competitive Algorithm (ICA) is employed to tune the proposed controller by minimizing Integral Square Error (ISE) performance criteria. The GRC linearity is considered to examine the superiority of the proposed method.

Authors in [36] have analyzed AGC of three areas with multi-unit generation. They proposed a fuzzy-based PID controller tuned with a Modified- Sine Cosine Algorithm (M-SCA). Various non-linearities like GRC, GDZ, and Boiler Dynamic (BD) have been considered to make the system practical. To show the efficacy of the proposed method they have extended the three areas system to five area systems considering hydrothermal generation. The performance of the M-SCA algorithm is compared to the Sine Cosine Algorithm (SCA), Genetic Algorithm (GA), and PSO. Further, the effectiveness of the proposed controller is also compared to other types of convention controllers such as PI, I and PID controllers. Guha et al. [37] introduced an evolutionary method known as the Backtracking Search Algorithm (SA) for the LFC problem of two areas IPS. Initially, the two areas with thermal power are deliberated and gains of PI and PID controllers are optimized using BSA. Further, the two areas system is extended to three and four area units including GRC, GDB, and BD. The efficiency of the proposed approach is related to Craziness based PSO (C-PSO) algorithm.

Yogendra Arya in [38] has used a fuzzy-based filter PID controller cascaded with fractional order integer (FPIDN-FOI) for AGC of two areas electric power system. The proposed controller is tuned by employing an imperialist competitive algorithm. The results yielded from the proposed method are compared to PID, PIDN, and FPIDN and conclude that the suggested approach provides a better transient response. Rajesh et al. have deliberate the LFC problem of five areas IPS considering with GRC and GDB. Fuzzy- based PID (FPID) is tuned with a hybrid Improved Firefly Algorithm (hIFA) with Pattern Search (PS). The proposed approach has been associated with other soft computing algorithms in the literature [39].

Authors in [40] analyzed the design of the Proportional Integral Double Derivative (PIDD) controller employing for AGC problem of a multi-areas multi-generation power unit. The gains of the PIDD controller are optimized with the TLBO algorithm. The authors compared the results yielded from the proposed method with traditional Ziegler Nichols (ZN) and metaheuristic algorithms such as FA, hIFA-PS, GA, and BFO for the same area of the interconnected unit. The results revealed that the PIDD controller with the TLBO algorithm superiorly performs as compared to other mentioned approaches in the literature. Ali et al. introduced a recent Multi-Verse Optimizer (MVO) metaheuristic optimization approach to developing LFC-based Model Predictive Control (MPC) embedded in a large multi-connected framework. The effect of GRC and GDB for multi-area with multi-generation are considered. The performance of the proposed approach is compared to GA and Intelligent Water Drops (IWD) techniques [41]. Similarly, numerous researchers have also applied meta-heuristic algorithms with different controllers to solve AGC problem such as Cookoo Search Algorithm (CSA) with Two Degree of freedom (2DOF) IDD

Controller [42], DE with 2DOF PID controller [43], PI controller optimized with a hybrid chemical reaction (HCR)- based PSO [44], DE optimized with Tilt Integral Derivative Filter (TIDF) controller [45], Biogeography-Based Optimization (BBO) with Fractional Order PI (FOPI) controller [46], Fuzzy based PI controller tuned with Self-Adaptive Modified Bat Algorithm (SAMBA) [47], Ant loin Optimizer (ALO) based PID plus Double Derivative (PID+DD) controller [48], FOPID controller optimized with DE [49], PD-Fuzzy-PID cascaded controller optimized with hybridization of Grey Wolf Optimization (GWO) based TLBO algorithm [50], Salp Swarm Algorithm (SSA) based PID controller [51], Fuzzy PID controller hybridized with PSO based levy flight algorithm [52], Lozi Chaotic Optimization Algorithm (LCOA) based PID controller [53], PI/PID based Bat algorithm [54], cascaded PID controller optimized with hybrid improved TLBO based DE (hITLBO-DE) algorithm [55], FA optimized 2DOF-Fractional Order (FO) PID Controller [56], FA with online wavelet filter based PI controller [57], Symbiotic Organism Search (SOS) with PID controller [58], [59], fuzzy based DE optimized PID controller [60], Improved PSO (IPSO) based FPPID and TID controller [61] and Social Spider Optimizer (SSO) based PID controller [62].

2.4 Deregulated Power System (DPS)

In the traditional power sector, DISCOs, GENCOs, and TRANSCOs are controlled by a single body that delivered power at a regulated tariff, known as Vertically Integrated Utility (VIU). However, development in power industries has changed the structure of VIU into a DPS in which GENCOs, TRANCOs, and DISCOs are owned by separate entities and they function independently in a competitive electricity market. Each company has the authority to contract others in the same or different control areas. In this aspect, numerous

researcher has contributed to solving the AGC problem in a deregulated environment. [63], [64], [65], [66].

Prakash et al. [67] proposed the 2-DOF Fractional Order (FO) Proportional Derivative Controller with filter (2-DOF-FPPDN) for AGC of the multi-generation DPS. Multi-source includes thermal, gas, wind, diesel, and hydro generation units. Different physical constraints including GRC, BD, and GDZ have been considered for a realistic model approach. The volleyball Premium league (VBL) metaheuristic algorithm is used to attain the tuned values of the suggested controller. The robustness and effectiveness of the proposed method were tested by comparing the same model with the published literature. Parmar et al. [68] highlighted the LFC problem in a deregulated environment with multi-generation power systems like thermal reheat, gas, and hydro units. An optimal output feedback controller with a less number of state variables is used for a realistic perspective on a large-scale IPS. The proposed controller address all potential transaction in the deregulated power sector. Sharma et al. [69] have used 2- DOF-Tilt Integral Derivative with filter (TIDN) controller for two areas IPS in deregulated environment considering physical constraint GRC, GDB, and BD. Two areas power system consists of Distribution Generations (DG, s) to include the outcomes of renewable energy sources permeation. The proposed controller is optimized by the hybridization of the salp swarm algorithm with DE. Authors in [70] have introduced a hybrid neuro-fuzzy approach based regulator for the AGC model in a deregulated scenario. The proposed model is evaluated on three-area hydrothermal power deregulated system including GRC for various contract conditions under different operating situations. The results yielded from the proposed approach are

assessed with Artificial Neural Networks (ANN), Real Coded Genetic Algorithm (RCGA) and hybrid chemical reaction based PSO controller to demonstrate its robust performance.

Prakash et al. proposed cascaded controller PIDF with FO derivative i.e (PIDF+1FOD) for a hydro-thermal unit in a restructured power system. The Salp Swarm Algorithm (SSA) is employed to attain the optimal gains of the suggested controller. The Static Synchronous Series Compensator (SSSC) is used with an HVDC tie-line to improve the power ability of IPS [71]. The authors in [72] considered the LFC problem of two areas with a thermal-thermal generation unit in a DPS by employing a Fuzzy Logic Controller (FLC). PSO algorithm is employed to tune the scaling gains of FLC controllers. Kumar and Romana [73] developed a wavelet-based Multi-Resolution PI (MRPI) controller for LFC of a two-area two-generation unit in the restructured scenario. The authors compare the efficacy of the suggested controller with the conventional PI controller.

Shahalami and Farsi introduced the Linear Quadratic Regulator (LQR) with Kalman Filter (KF) for the LFC of two- areas in a restructured environment. The proposed approach is tested on the thermal and hydro generation unit with and without the HVDC transmission line [74]. Sekhar et al. [75] have deliberate the LFC problem of multi-areas, multi-generation units in a restructured environment considering the effect of GRC and GDB. Fuzzy- based PID (FPID) controller are tuned with a Firefly Algorithm (FA). The proposed approach has been compared with other soft computing algorithms in the literature. Authors in [76] proposed Distributed Model Predictive Control (DMPC) for LFC of three areas two generation sources in a deregulated environment with and without load contract demands. The ideas of Area Participation Matrix (APM) and Disco Participation Matrix (DPM) is introduced in the deregulated environment by taking the effects of bilateral

trades. The DMPC is designed by model the LFC problem in the existence of both constraints and external disturbances that signify load reference point, and GRC respectively. Simulation results and analysis for the DPS indicate potential improvement in the closed-loop system.

Authors in [77] considered AGC of two areas deregulated system, each area comprised of two-generation and two distribution units. The performance of PI, I, PID and ID controllers are assessed for AGC in a deregulated environment. The proposed controller gains are optimized with the DE method and the results are compared with GA. Marzbali in [78] has proposed a PID controller for AGC of the four-areas multi-generation DPS. The author has considered a different contract in a restructured scenario including unilateral transactions, bilateral transactions, and contracts violation based transaction. The Modified Virus Colony Search (MVCS) algorithm is used to tune the PID controller. The efficacy of the proposed method is compared to PSO, ABC and Virus Colony Search (VCS) algorithm. The results reveal that the proposed approach performs superiorly in terms of transient response as compared to mentioned approaches.

Pappachen and Fatima introduced the design and implementation of an Adaptive Neuro-Fuzzy based Inference System (ANFIS) controller for four-areas with a thermal unit in a deregulated environment under various contractual scenarios considering standards of North American Reliability Council (NERC). The proposed controller is checked on the regional Indian grid systems and its performance is associated with the conventional PID controller. The outcomes obtained from simulation reveals that the ANFIS controller based on NERC standards is one of the best controllers under deregulated scenarios for the multi-area Indian regional grid systems [79].

2.5 Impact of Energy Storage and FACTS Devices in Power System.

The dynamic performance of the power system is enhanced by incorporating energy storage and FACTS devices which are reported in the literature. For instance, Nandi et al. [80] studied the impact of TCSC coordinated in tie-line for AGC of a deregulated system which consists of two areas with two generations and distributions unit in each area of an IPS. The PID controller is employed to tune its parameters by using Quasi Oppositional Harmony Search (QOHS) algorithm. Results achieved from the simulation reveals that QOHS based proposed PID controller is quite effective in DPS. Authors in [81] improved the performance of LFC in a deregulated environment by incorporating the combination of Thyristor Controlled Phase Shifters (TCPS) and Superconducting Magnetic Energy Storage (SMES) in its control areas. The application of the ANFIS controller is used to alleviate numerous issues of LFC in two-area restructured power networks. To examine the efficacy of the proposed approach, the performance of the system is assessed for different contract scenarios including bilateral, unilateral and contract violated based transaction and, the comparative results are also provided.

Ponnusam et al. [82] have analyzed the design of the Integral (I) controller for LFC of a DPS with various power generating sources using Imperialist Competitive Algorithm (ICA). The dynamic performance of the system is enhanced by integrating Capacitive Energy Storage (CES) along with Static Synchronous Series Compensator (SSSC). Results yielded from the simulation show that ICA based system employing CES and SSSC has better dynamic output without these factors.

Gorripotu et al. [66] proposed a PIDF controller for AGC of multi-source multi-area generation units in a deregulated scenario. The evolutionary algorithm Differential

Evolution (DE) is employed to tune the parameters of the PIDF controller. Additionally, the two-area system is incorporated with physical constraints including TD and GRC. Further, the performance of the system is enhanced by the inclusion of Redox Flow Batteries (RFB) in area-1 and Interline Power Flow Controller (IPFC) is retained in the tie-line power.

Sahoo et al. have used the Modified Differential Evolution (MDE) algorithm employed for the tuning of the optimized Fuzzy PID controller in the interconnected power system with the deliberation of non-linearities. Additionally, the TCSC model is used to enhance the dynamic performance of the LFC understudy system [83]. Similarly, Deepak and Ibrahim [84] also studied the impact of TCSC based FACTS devices on the performance of load following in two areas DPS.

Authors in [85] deliberate the impact of SMES and Unified Power Flow Controller (UPFC) integrated with the tie-line of two-area, multi-source generation. Further, the system is also made realistic by incorporating non-linearities like TD and GRC. Fuzzy logic based PID controller is employed in the system and the gains of the controller are tuned by Firefly Algorithm (FA). The effectiveness and robustness of the proposed approach are compared to other methods in the literature. Morsali et al. [86] discuss the dynamic performance of a realistic two areas multi-generation unit using a series Flexible AC Transmission System (FACTS). Various FACTS devices including TCPS, SSSC, and TCSC are used to compare the performance of the system. Simulation results show that TCSC based AGC performs well as compared to TCPS and SSSC based AGC.

Sahu et al. [87] considered the impact of RFB in area-1 of the two-area, multi-generation system and UPFC is integrated with the tie-line of LFC. Further, the system is

also made realistic by integrating non-linearities including GDB and GRC. Modified Integral Derivative (MID) controller is employed to the real system and the gains of the controller are tuned by hybrid (DE) and Pattern Search (PS). The effectiveness and robustness of the proposed method are compared to the other approaches in the literature.

Mostafa et al. [88] proposed a novel predictive functional modified PID controller for LFC of three areas with diverse generation units including wind, gas, hydro, diesel, and thermal unit considering GDB and GRC under deregulated environment. RFB is used to escalate the dynamic of the system and Grasshopper Optimization Algorithm (GOA) is employed to tune the gains of the proposed controller. Authors in [89] proposed a Tilt Integral Derivative (TID) controller for AGC of multi-source multi-area generation units in a restructured scenario. The hybridization of Teaching Learning Based Optimization (hTLBO) with Pattern Search (PS) algorithm is used to tune the parameters of the TID controller. Additionally, the two-area system is incorporated with physical constraints including BD, GDB, and GRC. Further, the performance of the system is enhanced by the inclusion of SMES in each area, and TCPS is placed in the tie-line. The supremacy of the proposed approach is demonstrated by comparing the outcomes with GA and DE based I/PI/PID controllers for the same test model.

Mishra and Kumar [59] have used IPFC to minimize system failure and power flow in the strongly loaded line, increase system reliability, and loadability. The Authors suggested the Disparity Line Usage Factor (DLUC) for optimal positioning and optimal tuning of IPFC using the Gravitational Search Algorithm (GSA) to regulate congestion in transmission lines. The proposed approach is executed on IEEE 30 bus bar system and IPFC is consequently located in the least congested and the most congested line linked to

the same bus. A decrease in the system's reactive power and an active power loss of approximately 6% is seen after the control system integrates an optimally tuned IPFC.

Morsali et al. [90] introduced a control approach and dynamic model for the SSSC to participate efficiently in the AGC of an interconnected restructured system. Fractional Order (FO) controller is used to design the effectiveness of the SSSC damping system. Modified Group Search Optimization (MGSO) and Improved PSO algorithm are used to tune the gains of the suggested controller. To obtain realistic outcomes in a competitive environment a multi-DISCO, multi GENCO with non-linear constraints, unilateral and bilateral transactions are taken into account at the same time. Authors in [91] have used the FOPID controller coordinated with TCSC for AGC considering the effect of GRC and GDB. Improved PSO technique is used to optimize the FOPID controller. Results yielded from simulation demonstrate that the proposed approach achieved better dynamic performance under various load perturbation conditions, as compared to conventional PID and phase lead-lag based TCSC controllers.

Arya and Kumar examine the effect of RFB in AGC of two-area multi-unit deregulated system. An optimal AGC regulator is employed to check the performance of the system by comparing the outcomes with the GA based optimized integral controller for the identical deregulated power system [92]. Hagh et al. [93] have proposed a Fractional Order Phase Lead lag Controller (FOPLC) coordinated with TCSC based frequency regulator to improve the transient response of the AGC system incorporated with GRC and GDB. The proposed FOPLC controller is tuned with the IPSO algorithm. The dynamic response of the proposed approach is compared to the classical phase lead-lag controller using time-domain analysis and eigenvalues simulations.

2.6 Nature-Inspired Metaheuristic Computational Techniques

Nature-inspired metaheuristic computational techniques are problem-independent optimization approaches that provide the best solution by iteratively exploring and exploiting the entire search space. A substantial amount of literature has already been published on the design and function of various metaheuristic algorithms, as well as their variants. In recent decades metaheuristic techniques have emerged in large numbers to address the issues associated with the efficient design and implementation of control methods for large and complex electrical power systems. Some of the most relevant meta-heuristic methods for AGC of regulated and deregulated power systems are deliberated in below subsection.

2.6.1 Genetic Algorithm (GA) Based AGC Power System

The genetic algorithm (GA) is a population based nature inspired algorithm relies on natural selection and genetics to find an optimal results. GA begins a loop of evolution processes consisting of selection, crossover, and mutation from a random initial population in order to increase the population's average fitness function [94]. The authors in [95] have used GA based PI controller for a two area network of an interconnected power system. Similarly the authors in [96], [97] employed I, PID and fuzzy based controllers optimized with genetic algorithm for two and three area interconnected power networks under restructured environment.

2.6.2 Artificial Bee Colony (ABC) Based AGC Power System

ABC is a nature inspired metaheuristic algorithm has been developed by Karaboga to search the swarming actions of the bees. In short there are different types of bees: queen

bees (responsible for making decision and produce offspring), worker bees (works under the command of queen bees) and scout bees (responsible for exploring environment and exploit the desirable targets). Authors in [98] presented market-based LFC architecture using PID controller optimized with ABC algorithm in a two-area thermal deregulated power system. The results yielded from proposed method shows better performance as compared to GA and PSO based tuned PID controller.

The authors of [99] used artificial bee colony (ABC) algorithms to introduce a strategic virtual inertia regulation for wind power conversion systems connected to the grid. The proposed control scheme and its robustness were assessed using LFC for three transaction cases in an integrated open-energy market, and validation was performed using eigenvalue analysis.

2.6.3 Bacterial Foraging Optimization Algorithm (BFOA) Based AGC Power System

The BFOA is a nature-inspired computational technique in which the total solution space is searched with a much larger number of parameters than GA. This algorithm is influenced by natural selection, which aims to exclude animals with ineffective foraging tactics and prefer those with successful foraging strategies. Authors in [100] analyzed the design of the Proportional Integral (PI) controller employing for AGC problem of a multi-areas multi-generation deregulated power unit. The gains of the PI controller are optimized with the BFO algorithm and the comparative studied has been conducted for various type of transactions.

Thirunavukarasu et al. [101] have analyzed the design of the proportional double integral (PI^2) controller for LFC of a DPS with various power generating sources using

Bacteria Foraging Optimization (BFO) algorithm. The dynamic performance of the system is enhanced by integrating RFB with UPFC. Results yielded from the simulation show that BFOA based system employing RFB and UPFC has better dynamic output without these factors.

2.6.4 Grasshopper Optimization Algorithm (GOA) Based AGC Power System

The Grasshopper Optimization Algorithm (GOA) is a meta-heuristic technique based on Grasshopper's life cycle that damages cropping and agricultural production. Grasshoppers have a swarming behavior in which they grow from nymphs into rolling cylinders and then mature into adults, forming a swarm in the air. This is the mechanism by which these insects or pests move over a vast distance from one form to another. The authors in [102] designed filter based PD controller integrated with (1 + PI) controller tuned with GOA for AGC of diverse generation of reheat thermal, hydro, wind and diesel unit.

Tripathy et al. [103] have deliberate the LFC problem of three areas of thermal, solar thermal and wind generation unit. Fuzzy- based PD cascaded with PI controller is tuned with a GOA. Further, the proposed approach has been associated with PI controller optimized with other soft computing algorithms including PSO, TLBO and PSO.

2.6.5 Ant Colony Optimization Based AGC Power System

The ACO technique mimics the foraging behavior of certain natural real ant species by using a liquid substance known as pheromone to find the shortest path from food source to nest. This route is more useful in identifying the path of other ants in the same colony. During the optimization process, the ACO technique has three major phases: initialization, building ant solutions, and updating pheromone concentration. Jagatheesan et al. [104] have employed ACO technique for AGC of multi area thermal power system using various

multi-objective function. Similarly, authors in [105] have also used ant colony optimization for different generation units of multi-area AGC system.

Chapter 3. AGC of Interconnected Power System

This chapter provides the designing and implementation of the Proportional Integral Derivative (PID) controller and their modified form called as Integral-Proportional Derivative (I-PD) controller. A, meta-heuristic algorithms known as Particle Swarm Optimization (PSO), Fitness Dependent Optimizer (FDO), Teaching Learning Based Optimization (TLBO) and Firefly Algorithm (FA) are employed for the optimization of proposed controllers. The rest of this chapter is outlined as follows: The subsequent section is comprised of mathematical modeling of the power system, controller structure, fitness function and optimization techniques while the last section described the implementation of the proposed approach and its results.

3.1 Mathematical Modeling of a Power System

In a power system, synchronous generators are typically powered by primary movers receiving energy from sources like gas, hydro, thermal, wind etc. Each turbine is fitted with a speed control system to provide a means for starting the turbine, running up to the operating speed and operating on load with the necessary power output. The power system gains constant (K_p), damping load (D), area frequency bias characteristics (β) and power system time constant (T_P) are given in below equations respectively [64].

$$K_p = \frac{1}{D} \quad \text{Hz/puMW} \tag{3.1}$$

$$D = \frac{\partial P_L}{\partial F}\frac{1}{P_r} \quad \text{puMW/Hz} \tag{3.2}$$

$$\beta = D + \frac{1}{R} \quad \text{puMW/Hz} \tag{3.3}$$

$$T_p = \frac{2H}{FD}\ s \tag{3.4}$$

Where ∂P_L represent the nominal operating load, P_r denote the total area capacity, H represents the inertia constant, F represent frequency of the system and R shows the regulation constant of the power system.

3.1.1 Modeling of Two Area Reheat Thermal Power System

In thermal power plants, the fuel's energy is used to produce high temperature and high-pressure steam in the boiler. In axial flow steam turbines, steam energy is then converted into mechanical energy. The steam exerted force on the blades of the turbine and as a result, the turbine rotates and energy is produced. The Transfer Function (TF) model of thermal reheat power with a two-area interconnected system is provided in Fig 3.1. Rth1 and Rth2 denote the droop constant of area 1 and area 2 respectively, whereas ΔPD indicates the change in load perturbation. Similarly, ΔF1 and ΔF2 represent the change of frequency in area 1 and area 2 respectively. The TF of the governor, reheat thermal, turbine and load generator for area 1 and area 2 are represented in Eq (3.5)- Eq (3.8) [2].

$$G_{11}(s) = G_{21}(s) = \frac{1}{T_t S+1} \tag{3.5}$$

$$G_{12}(s) = G_{22}(s) = \frac{k_1 T_r S+1}{T_r S+1} \tag{3.6}$$

$$G_{13}(s) = G_{23}(s) = \frac{1}{T_1 S+1} \tag{3.7}$$

$$G_{p1}(s) = G_{p2}(s) = \frac{Kp}{T_p S+1} \tag{3.8}$$

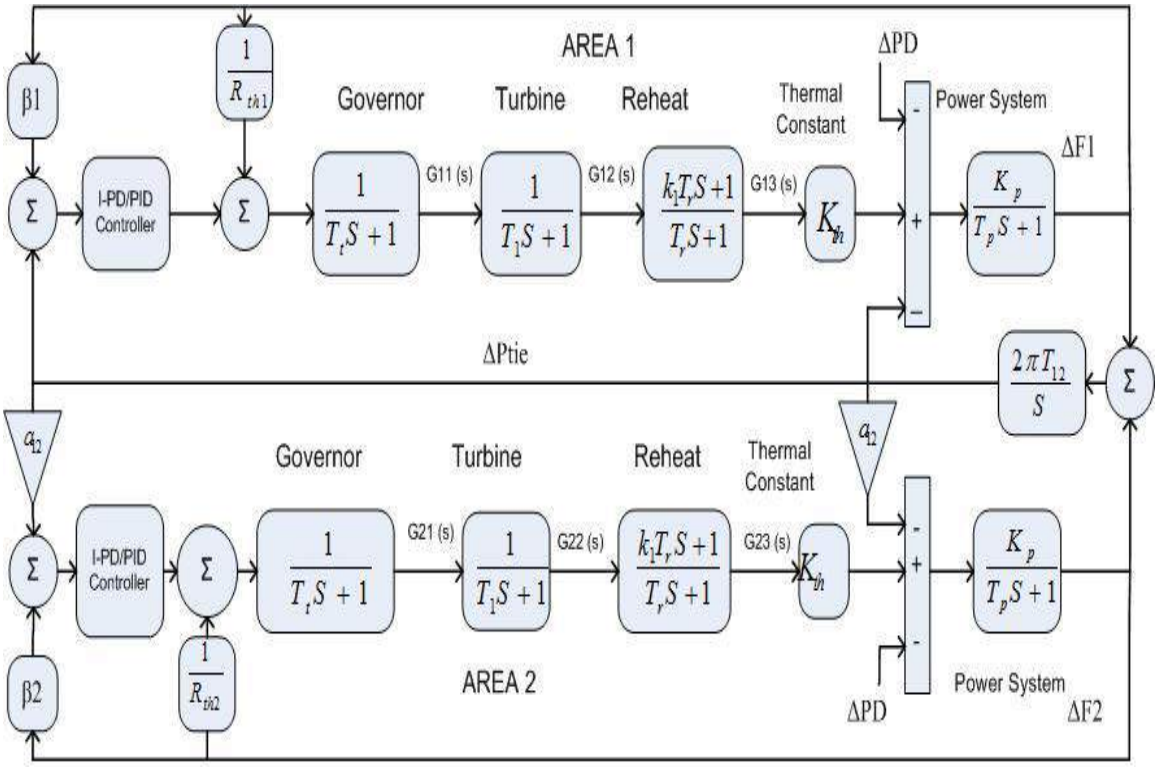

Figure 3.1 Two- area model with reheat thermal power unit.

3.1.2 Modeling of Two Area Hydro Power System

The transfer function (TF) diagram for the hydropower system with two areas is shown in Fig 3.2. Where Kh represents the hydro constant and Rh1, Rh2 represent the droop constant of the hydro unit for areas 1 and 2 respectively. The TF of the governor, penstock turbine, and transient droop compensation for area 1 and area 2 are represented in Eq (3.9) - Eq (3.11) [2].

$$G_{11}(s) = G_{21}(s) = \frac{1}{T_{gh}S+1} \tag{3.9}$$

$$G_{12}(s) = G_{22}(s) = \frac{-T_wS+1}{0.5T_wS+1} \tag{3.10}$$

$$G_{13}(s)=G_{23}(s)=\frac{T_rS+1}{T_{rh}S+1} \tag{3.11}$$

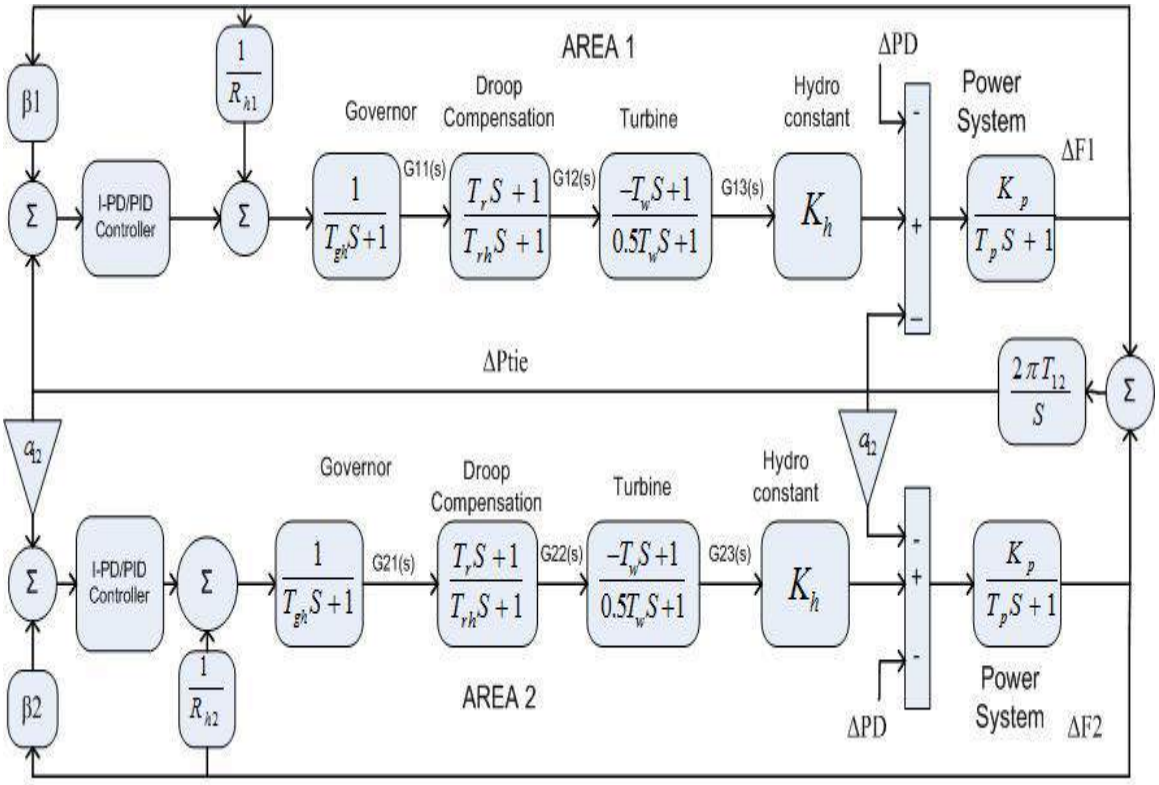

Figure 3.2 Two- area model with hydro power unit.

3.1.3 Modeling of Two Area Gas Power System

The Transfer Function (TF) diagram of two area gas power generation is depicted in Fig 3.3. Where Rg1, Rg2 represent the droop constant of the gas unit for areas 1 and 2 respectively and Kg represents the hydro constant. The transfer function of the valve position, speed governor, compressor discharge, and fuel with combustion reaction for area 1 and area 2 are represented in Eq (3.12)- Eq (3.15) [2].

$$G_{11}(s) = G_{21}(s) = \frac{1}{b_g S + x_g} \tag{3.12}$$

$$G_{12}(s) = G_{22}(s) = \frac{x_c S + 1}{y_c S + 1} \tag{3.13}$$

$$G_{13}(s) = G_{23}(s) = \frac{1}{T_{cd} S + 1} \tag{3.14}$$

$$G_{14}(s) = G_{24}(s) = \frac{T_{cr}S-1}{T_f S+1} \tag{3.15}$$

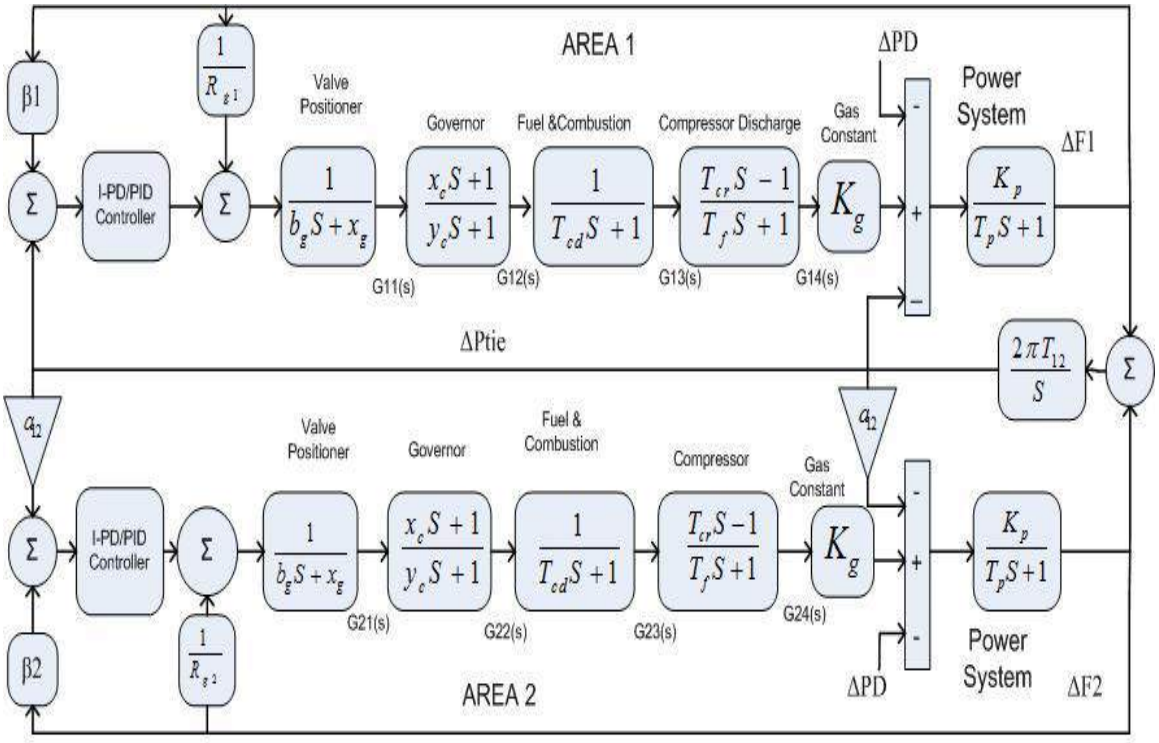

Figure 3.3 Two- area model with gas power unit.

3.1.4 Modeling of Two Area Multi-Source Power System

The Transfer Function (TF) diagram for multi-source with two-area IPS is depicted in Fig 3.4. In each control area, the system is equipped with thermal reheat, gas power and hydro generation unit which makes the system more complicated as compared to other generation units which are individually applied in two area power units.

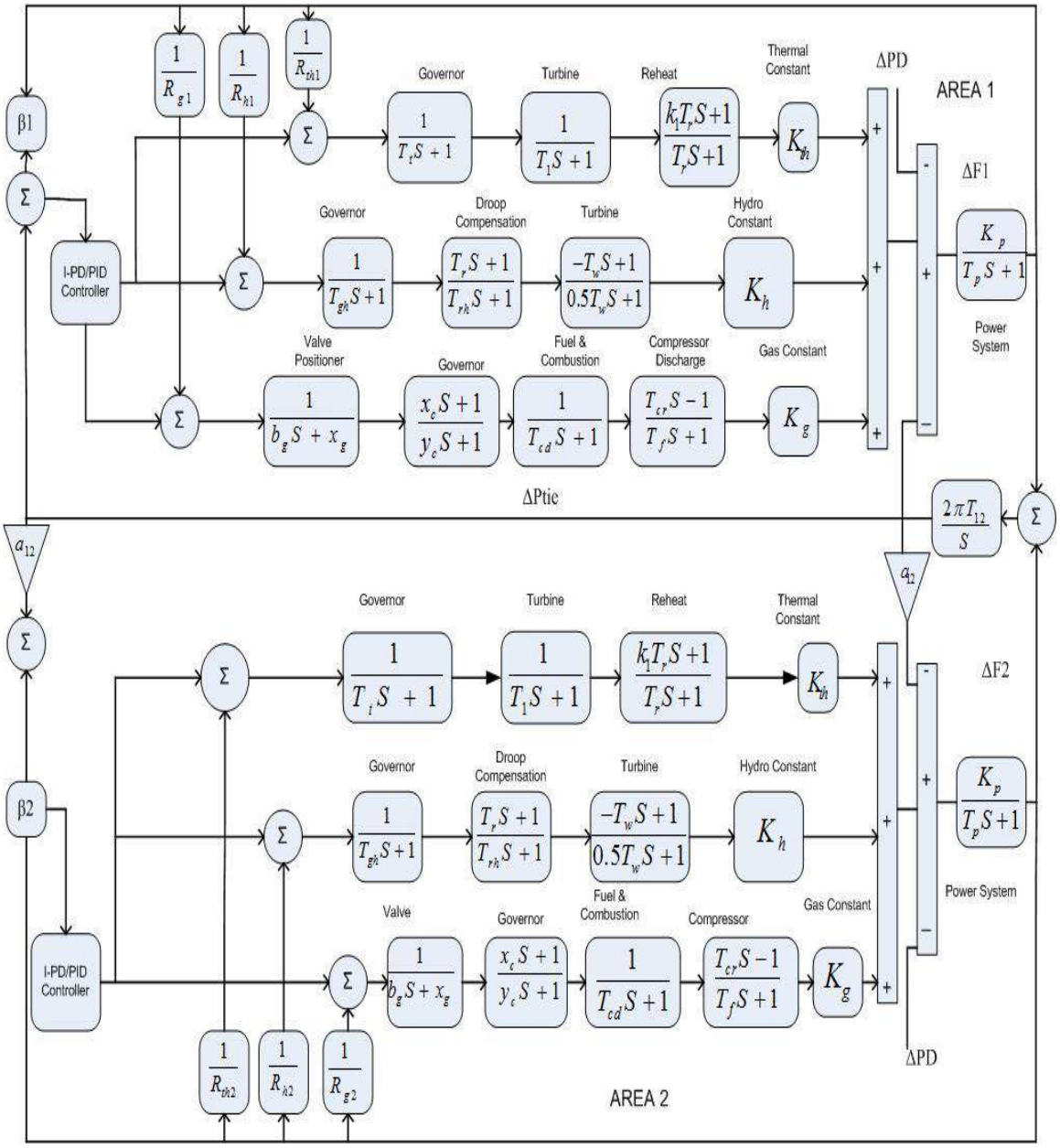

Figure 3.4 Two- area model with multi-source power unit [29].

3.2 Controller Structure and Optimization Techniques

The integral controller is typically used for automatic generation control due to its simple structure. However, it has a drawback of slow response time in which the use of Proportional Integral (PI) controller improves the setback. PI controller can improve the dynamic response of the integral controller, in addition to being low cost, easy to

implement as well as having a simple configuration. PI controller however still exhibits a slow response time to a highly non-linear system. This problem, however, can be solved by using a PID controller. PID controller is used frequently in industries nowadays due to its strong dynamic performance, robustness, and its easy implementation. The typical structure of the proposed PID controller is depicted in Figure 3.5.

In this thesis, an improved form of PID controller term as the Integral-Proportional Derivative (I-PD) controller is designed for the AGC system. I-PD controller has advantages of simplicity, functionality, ease to use, and capability of improving the transient response of the controller, especially the overshoot time without affecting the other parameters of the controller [106], [107], [108], [109]. The structure of the proposed I-PD controller is depicted in Figure 3.6.

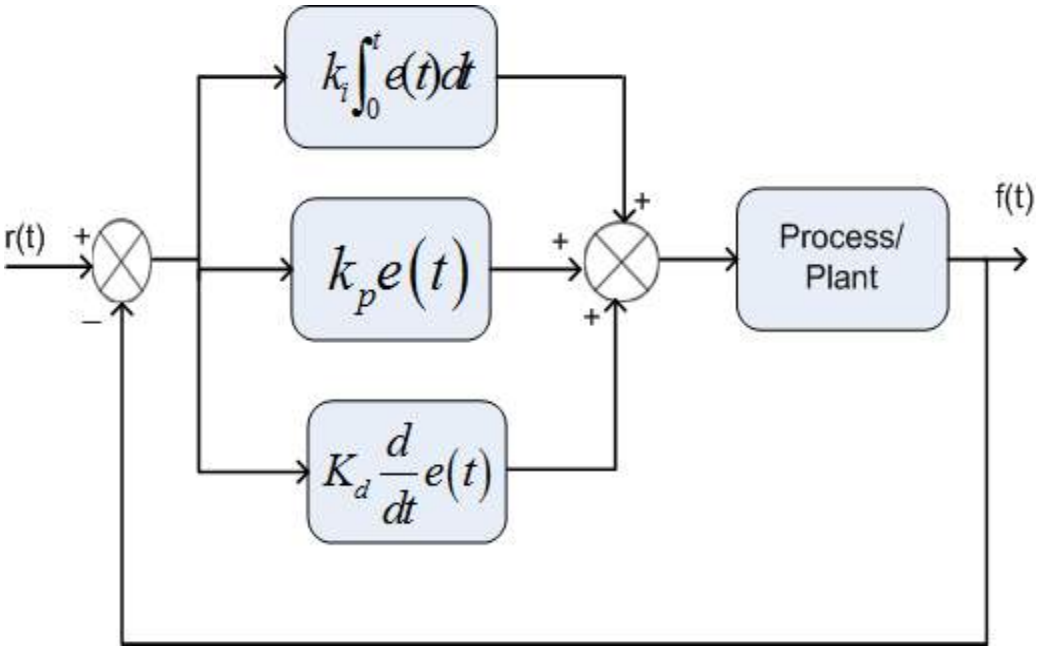

Figure 3.5 Structure of PID controller.

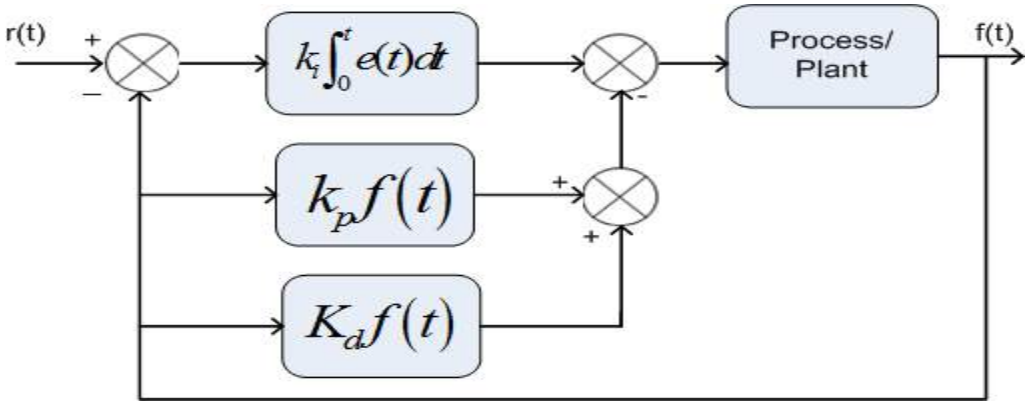

Figure 3.6 Structure of I-PD controller.

The output of the PID and I-PD controllers is given by Eq. (3.16) and Eq. (3.17) below, respectively.

$$u(t) = k_p e(t) + \int K_i e(t)\,dt + K_d \frac{d}{dt} e(t) \tag{3.16}$$

$$u(t) = \int K_i e(t) - [k_p y(t) + k_d \frac{d}{dt} y(t)] \tag{3.17}$$

The input of the I-PD/PID controller for areas 1 and 2 is the area control error (ACE) which is given by Eq. (3.18) and Eq. (3.19) [11].

$$ACE_1 = \beta_1 \Delta F_1 + \Delta P_{tie12} \tag{3.18}$$

$$ACE_2 = \beta_2 \Delta F_2 + \Delta P_{tie21} \tag{3.19}$$

To attain a good system performance, it is vital to properly optimize the parameters of the controller while choosing appropriate performance criteria as an objective function. In literature, four different performance indices are used including ITSE, ITAE, IAE, and ISE. However, ITAE [12,16,17,32], ITSE [3,10,11,21] and ISE [14,18,20,29] are more frequently used for AGC problem. For the comparison among various performance indices, Eq (3.20)

to Eq (3.23) is implemented in Matlab for two area multi-source IPS and achieved minimum fitness values for ITSE as compared to ITAE, ISE, and IAE which is depicted in Table 3.1. Therefore, ITSE is used as a cost function for the said AGC problem.

$$J_1 = \text{ITSE} = \int_0^t \left[\Delta F_1^{\,2} + \Delta F_2^{\,2} + \Delta P^2_{tie12} \right] \text{t}\, dt \tag{3.20}$$

$$J_2 = \text{ISE} = \int_0^t \left[\Delta F_1^{\,2} + \Delta F_2^{\,2} + \Delta P^2_{tie12} \right] dt \tag{3.21}$$

$$J_3 = \text{ITAE} = \int_0^t \left[| \Delta F_1 | + | \Delta F_2 | + | \Delta P_{tie12} | \right] \text{t}\, dt \tag{3.22}$$

$$J_4 = \text{ITAE} = \int_0^t \left[| \Delta F_1 | + | \Delta F_2 | + | \Delta P_{tie12} | \right] dt \tag{3.23}$$

3.2.1 Particle Swarm Optimization (PSO)

Particle swarm optimization (PSO) is a global optimization heuristic approach proposed by Kennedy and Eberhart in 1995. PSO is a population-based optimization technique inspired by the movement of flocks of birds and schools of fish. PSO consist of the following steps [72, 106].

Step 1 (Initialization): A random population of swarm particle is initialized in the quest space.

Step 2 (Fitness value): The fitness value for each particle is computed.

Step 3 (Determination of velocity): For each particle the particle velocity can be determined using below equation.

$$\begin{aligned} &V_{xy}(n) = V_{xy}(n\text{-}1) + r_1(P_{xy} - b_{xy}(n\text{-}1)) + r_2(P_{gy} - b_{xy}(n\text{-}1)) \\ &1 \le x \le X; 1 \le y \le Y \end{aligned} \tag{3.24}$$

Where P_x represent local best and g_y represent global best. The vectors r1 and r2 can be visualized as random vectors containing values that are uniformly distributed between 0 and 1.

Step 4 (Update position): The particle position can be updated using below equation

$$b_{xy}(n) = b_{xy}(n\text{-}1) + V_{xy}(n) \tag{3.25}$$

Step 5 (Termination criteria): The fitness value of each scout bee is calculated until a solution is achieved or a termination criterion is reached. The basic steps for the PSO flow chart as given in Figure 3.7

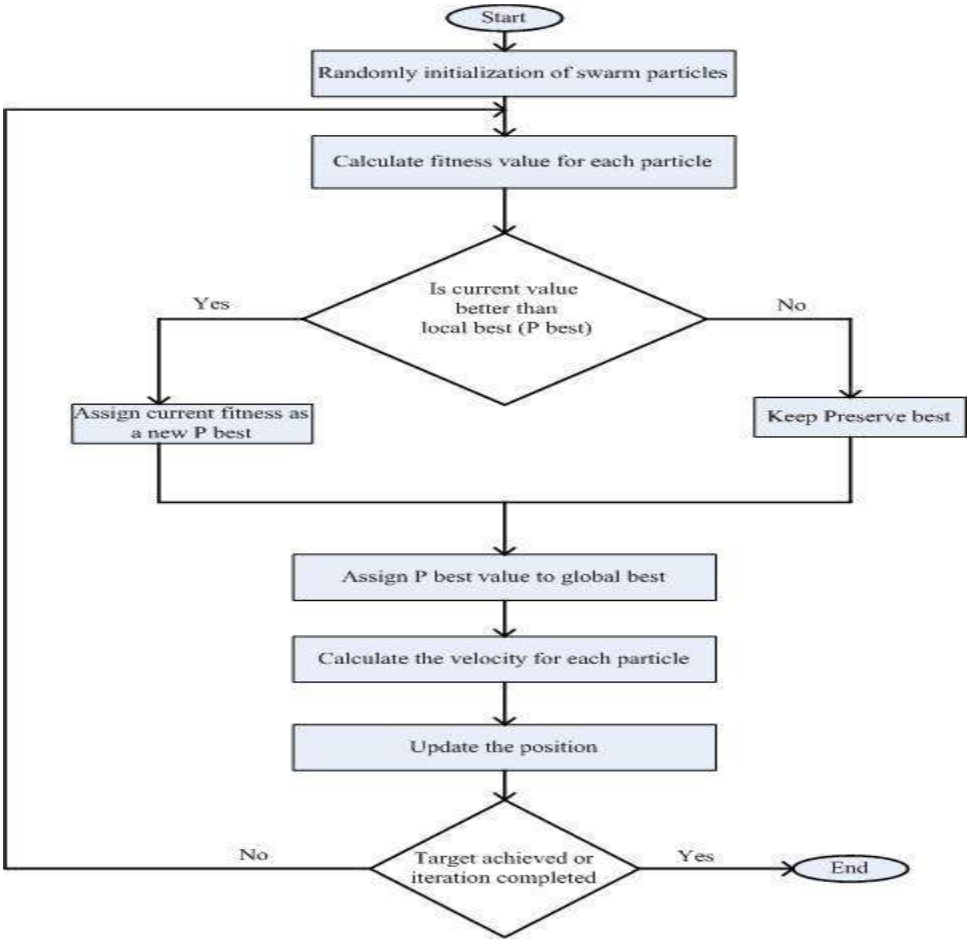

Figure 3.7 Flow chart of Particle Swarm Optimization (PSO) [106].

3.2.2 Firefly Algorithm (FA)

Insects or winged beetles that yield light and blink at night are known as fireflies. Bioluminescence is a light with no ultraviolet or infrared frequency that is chemically generated from the lower abdomen. They use the flash light to attract mates or prey in particular. The flash light also served as a warning system for the fireflies, reminding them of potential predators. The Firefly algorithm developed by Yang, is a heuristic algorithm which is inspired by the phenomenon of bioluminescent communication in fireflies and consist of the following molds [57, 85].

1) Because fireflies are unisexual, they will attract each other regardless of sex.

2) While the less attractive firefly will be attracted to the brighter firefly, attractiveness is proportional to their brightness. As the distance between the two fireflies increased, their attractiveness decreased.

3) Fireflies will move randomly if the brightness of both of them is the same.

The algorithm is based on the fireflies' ability to communicate globally. As a result, it can find both global and local optimal solutions at the same time. The majority of the numbers used by FA are real random numbers. Different fireflies operate independently, allowing for parallel implementation. The basic steps for the FA flow chart as given in Figure 3.8.

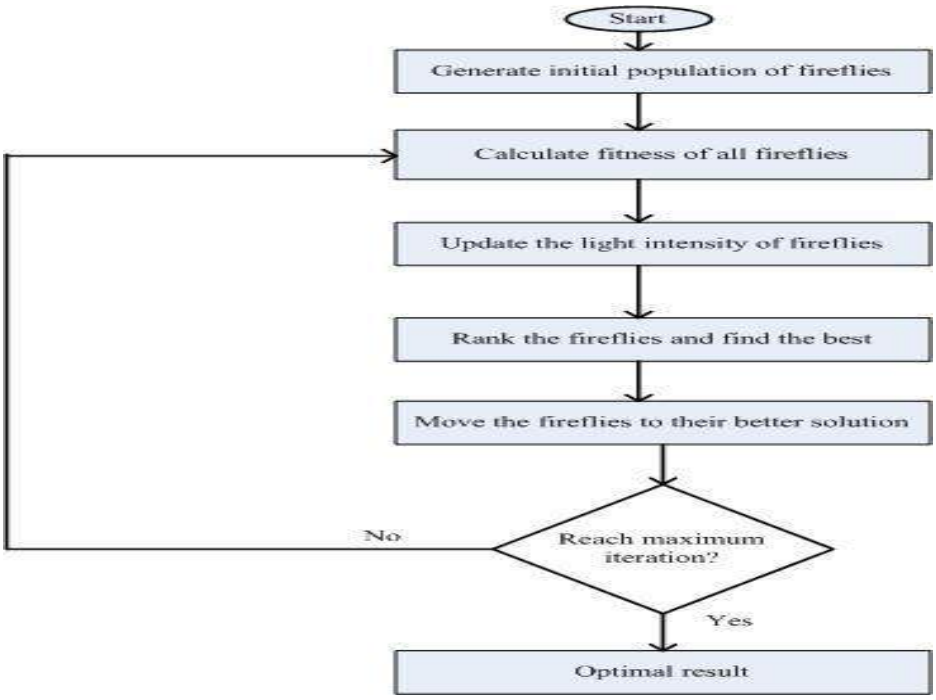

Figure 3.8 Flow chart of Firefly Algorithm (FA) [85].

3.2.3 Teaching Learning Based Optimization (TLBO)

TLBO is a Meta heuristic algorithm developed by Rao et al that is inspired by simulation of the learning and teaching process behaviors in a classroom. The teacher works hard to educate all of the students in the class. The students then interact with one another to modify and improve their newly acquired knowledge. The TLBO algorithm is a population-based Meta heuristic algorithm in which the population is a group or class of students. As a result, a classmate represents a viable solution to the problem [40, 89]. The TLBO algorithm is divided into two phases: teacher and learner.

Teacher phase: In the teaching phase, the teacher's role is to study the students. The most experienced, knowledgeable, and highly learned person in the society is considered a teacher, according to the teaching-learning philosophy. The teacher aims to improve students' knowledge and assist them in achieving good grades. However, students gain

knowledge and receive grades based on the quality of the teacher's instruction and the quality of the students in the class.

Learner phase: Students gain knowledge through mutual interaction during this phase. Students talk with one another to better understand the class material. It is possible for a student (x) to learn something new from a classmate who is more knowledgeable than the student (x). As a result, if student (y) performs significantly better than student (x), student (x) is moved closer to student (y). Alternatively, student (x) is re-positioned away from student (y). The basic steps for the TLBO flow chart as given in Figure 3.9.

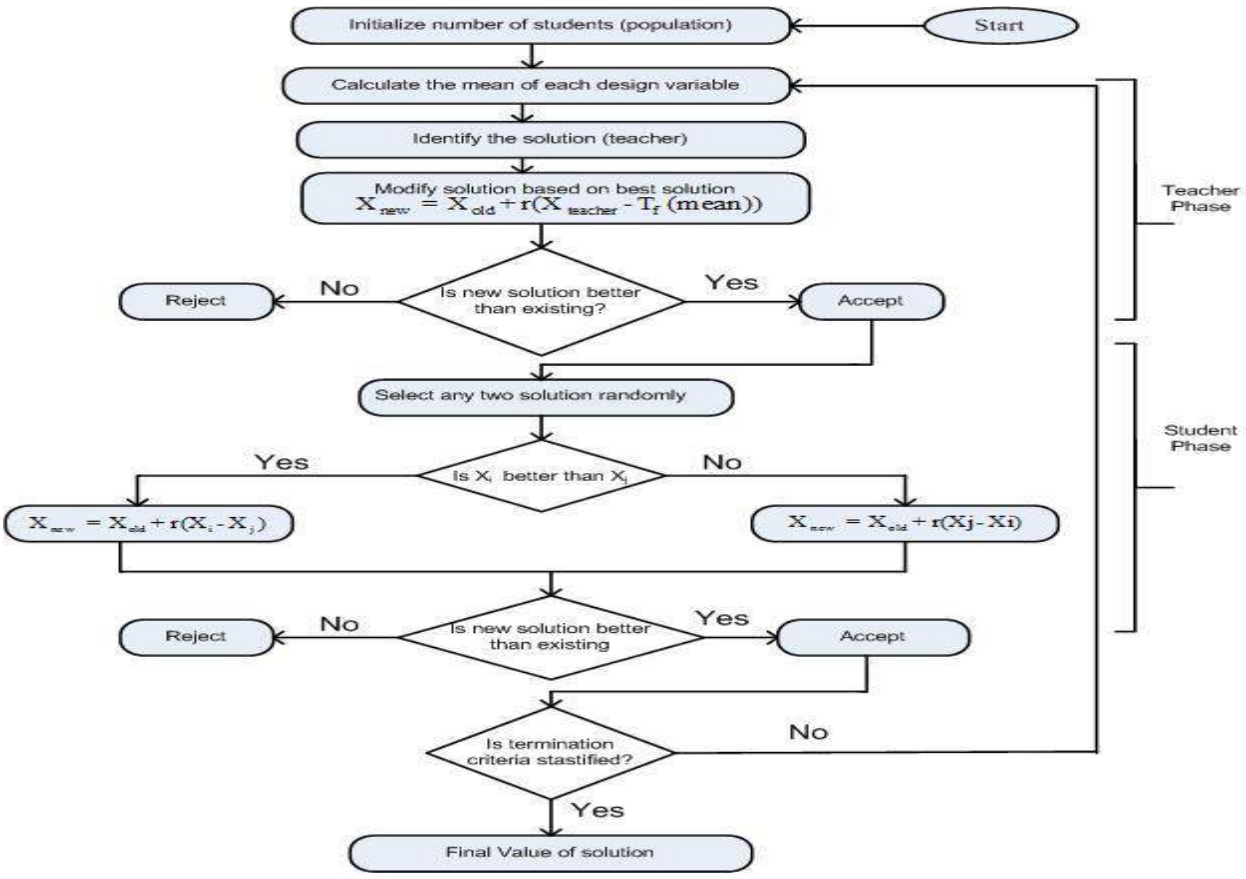

Figure 3.9 Flow chart of Teaching Learning Based Optimization (TLBO) algorithm [89].

3.2.4 Fitness Dependent Optimizer

Fitness Dependent Optimizer (FDO), developed by Abdullah and Tariq [110] is applied for the tuning of controllers of AGC with multi-source IPS. The adaptive-based FDO has been also used for the bin packing problem [111]. FDO has a fast convergence rate, dynamics, and able to solve nonlinear problems. FDO consist of the following points:

1) A random population of scout is initialized in the quest space, X_k (k=1, 2, 3……n).

2) The scout bees are randomly searching for a better hive. Once a better position is found, the previous one is discarded. Thus, at each position, a new optimum solution is identified by the algorithm. However, if the current forward direction doesn't give any optimal solution it will go back to its previous direction looking for the best solution.

3) In searching for an optimal solution, scout bees add pace to their current position and their moment can be shown as below [110].

$$\mathbf{X}_{k,t+1} = \mathbf{X}_k + \mathbf{P} \tag{3.26}$$

Where X indicates the scout bees, K is the current position, t is the iteration of scout bees and P represents the direction and the forward moment rate.

4) The pace depends upon a factor term known as fitness weight (FW). Though, the momentum of the pace is random. The FW can be expressed as [111]

$$\mathrm{FW} = \left| \frac{\mathbf{X}^*_{K,t,f}}{\mathbf{X}_{k,t,f}} \right| - \gamma \tag{3.27}$$

The $X^*_{K,t,f}$ denotes the value of fitness function (FF) for the global best solution, $X_{k,t,f}$ represents the objective value for the current solution while ϒ represents the weight factor

taking the value of either 0 or 1 to control the FW. When ϒ=1, it shows the high rate of convergence, and if ϒ= 0, then it does not affect the above equation. In many cases, ϒ is usually 0 for a stable search. However, this condition is problem-dependent.

5) The FW should be in the range of [0, 1]. The value of FW will be one when $X^{*}_{K,t,f}$ and $X_{k,t,f}$ have the same values.

The Value of FW will be zero when $X^{*}_{K,t,f} = 0$. To avoid $X_{k,t,f} = 0$ the following rules should be applied [110].

$$P = a\, X_{K,t,f} \text{ If } WF = 0, \vee WF = 1, \vee X_{K,t,f} = 0 \quad : \tag{3.28}$$

$$P = \begin{Bmatrix} WF(X_{k,t,f} - X^{*}_{k,t,f}) - 1; \text{If } WF < 1 \wedge WF > 0 \wedge \alpha < 0 \\ WF(X_{k,t,f} - X^{*}_{k,t,f}); \text{If } WF < 1 \wedge WF > 0 \wedge \alpha \leq 0 \end{Bmatrix} \tag{3.29}$$

Where α is a random integer in the range of [-1, 1]. The basic steps for the FDO flow chart as given in Figure 3.10.

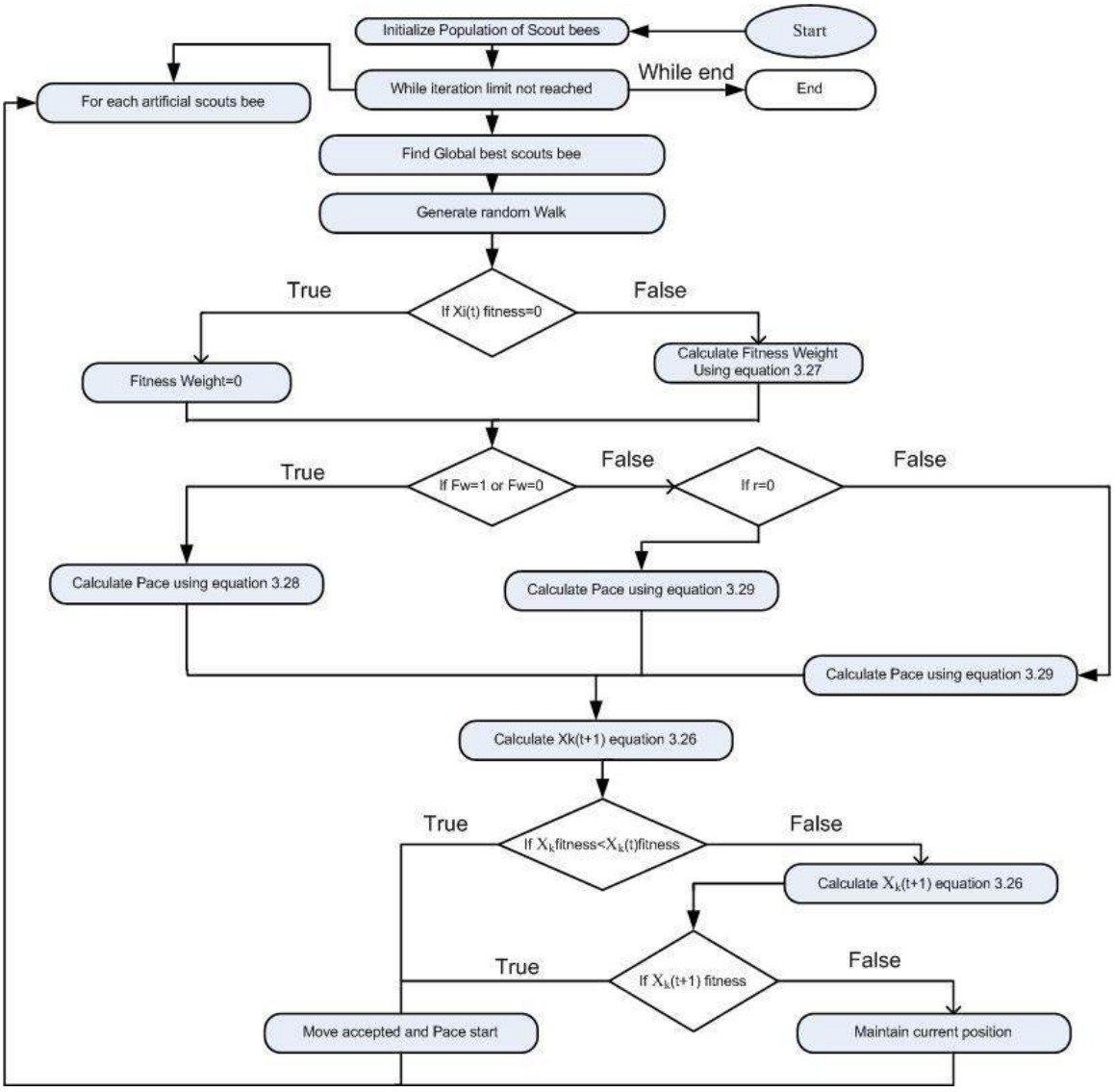

Figure 3.10 Flow chart of Fitness Dependent Optimizer [111].

3.3 Implementation and Results

In this section, the PID/I-PD controller is designed and implemented in two areas, a multi-unit interconnected power system considering different generation sources of a hydro, reheat-thermal, and gas generation system. To show the efficacy of the proposed technique, it has been simulated on two area multi-source IPS with 1% step load perturbation (SLP)

in area-1 considering four different scenarios. The first scenario is a two-area IPS with a reheat thermal unit while the second and third scenario is a two-area IPS with hydro and gas generation units respectively. Finally, in the last scenario, all the generating units are collectively applied for two areas system called as two- area multi-source system. The parameters of the proposed I-PD/PID are optimized with fitness dependent optimizer using ITSE as a cost function. To optimize the parameters of the controller the values of FDO parameters have been considered from the Appendix (Table 2). The optimization method was 30 times performed and the best optimum values of the 30 runs are selected as an ultimate gain of controller. The best optimum value for two areas IPS with thermal reheat, hydro, gas and collectively all the generation units are provided in Table 3.2, 3.4, 3.6, and 3.8 respectively. Results achieved from the proposed technique are compared with a few other techniques such as TLBO, PSO, and FA used to develop and optimize the PID/I-PD controllers. The convergence diagram for fitness values with different techniques is provided in Figure 3.11. The convergence profile provided in Figure 3.11 plotted against different evolutionary algorithms indicates that FDO algorithm converge quickly for 60 iterations as compared to TLBO, FA and PSO techniques. Further, Table 3.1 also illustrate that our proposed FDO algorithm have better ITSE (0.00056) as compared to TLBO-ITSE (0.00070), PSO-ITSE (0.00090) and FA –ITSE (0.00014). Similarly, FDO based ISE, ITAE, and IAE performance indices superiorly perform as compared to TLBO, FA and PSO algorithms with same performance indices.

Table 3.1: Comparative performance for different indices criteria.

Techniques	Performance Indices			
	ITSE	ITAE	ISE	IAE
FDO-PID	0.00056	0.00093	0.00067	0.0147
FDO-I-PD	0.00026	0.00019	0.00056	0.0036
PSO-PID	0.00030	0.00210	0.002300	0.0096
PSO-I-PD	0.00090	0.00560	0.009600	0.0663
FA-PID	0.00050	0.00100	0.004900	0.0023
FA-I-PD	0.00094	0.00080	0.004900	0.0196
TLBO-PID	0.00055	0.00020	0.002100	0.0210
TLBO-I-PD	0.00070	0.00900	0.001100	0.0020

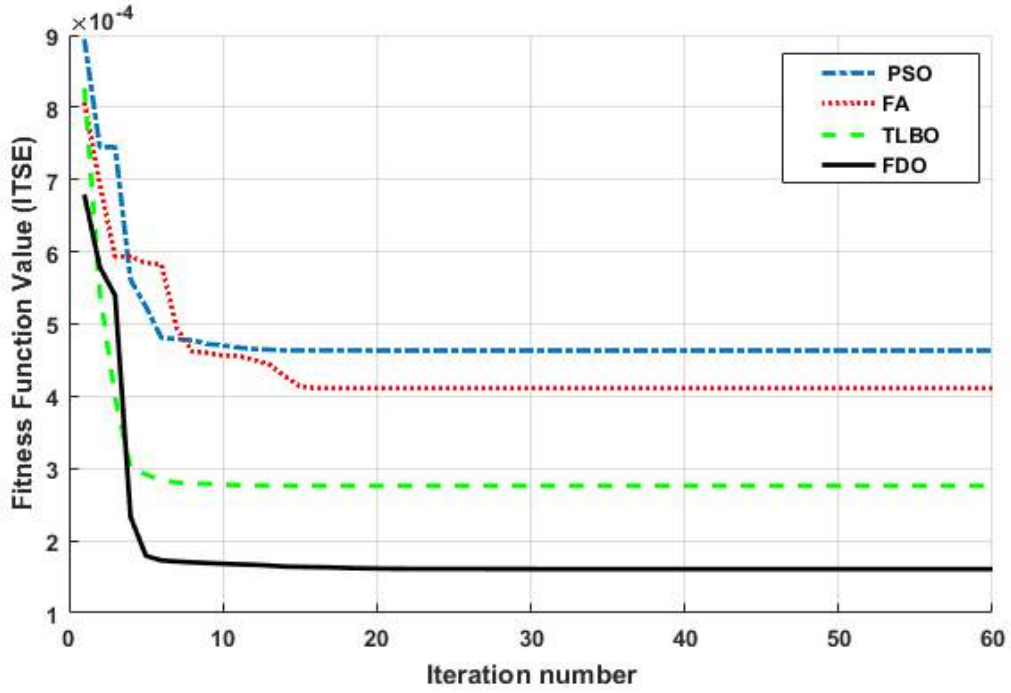

Figure 3.11 Convergence rate comparison of different techniques.

3.3.1 Implementation of Two Area Reheat Thermal Power System

The TF diagram for two-area reheat thermal IPS is developed in Matlab/Simulink using the values of the gains from the Appendix (Table 1). The system is evaluated with I-PD/ PID controllers with 1% SLP at t = 0 sec. Fig 3.12 – Fig 3.17 depicts the responses of load

frequency in each area and tie-line power. In pursuance to examine the effectiveness of the FDO-PID and FDO-I-PD control strategies, the output responses are compared with several other algorithms including PSO- PID/I-PD, FA-I-PD, and TLBO-PID/I-PD. The comparison of transient response specifications is quantified and presented in Table 3.3.

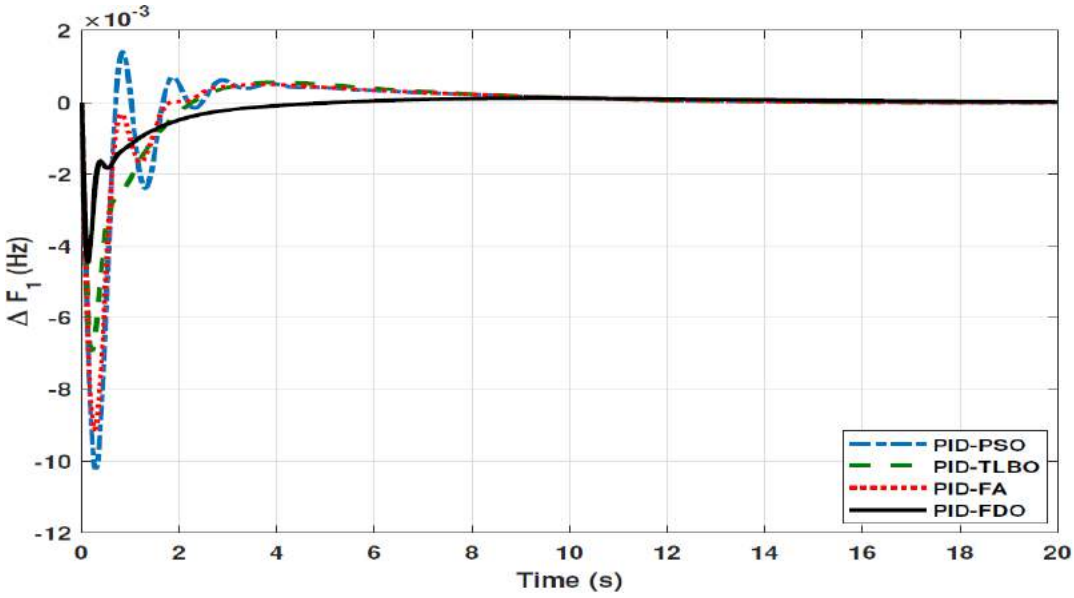

Figure 3.12 Results of reheat thermal unit for ΔF1 with PID controller.

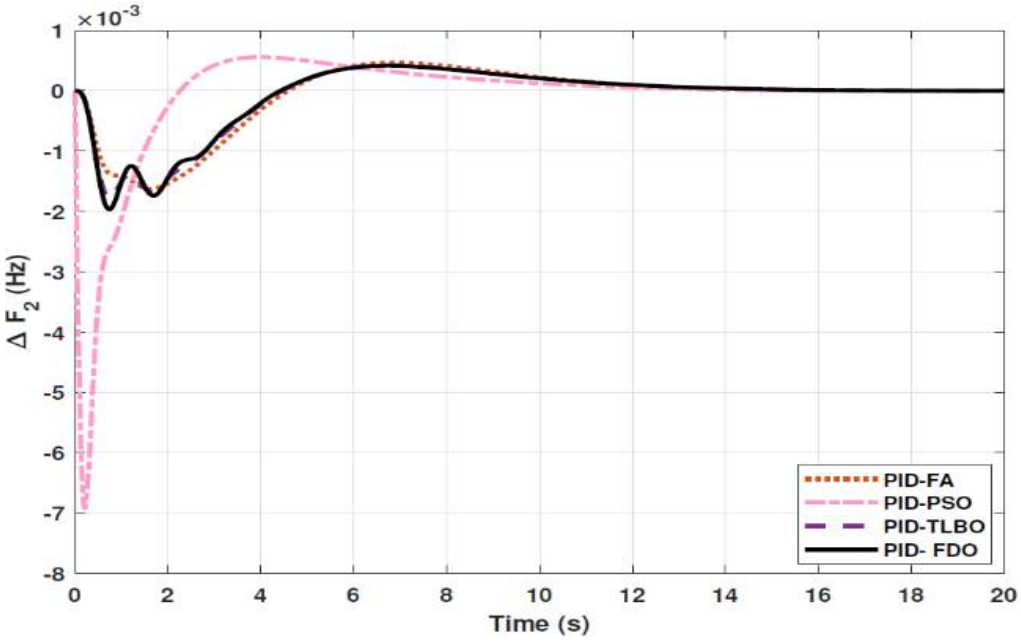

Figure 3.13 Results of reheat thermal unit for ΔF2 with PID controller.

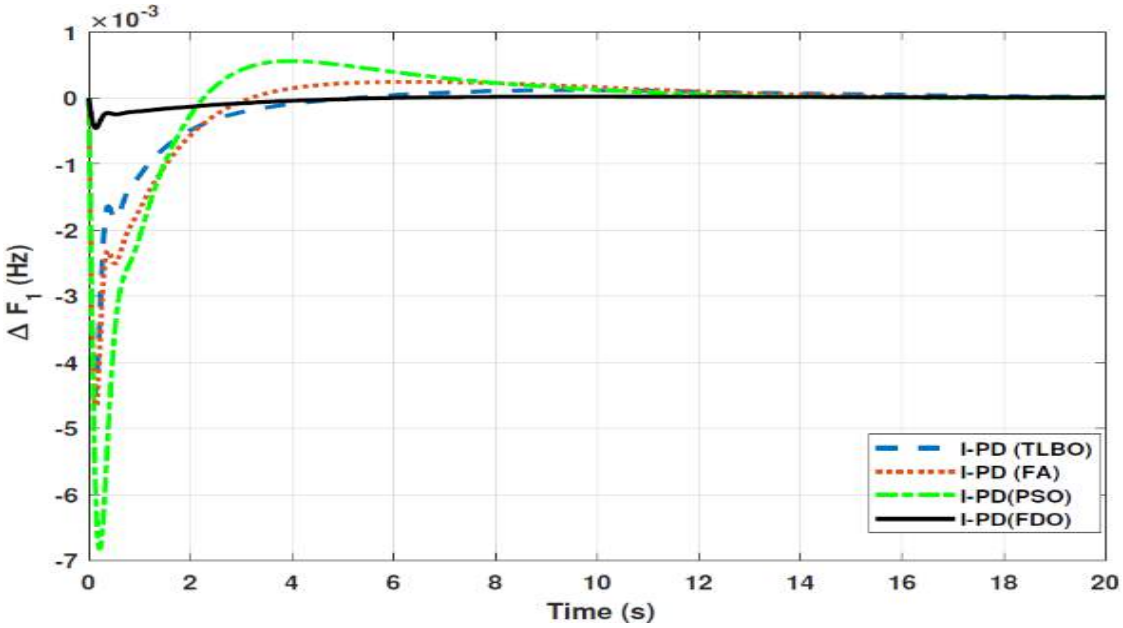

Figure 3.14 Results of reheat thermal unit for ΔF1 with I-PD controller.

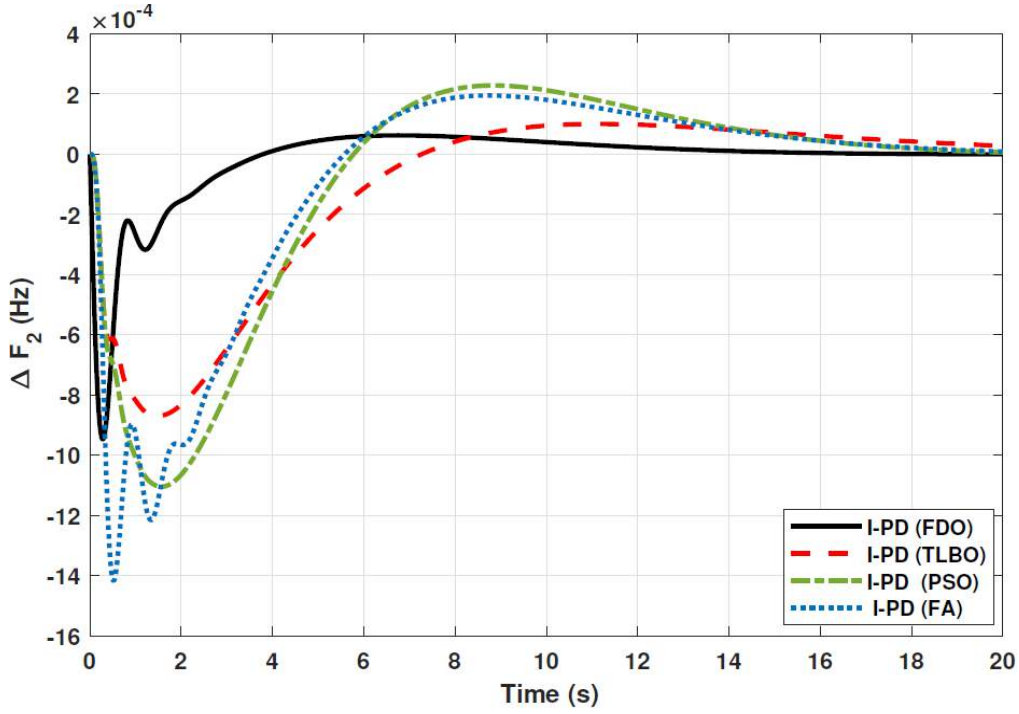

Figure 3.15 Results of reheat thermal unit for ΔF2 with I-PD controller.

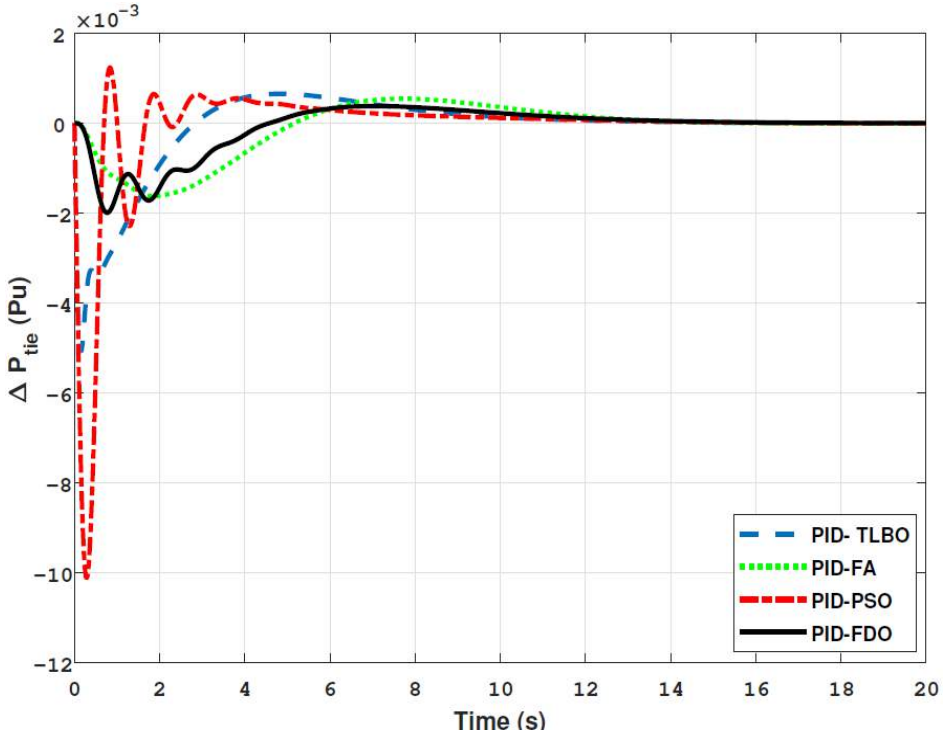

Figure 3.16 Results of reheat thermal unit for ΔPtie with PID controller.

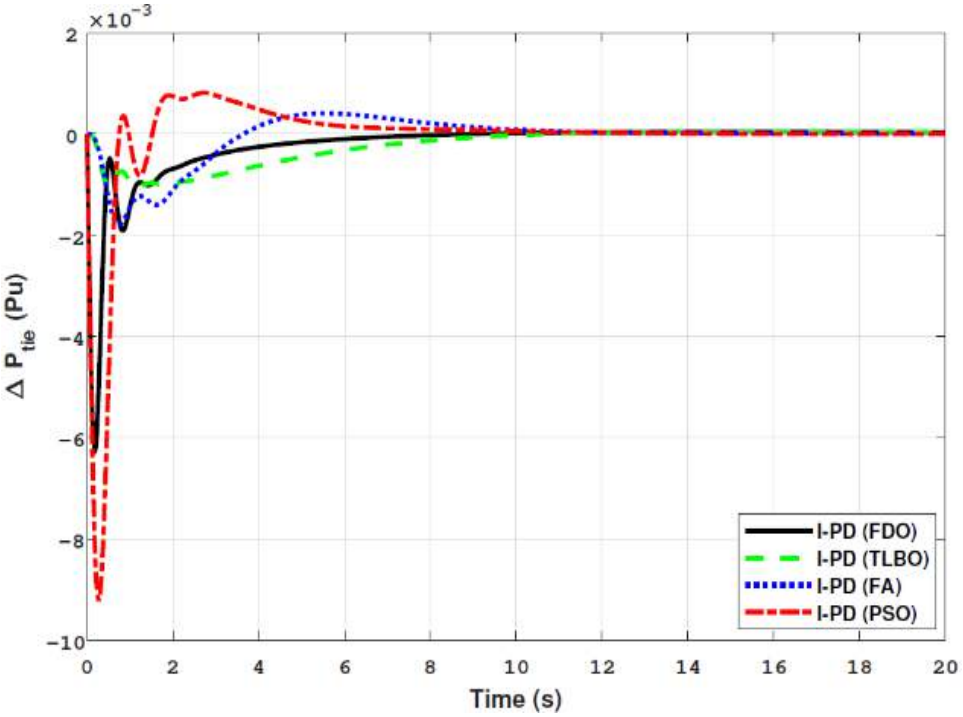

Figure 3.17 Results of reheat thermal unit for ΔPtie with I-PD controller.

Table 3.2 Optimum gains of PID /I-PD controllers for reheat thermal unit.

Controller with different Techniques	Controller gains of reheat thermal unit		
	K_p	K_i	K_d
I-PD-FDO	1.023	1.000	-0.223
I-PD-TLBO	1.305	0.011	-0.435
I-PD –FA	0.450	1.204	0.203
I-PD –PSO	1.006	1.230	-0.067
PID-FDO	1.109	1.460	0.023
PID-TLBO	1.203	1.804	0.045
PID –FA	1.703	1.904	0.293
PID –PSO	1.464	1.984	-0.056

The comparison results from Fig 3.12 and Table 3.3 reveal that the FDO-PID controller eliminates overshoot Osh as compared to PSO, FA, and TLBO based PID controller which is the dire need of a controller for the system stability. Further, settling time (Ts) and undershoot (Ush) yielded by FDO-PID are better than PSO/FA/TLBO based PID controller. The results are depicted in Fig 3.13 further reveal that the FDO-PID controller provides less Osh than PSO-PID however, at the cost of a slight increase in Ts, but better than FA-PID and TLBO-PID. The results are given in Fig 3.14 and 3.15 further shows that the FDO-I-PD controller for both areas 1 and area 2 outperform in terms of Ts, Osh, and Ush which is less than PSO/FA/TLBO base tuned PID controllers. The results shown in Fig 3.16 reveals that FDO-PID has lesser Osh as compared to other controllers at the cost of an increase in settling time for PSO-PID and FA-PID but still better than TLBO-PID. The outcome is given in Fig 3.17 expresses the overall superiority of FDO-I-PD over other controllers in all aspects i.e less Ts, Osh, and Ush. The overall comparison of the results for areas 1 and 2 for the reheat thermal power unit is quantified and presented in Table 3.3.

Table No 3.3 Comparative performance of various techniques for two areas reheat thermal unit.

Techniques	Settling Time Ts (s)			Overshoot Osh			Undershoot Ush		
	ΔF 1	ΔF 2	ΔP tie	ΔF 1	ΔF 2	ΔP tie	ΔF 1	ΔF 2	ΔP tie
FDO-PID	2.9	9.2	10.3	0.00000	0.00250	0.0002	-0.00400	-0.0020	-0.00200
FDO-I-PD	1.9	10.1	4.9	0.00000	0.00012	0.0000	-0.00050	-0.0009	-0.00620
PSO-PID	6.5	9.1	8.4	0.00180	0.01630	0.0016	-0.01000	-0.0069	-0.01010
PSO-I-PD	8.2	14.2	6.2	0.00150	0.00030	0.0093	-0.00680	-0.0013	-0.00910
FA-PID	6.3	10.4	8.7	0.01200	0.00280	0.0008	-0.08400	-0.0170	-0.00500
FA-I-PD	10.9	16.5	9.3	0.00072	0.00025	0.0071	-0.00480	-0.0011	-0.00180
TLBO-PID	6.4	10.2	11.6	0.01300	0.00270	0.0009	-0.06300	-0.0180	-0.00160
TLBO-I-PD	**3.8**	**14.3**	**8.3**	**0.00020**	**0.00310**	**0.0000**	**-0.00460**	**-0.0007**	**-0.01100**

3.3.2 Implementation of Two Area Hydro Power System

The TF model of a two-area hydropower system has been assessed with FDO-PID and FDO-I-PD controllers. The outcomes yielded from the proposed controller are compared with I-PD/PID based other tuning techniques i.e PSO, TLBO, and FA. The results obtained from the two-area hydropower system with I-PD and PID controllers are given in Fig 3.18- Fig 3.23. The best optimal gains value for PID and I-PD controllers for hydro power units are provided in Table 3.4 which is obtained by running each algorithm to 30 times and the best values among each optimization is .picked as optimal parameters of the proposed controller.

Table 3. 4 Optimum gains of PID/ I-PD controllers for hydropower unit.

Controller with different Techniques	Controller gains of hydropower unit		
	K_p	K_i	K_d
I-PD-FDO	1.163	1.962	-0.003
I-PD-TLBO	1.200	1.012	1.001
I-PD –FA	1.962	0.003	0.002
I-PD –PSO	1.012	1.001	1.012
PID-FDO	1.002	1.002	0.001
PID-TLBO	1.013	1.012	0.080
PID –FA	1.110	1.002	-0.103
PID –PSO	1.004	0.119	0.001

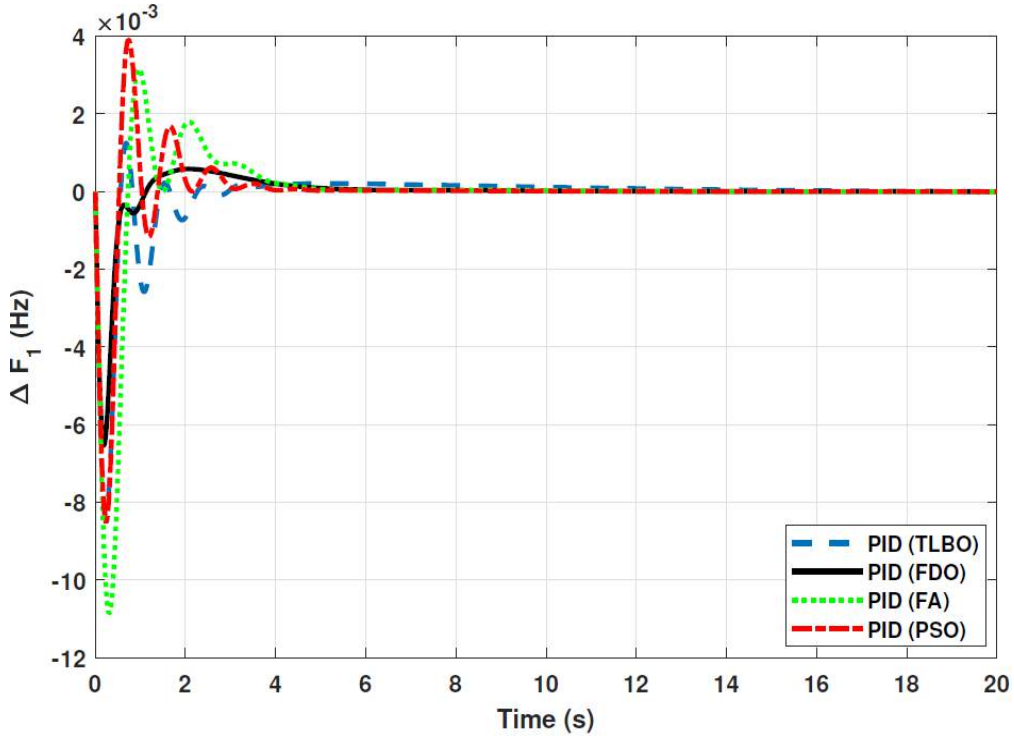

Figure 3.18 Results of hydro unit for ΔF1 with PID controller.

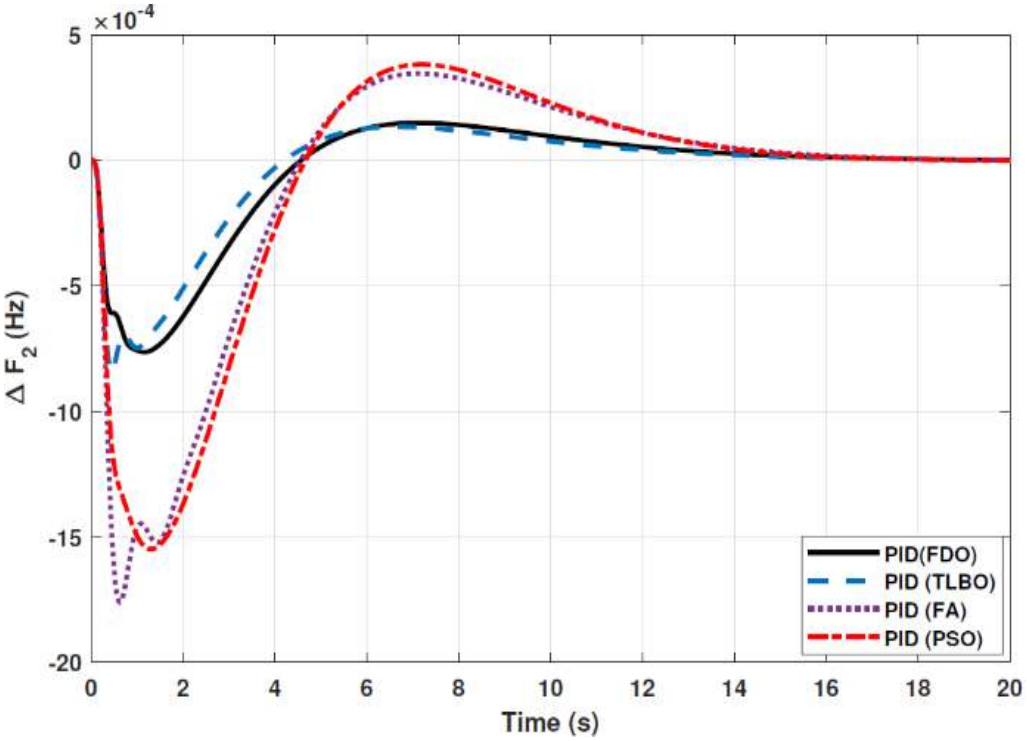

Figure 3.19 Results of hydro unit for ΔF2 with PID controller.

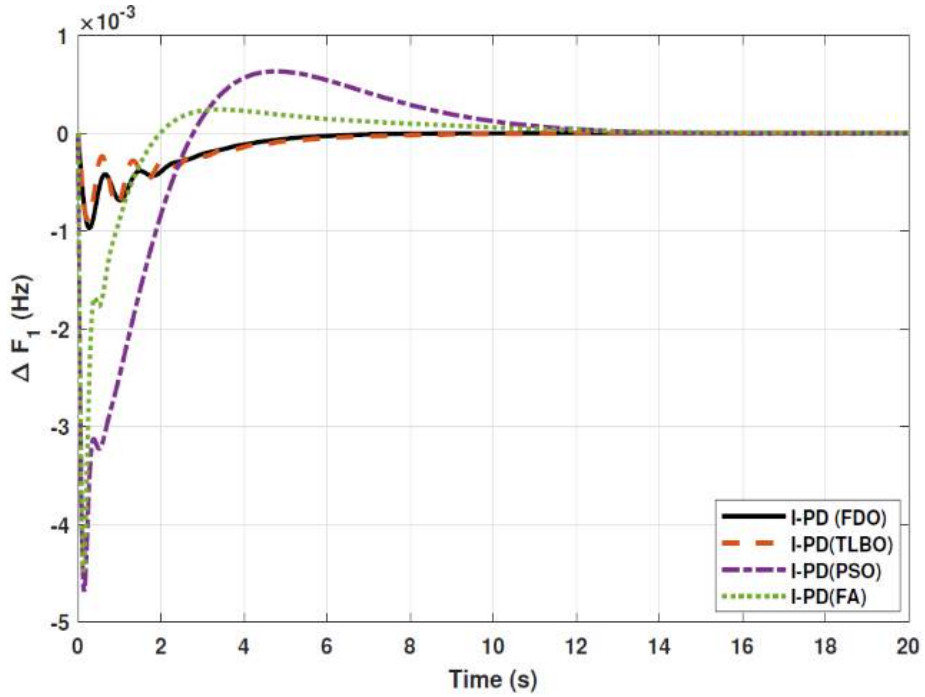

Figure 3.20 Results of hydro unit for ΔF1 with I-PD controller.

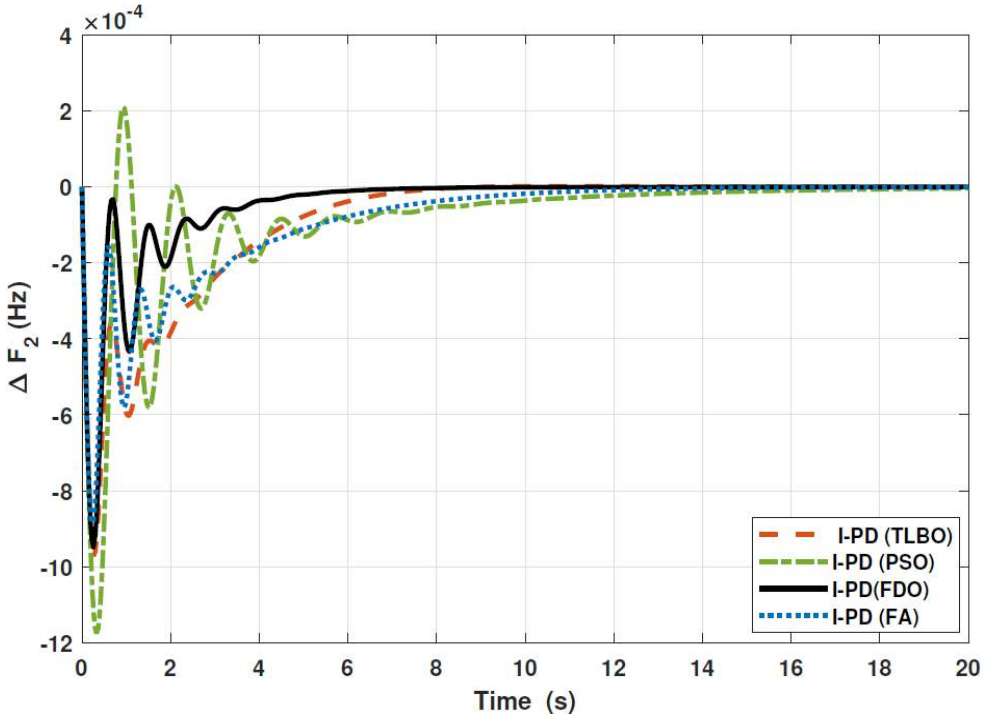

Figure 3.21 Results of hydro unit for ΔF2 with I-PD controller.

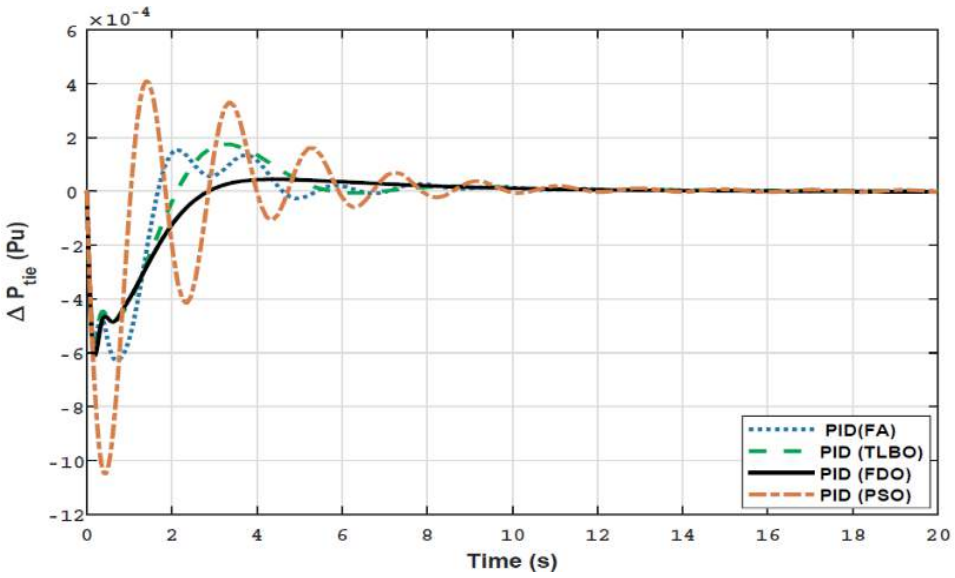

Figure 3.22 Results of hydro unit for ΔPtie with PID controller.

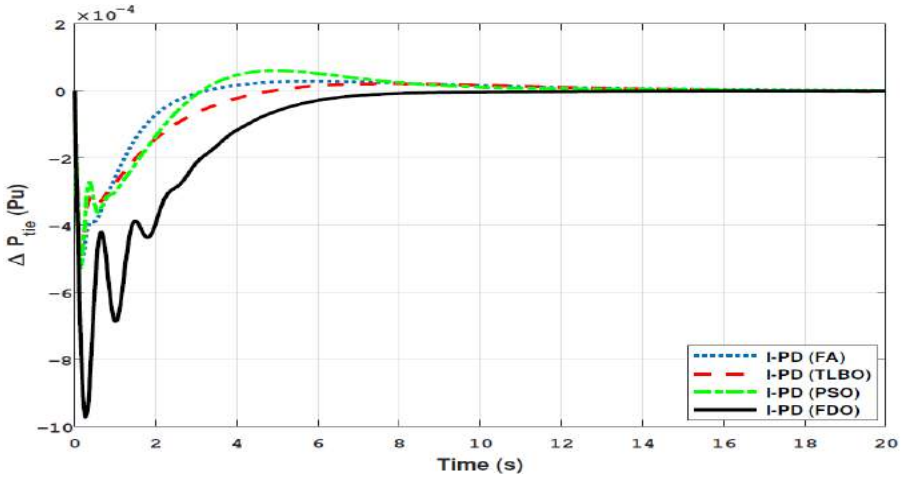

Figure 3.23 Results of hydro unit for ΔPtie with I-PD controller.

The results obtained from the interconnected hydropower system with a PID controller are given in Fig 3.18 which shows the better performance of the FDO-PID controller as compared to the FA/TLBO/PSO based PID controller. The results in Fig 3.19 reflect that FDO-PID provides output response with zero overshoot (Osh = 0.0000) as compared to PSO-PID (Osh = 0.0029), FA-PID (Osh = 0.0019) and TLBO-PID (Osh = 0.0006) controllers. Similarly, the results also express that FDO-PID yields lesser Ush and Ts as compared to a PID controller with other tuning techniques. The results depicted in Fig 3.20

indicate that the FDO-I-PD controller provides excellent results with zero Osh in load frequency of area 1, less settling time, and undershoot as associated with other techniques like PSO, FA, and TLBO with same controllers. The results illustrated in Fig 3.21 express that the FDO base tuned PID controller has less settling time, undershoot, and overshoot than PSO, TLBO, and FA base tuned PID controller. However, a minor change of 0.001 in overshoot can be seen as a PID based controller optimized with the FDO algorithm. From Fig 3.22 it can be seen that the FDO base tuned algorithm has less settling time nonetheless of minor increased in overshoot which is eliminated by FDO based tuned I-PD controller which is indicated in Fig 3.23 but still better than other used techniques in terms of Ts, Osh, and Ush. A comprehensive comparison results for two-area hydropower systems and change in tie-lines in respect of Ts, Osh, and Ush are given in Table 3. 5. The representation of bold values indicates the best results.

Table No 3.5 Comparative performance of various techniques for two area hydropower units.

Techniques	Settling Time (T_s)			Overshoot (O_{sh})			Undershoot (U_{sh})		
	ΔF 1	ΔF 2	ΔP tie	ΔF 1	ΔF 2	ΔP tie	ΔF 1	ΔF 2	ΔP tie
FDO-PID	**2.83**	**2.30**	**3.20**	**0.0000**	**0.0000**	**0.0002**	**-0.00760**	**-0.00430**	**-0.0002**
FDO-I-PD	**2.90**	**5.30**	**4.00**	**0.0000**	**0.0010**	**0.0000**	**-0.00410**	**-0.00190**	**-0.0010**
PSO-PID	7.30	6.40	10.1	0.0029	0.0019	0.0062	-0.0640	-0.00520	-0.0130
PSO-I-PD	6.70	9.80	8.70	0.0060	0.0050	0.0070	-0.0042	-0.00130	-0.0046
FA-PID	4.30	5.60	10.2	0.0019	0.0006	0.0041	-0.0430	-0.00700	-0.0060
FA-I-PD	5.40	10.1	6.80	0.0080	0.0070	0.0040	-0.0093	-0.00150	-0.0043
TLBO-PID	2.40	4.20	4.60	0.0006	0.0005	0.0010	-0.0620	-0.00560	-0.0050
TLBO-I-PD	3.10	6.20	4.40	0.0021	0.0030	0.0000	-0.0042	-0.00170	-0.0090

3.3.3 Implementation of Two Area Gas Power System

The TF model of the two-area gas power system is established in Matlab/Simulink using Appendix (Table 1). The system is assessed with FDO base optimized I-PD/PID controllers to evaluate the achievement of the proposed techniques and their outcomes are

compared with some recent optimization algorithms like TLBO, FA, and PSO. The results obtained from a two-area gas power system for areas 1 and 2 with I-PD and PID controllers are given in Fig 3.24 – 3.29. The best optimal gains value for PID and I-PD controllers for gas generation units are provided in Table 3.6 which is obtained by running each algorithm to 30 times and the best values among each optimization is .picked as optimal parameters of the proposed controller.

Table 3.6 Optimum gains of PID/ I-PD controllers for the gas unit.

Controller with different Techniques	Controller gains of Gas unit		
	K_p	K_i	K_d
I-PD-FDO	0.723	0.112	-1.012
I-PD-TLBO	0.305	0.811	0.029
I-PD –FA	0.405	0.001	0.112
I-PD –PSO	1.060	0.723	0.687
PID-FDO	1.109	0.811	-0.273
PID-TLBO	0.062	1.100	0.458
PID –FA	1..072	1.007	-0.238
PID –PSO	1.061	00.90	0.56

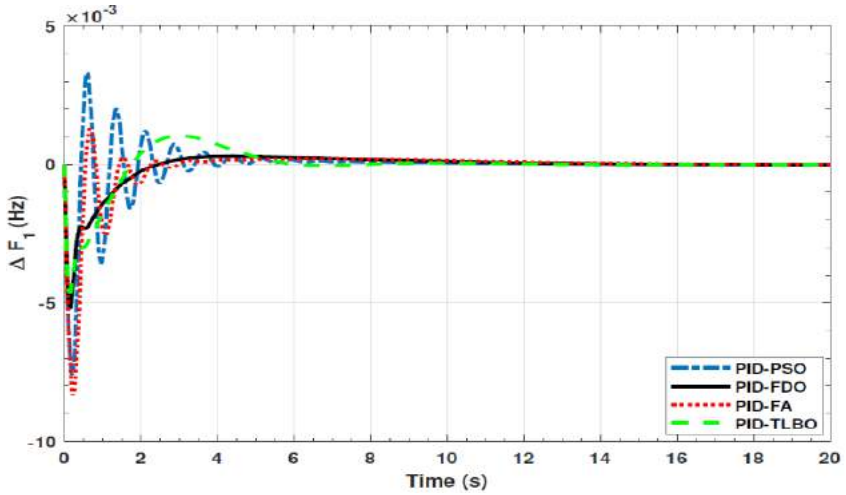

Figure 3.24 Results of the gas power unit for ΔF1 with the PID controller.

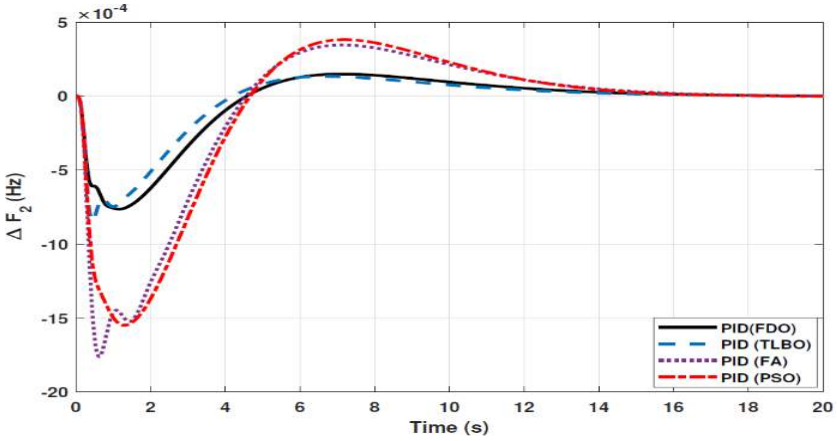

Figure 3.25 Results of the gas power unit for ΔF2 with a PID controller.

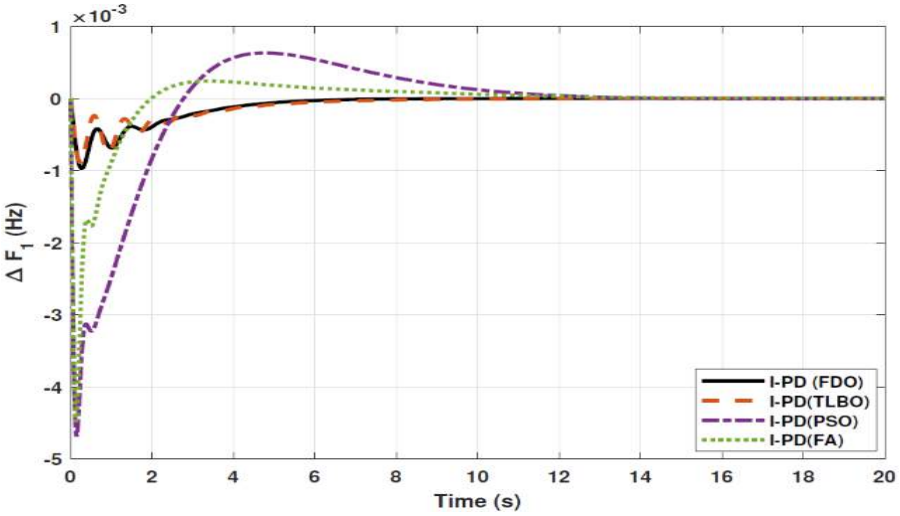

Figure 3.26 Results of the gas power unit for ΔF1 with the I-PD controller.

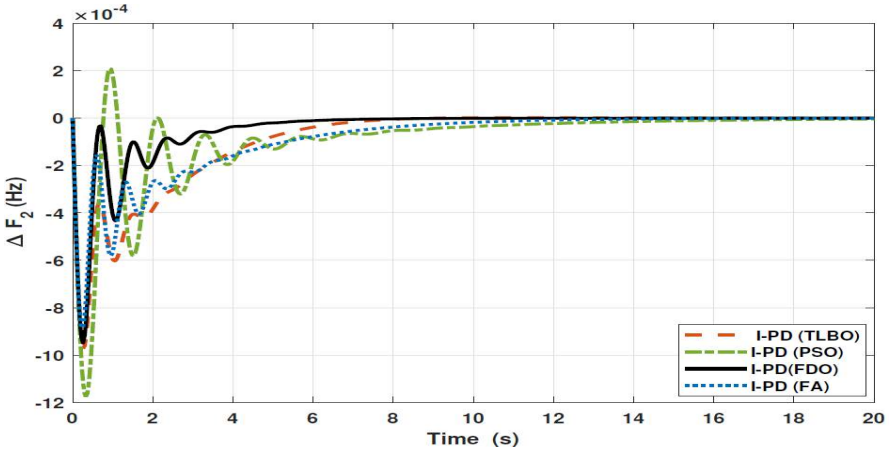

Figure 3.27 Results of the gas power unit for ΔF2 with the I-PD controller.

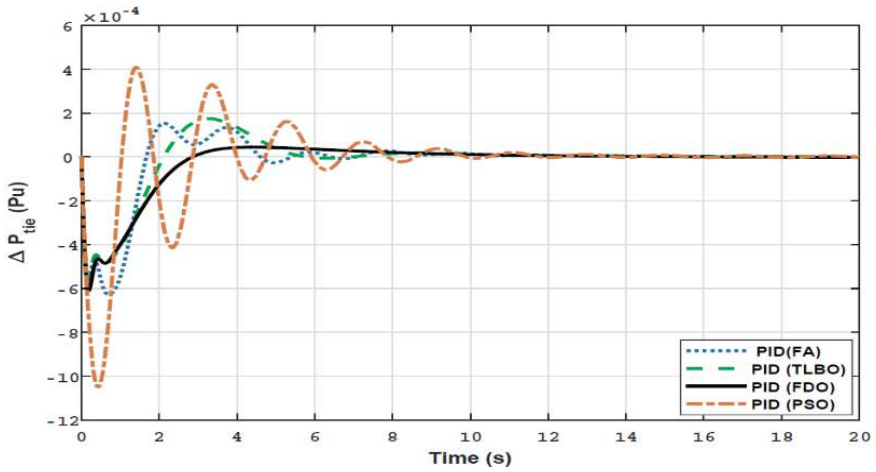

Figure 3.28 Results of the gas power unit for ΔPtie with PID controller.

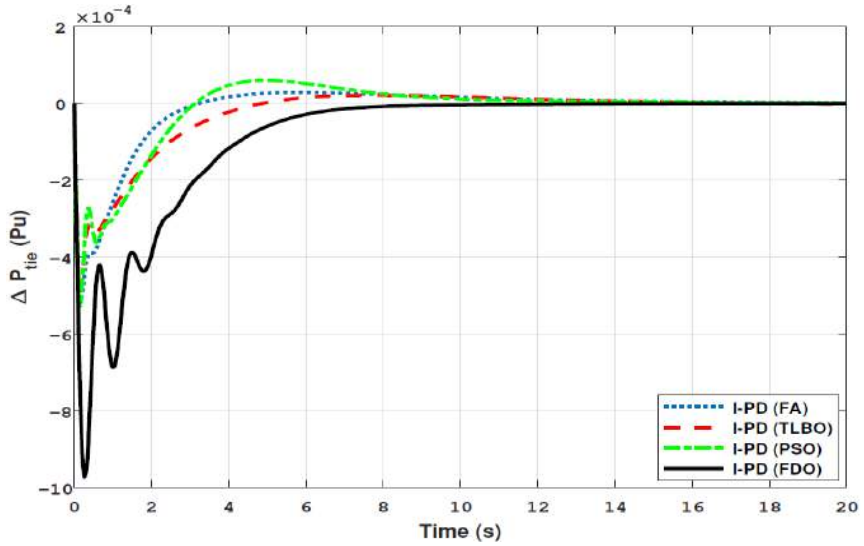

Figure 3.29 Results of the gas power unit for ΔPtie with the I-PD controller.

In Fig 3.24 the results reveal that FDO base PID controller completely eliminate the overshoot (Osh = 0.000), less settling time (Ts = 2.1) and undershoot (Ush = −0.0048) as compared to PSO (Osh = 0.0036, Ts = 5.9s, Ush = −0.0072), FA (Osh = 0.021, Ts = 3.9s, Ush = −0.0083), and TLBO (Osh = 0.019, Ts = 5.2s, Ush = 0.0049) base PID controller. The results depicted in Fig 3.25 express that the FDO base tuned PID controller have a similar settling time and overshoot but less undershoot than the TLBO base tuned PID controller, nonetheless better than remaining techniques i.e. FA and PSO. The results are given in Fig 3.26 and 3.27 indicates that the FDO base tuned I-PD controller for change

in frequency with area 1 and area 2 have good performance in terms of Ts, Osh, and Ush which is less than PSO/FA/TLBO base tuned PID controllers. In an inclusive comparison of the results for areas 1 and 2 of the gas power system in settling time, overshoot, undershoot, and different performance indices are given in table 3.7. The outcome is shown in Fig 3. 28 articulates that the FDO base tuned PID controller for change in tie-line power has better results in all aspects i.e T_S, Osh, and Ush from other applied techniques with the same controller. From Fig 3.29 it can be observed that the FDO base optimized I-PD controller has a better result than the same controller tuned with PSO/FA/TLBO in terms of lesser Osh, TS and USh. The best results are indicated with bold formats.

Table 3.7 Comparative performance of various techniques for two area gas power unit.

Techniques	**Settling Time** T_s			**Overshoot** O_{sh}			**Undershoot** U_{sh}		
	ΔF_1	ΔF_2	ΔP_{tie}	ΔF_1	ΔF_2	ΔP_{tie}	ΔF_1	ΔF_2	ΔP_{tie}
FDO-PID	**2.1**	**10.2**	**3.1**	**0.00000**	**0.00013**	**0.00003**	**0.00730**	**-0.00720**	**-0.00059**
FDO-I-PD	**4.0**	**3.9**	**5.2**	**0.00000**	**0.00000**	**0.00000**	**-0.00100**	**-0.00084**	**-0.00047**
PSO-PID	5.9	12.4	10.4	0.0360	0.0039	0.00040	-0.00480	-0.00160	-0.00110
PSO-I-PD	8.7	9.6	5.9	0.0073	0.0020	0.00930	-0.00460	-0.00019	-0.00054
FA-PID	3.9	12.3	7.9	0.0021	0.0032	0.00016	-0.00490	-0.00170	-0.00064
FA-I-PD	6.8	9.2	6.3	0.0049	0.0000	0.00021	-0.00430	-0.00082	-0.00052
TLBO-PID	5.2	10.2	6.8	0.0100	0.0001	0.00017	-0.00830	-0.00080	-0.00061
TLBO-I-PD	4.4	5.9	10.1	0.0000	0.0000	0.00000	-0.00900	-0.00089	-0.00096

3.3.4 Implementation of Two Area Multi-Source Power System

The two-area multi-source interconnected power systems have been developed in Matlab/ Simulink and the values have been used from Appendix (Table 1). The system is assessed with FDO base tuned I-PD/ PID controllers and the superiority of the proposed techniques are compared with other techniques i.e TLBO, FA, and PSO. The results are depicted in Fig 3.30 – Fig 3.35.

Table 3.8 Optimum gains of PID/ I-PD controllers for the multi-source unit.

Controller Techniques	Gains of thermal unit			Gains of hydro power unit			Gains of gas power unit		
	K_p	K_i	K_d	K_p	K_i	K_d	K_p	Ki	K_d
PID-PSO	0.013	0.910	0.123	1.96	1.000	0.011	0.32	1.000	0.110
PID-FA	0.335	0.021	0.245	1.60	1.202	0.009	0.30	1.202	0.121
PID-TLBO	0.230	0.004	-0.023	1.20	1.321	0.102	0.40	1.321	0.104
PID-FDO	1.06	0.030	0.687	0.47	0.232	-0.120	1.06	0.232	0.130
I-PD (PSO)	1.209	0.360	-0.273	1.63	1.012	1.001	1.10	1.012	0.060
I-PD (FA)	0.109	0.914	0.458	1.16	1.962	-0.033	0.06	1.962	0.014
I-PD (TLBO)	1.703	1.094	-0.238	1.20	1.012	1.011	0.07	1.012	1.104
I-PD (FDO)	1.464	0.234	0.56	1.30	1.100	0.001	0.06	1.100	0.004

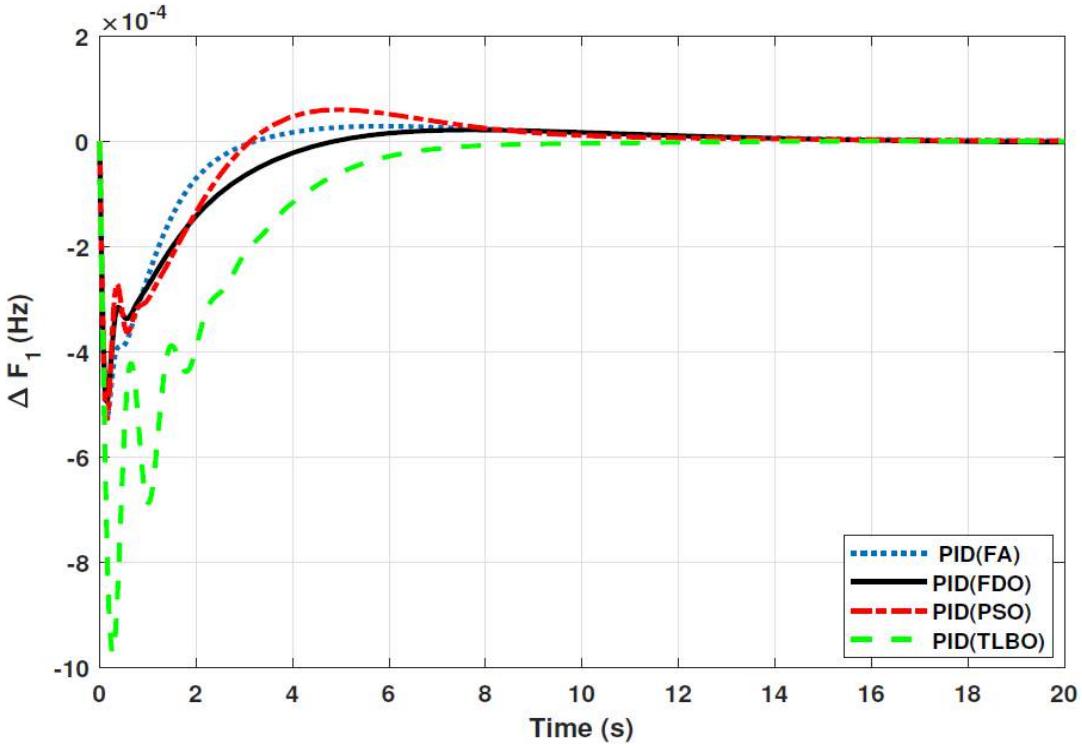

Figure 3.30 Results for multi-source in area 1 with PID controller.

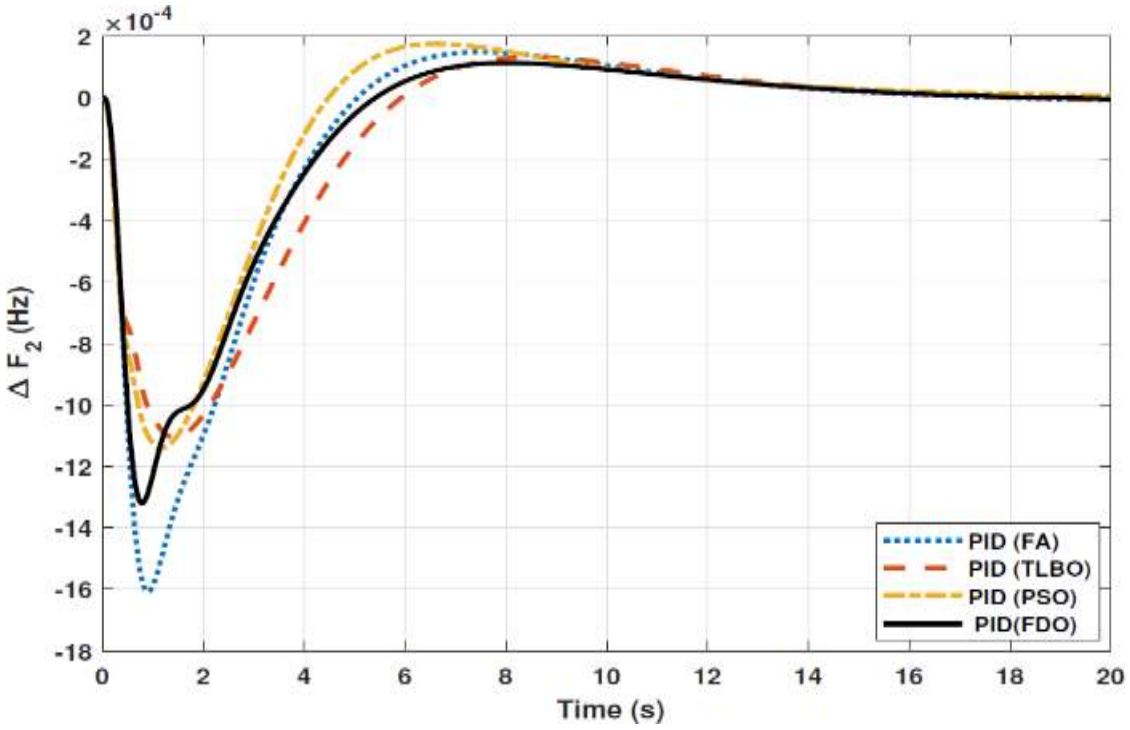

Figure 3.31 Results for multi-source in area 2 with PID controller.

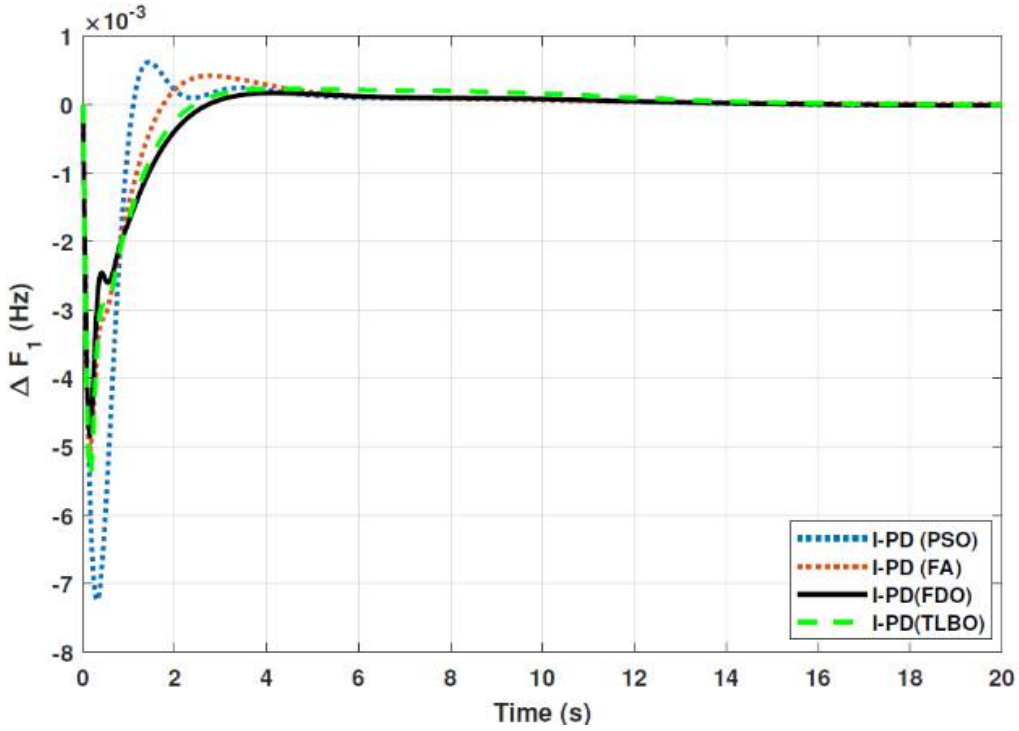

Figure 3.32 Results for multi-source in area 1 with I-PD controller.

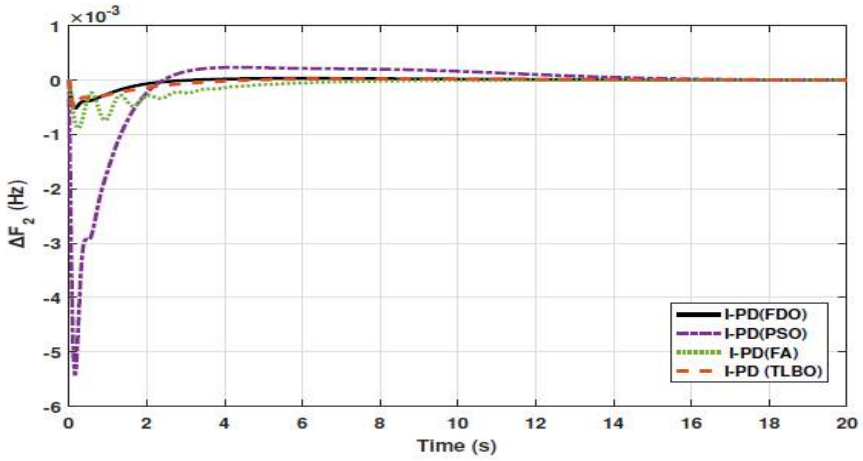

Figure 3.33 Results for multi-source in area 2 with I-PD controller.

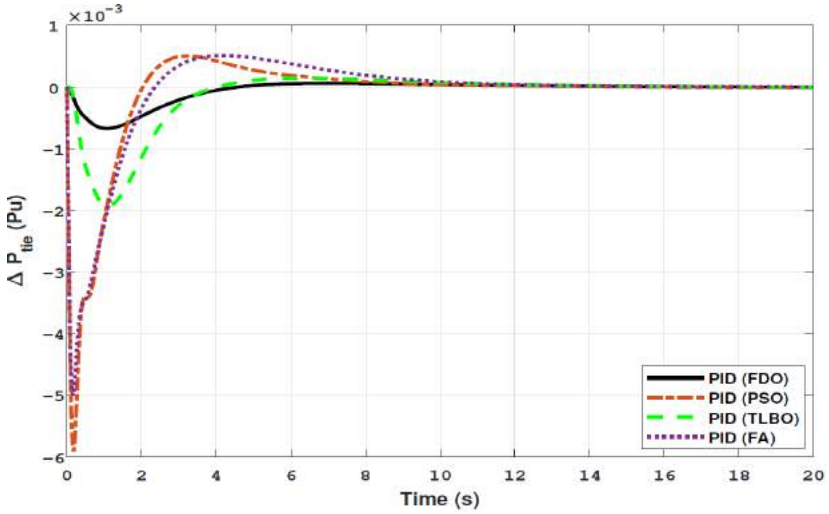

Figure 3.34 Results for multi-source of tie-line power with PID controller.

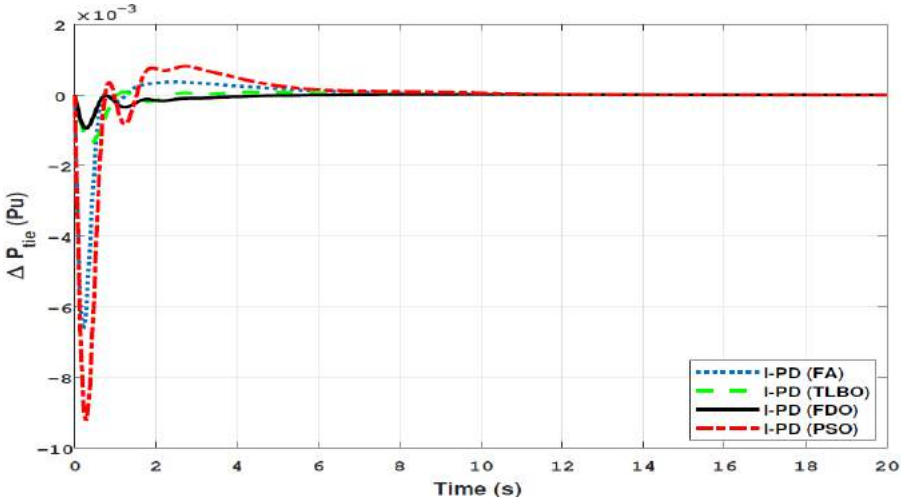

Figure 3.35 Results for multi-source of tie-line power with I-PD controller.

The results shown in Fig 3.30 for the multi-source interconnected power system of area 1 reveals that the PID controller with the FDO base algorithm has no overshoot, less settling time, and undershoot as associated with other techniques like PSO, TLBO, and FA. The results depicted in Fig 3.31 express that the FDO base tuned PID controller has less overshoot and settling time than the TLBO and FA base tuned PID controller however at the cost of 0.001 increase in undershoot but shows better improvement than PSO base tuned PID controller. The results shown in Fig 3.32 express that FDO-PID has less settling time Ts, undershoot Ush and overshoot Osh than PSO-PID, TLBO-PID, and FA-PID. However, a minor change of 0.001 in Osh can be seen as FDO-PID. The results given in Fig 3.33 indicate that the FDO-I-PD technique for change in frequency of area 2 has no overshoot, less settling time, and undershoot as compared with other techniques like PSO/ FA/TLBO with I-PD controller. The results are given in Fig 3.34 and 3.35 reflect that FDO-I-PD for change in tie-line power has good performance in terms of Ts, Osh, and Ush which is less than PSO/FA/TLBO base optimized PID/I-PD controllers. A comprehensive comparison results for two-area multi-source power systems and tie lines in terms of Ts, Osh, and Ush are given in Table 3.9 and the percentage improving comparing with different techniques is shown in the bar chart of Figure 3.36. The representation of bold values indicates the best results.

TABLE 3.9. Comparative performance between different algorithms for two areas multi-source power system.

Techniques	Settling time T_s			Overshoot O_{sh}			Undershoot U_{sh}		
	ΔF_1	ΔF_2	ΔP_{tie}	ΔF_1	ΔF_2	ΔP_{tie}	ΔF_1	ΔF_2	ΔP_{tie}
FDO-PID	**5.20**	**12.70**	**4.30**	**0.00000**	**0.00021**	**0.00020**	**-0.00047**	**-0.00130**	**-0.00056**
FDO-I-PD	**2.30**	**1.65**	**2.10**	**0.00000**	**0.00000**	**0.00000**	**-0.00450**	**-0.00500**	**-0.00058**
PSO-PID	5.90	13.40	9.30	0.00930	0.00250	0.00630	-0.00054	-0.00016	-0.00580
PSO-I-PD	2.90	9.20	6.80	0.00400	0.00400	0.00080	-0.00720	-0.05500	-0.00910
FA-PID	6.30	13.10	7.10	0.00021	0.00036	0.00610	-0.00052	-0.00110	-0.00510
FA-I-PD	4.30	4.10	5.90	0.00000	0.00000	0.00043	-0.00490	-0.00900	-0.00640
TLBO-PID	9.37	3.76	4.76	0.00172	0.00043	0.00017	-0.01972	-0.01279	-0.00307
TLBO-I-PD	2.20	2.20	2.20	0.00000	0.00000	0.00011	-0.00530	-0.00500	-0.00130
LUS-TLBO Fuzzy-PID [28]	5.26	2.96	2.36	0.00055	0.00021	0.00008	-0.00895	-0.00301	-0.00096
DE-PID [27]	13.84	8.35	9.35	0.00203	0.00077	0.00019	-0.02657	-0.02214	-0.00475

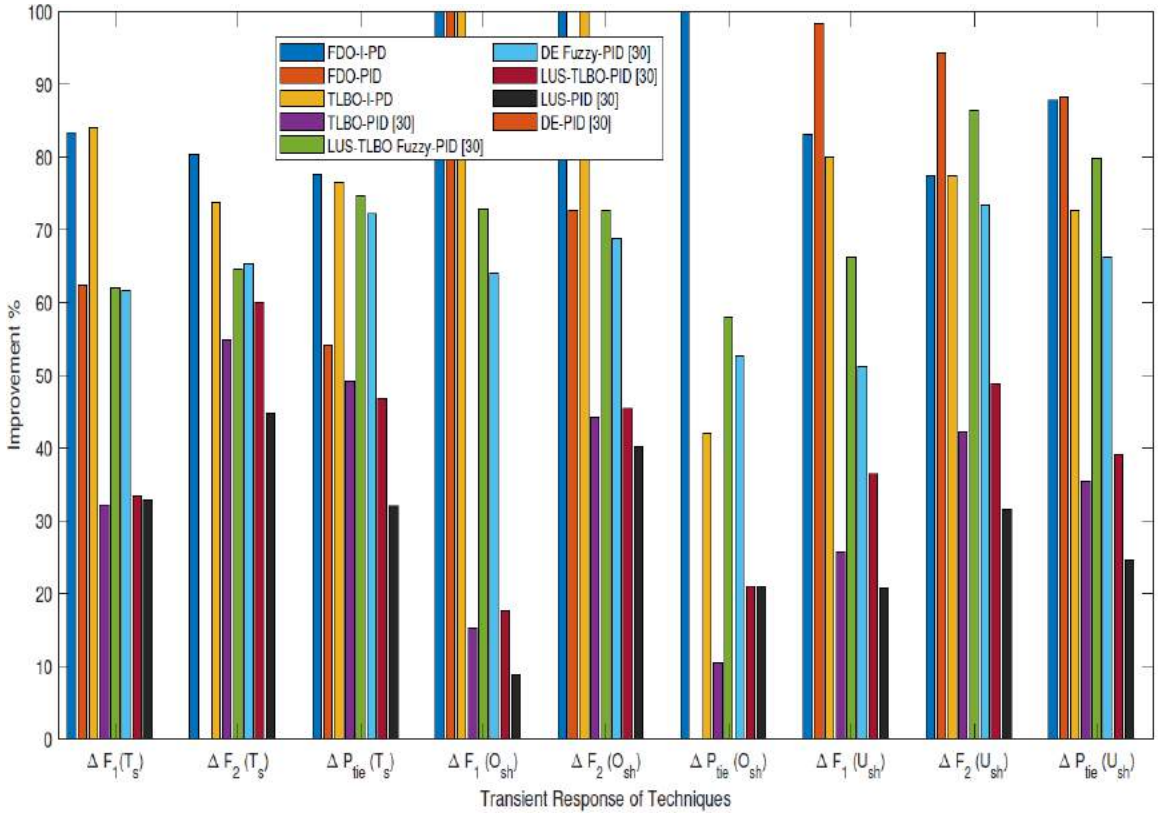

Figure 3.36 Percentage comparison in terms of TS, Osh and Ush.

Chapter 4. AGC of Power System Model Incorporated with Non-linearity

A physical system is composed of several components that are interconnected and perform a specific task. Practically, it is difficult to identify all the components of the physical system. In this dissertation, we have attempted to consider all the probable non-linearities such as Generation Rate Constraint (GRC), Governor Dead Zone (GDZ), Time Delay (TD), and Boiler Dynamics (BD) which make the system model more practical which are described as below:

4.1 Generation Rate Constraint (GRC)

In the real world, electrical power plants can not too hastily adjust their power outputs due to the limitations of mechanical and thermal movements called is GRC. GRC is specified in percentage of generator output per unit time. This constraint is due to the limitation of the turbine concerning the rate of change in a generation. Its main effect is on the performance of the power unit due to its characteristic of non-linear behavior. GRC impacts must be incorporated into a realistic AGC study. Under GRC's non-appearance, generators are forced to chase huge provisional disturbance that may turn network generation into instability. The time response of the system with GRC indicates greater overshoots and higher time settling relative to the GRC-free system. Further, if the controller gain is not optimized appropriately, the power system may get unstable in the occurrence of GRC. Larger thermal heat generators have relatively low GRCs of about ±3 percent per minute and typically GRCs are used for gas units of ±20 percent per minute. For hydro units, higher GRC values of +270 percent per minute, i.e. 4.5 percent / s for

generation increase and 360 percent per minute, i.e. 6 percent / s for generation decrease, are considered [112], [113], [114].

4.2 Governor Dead Band (GDB)

The GDB or dead zone (DZ) non-linearity is another major concern in power system performance. The speed governor responds not instantly until the input meets a certain value by adjusting the input signal. The GDB is defined as the total quantity of a continuous speed variation within the governor where the valve point of the turbine does not change. For larger steam turbines the typical values of GDB are 0.06%. As the system oscillates, GDB greatly affects the dynamic of the AGC system. The GDB's output of AGC regulator has been studied [115], [116] and different AGC strategies are applied in restructured power systems [117], [118], [119]. The transfer function model for GDB is given below [119].

$$G(s) = N_1 + SN_2 \tag{4.1}$$

Where $N_1 = 0.8$ and $N_2 = -\frac{0.2}{\pi}$ so Eq (4.1) becomes

$$G(s) = 0.8 - S\frac{0.2}{\pi} \tag{4.2}$$

4.3 Boiler Dynamic (BD)

The boiler is used to create pressure steam. It receives preheated feed water from the economizer and produces saturated steam. Recirculation boilers are called drum form boilers which isolate the steam from the recirculation of water. Turbine control valves begin the change in generation and the boiler controls react with a critical steering motion, changes in the flux of steam, and changes in the throttle compression, the burning rate, and

thus the boiler output. To start long-term fuel and steam flow dynamics at drum-type boiler pressure and its dynamics are built into thermal units [120], [121], [122],[123]. The blocked diagram of the drum-type boiler is given in Fig 4.1. The parameters of the value for BD are taken from and are given in the Appendix (Table 1).

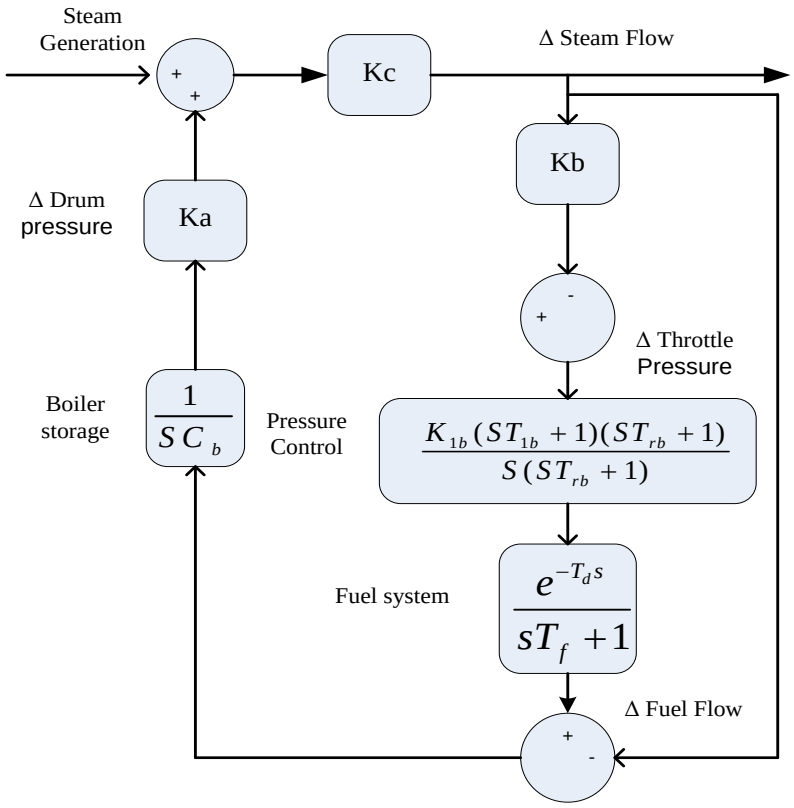

Figure 4.1 TF model of drum-type boiler.

4.4 Time Delay (TD)

The time delay (TD) in the electrical generation unit is due to delays in filters, signal processing units, and communication channels (CCs). The TD in the AGC is largely maintained by the CCs between the operating stations and the control center; particularly on the prescribed frequency and connecting power line from remote terminal units (RTUs) towards the control region and the delay up / down signal from the control center towards each generation unit. The time delay related to AGC can affect the performance of the

system if it is not addressed properly. However, in certain cases, it may interrupt the stability of the system [124], [125], [126]. In this work, we have considered the time delay for the AGC problem is 2 sec, which is used more practically.

To show the potency of the proposed I-PD/PID controllers with FDO techniques the two area multi-source IPS with several non-linearities have been tested in which two cases are deliberated.

4.5 Case (a): System model with considering two non-linearities GRC and GDB

In the first case, the linear system model with multi-source generation including reheat thermal, gas, and hydropower unit are used with the addition of two non-linearities i.e. GRC and GDB. The said model has been developed in Matlab/Simulink and the values have been used from Appendix (Table 1). Further, the efficacy of the proposed approach has been assessed with FDO tuned PID/I-PD controller to show. The outcomes are shown in Fig 4.2 – 4.7 and the comparative transient time response of the system with different algorithms is presented in Table 4.1.

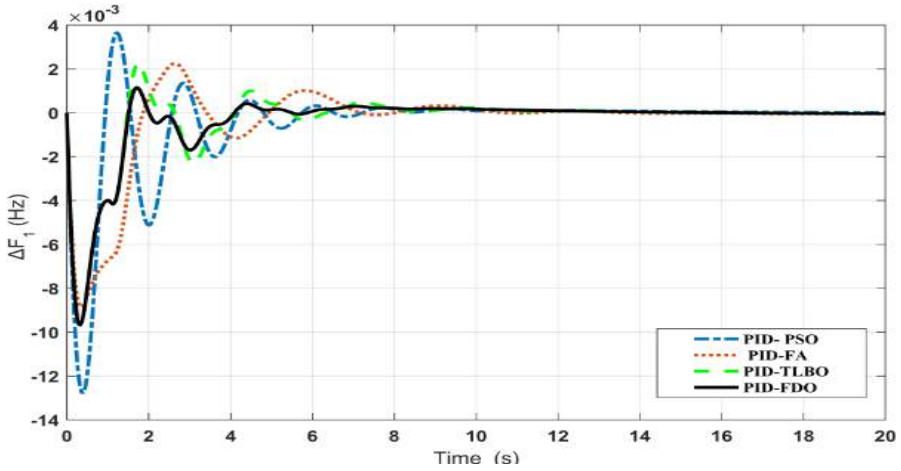

Figure 4.2 Results of multi-source with GDB and GRC for ΔF1 with a PID controller.

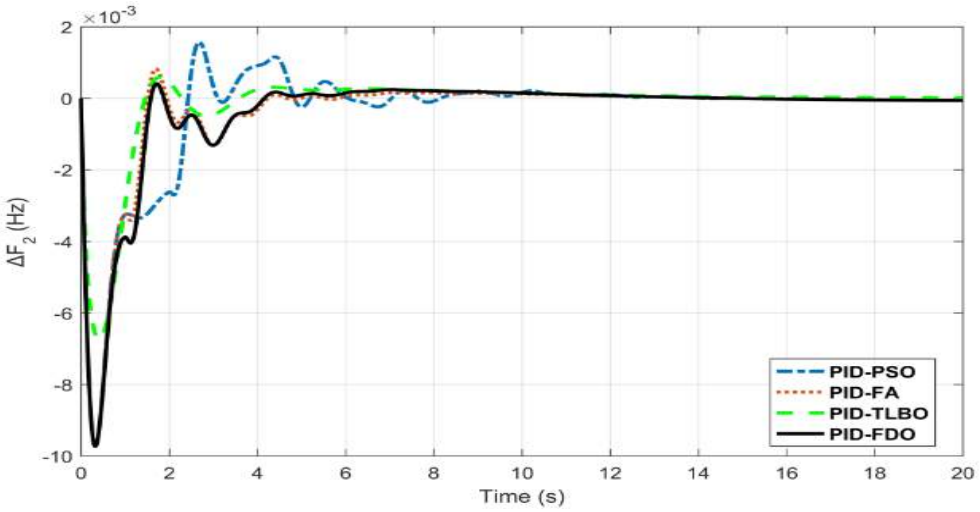

Figure 4.3 Results of multi-source with GDB and GRC for ΔF2 with PID controller.

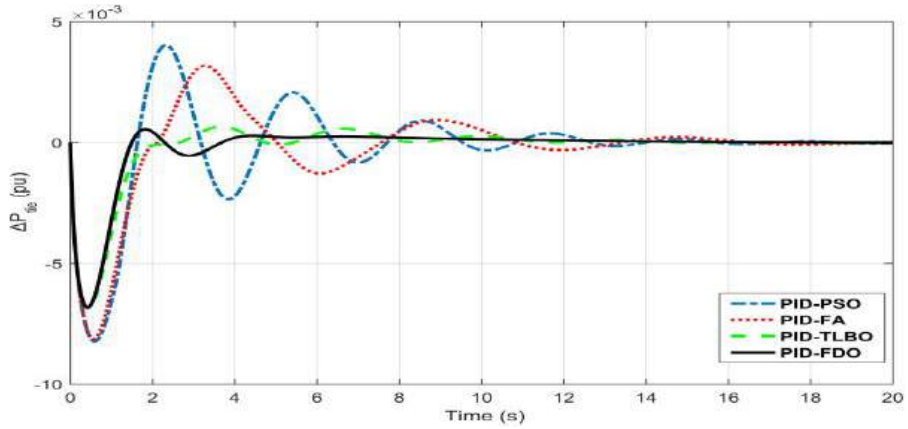

Figure 4.4 Results of multi-source with GDB and GRC for ΔPtie with PID controller.

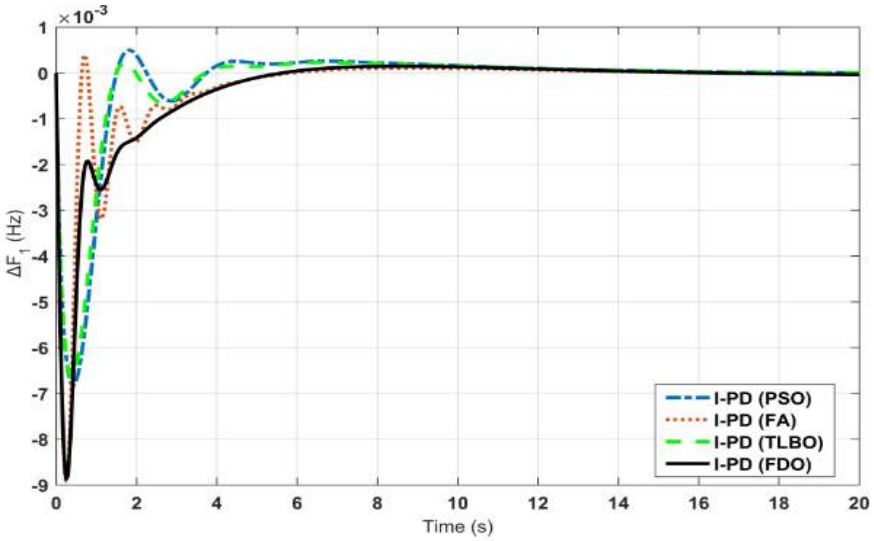

Figure 4.5 Results of multi-source with GDB and GRC for ΔF1 with I-PD controller.

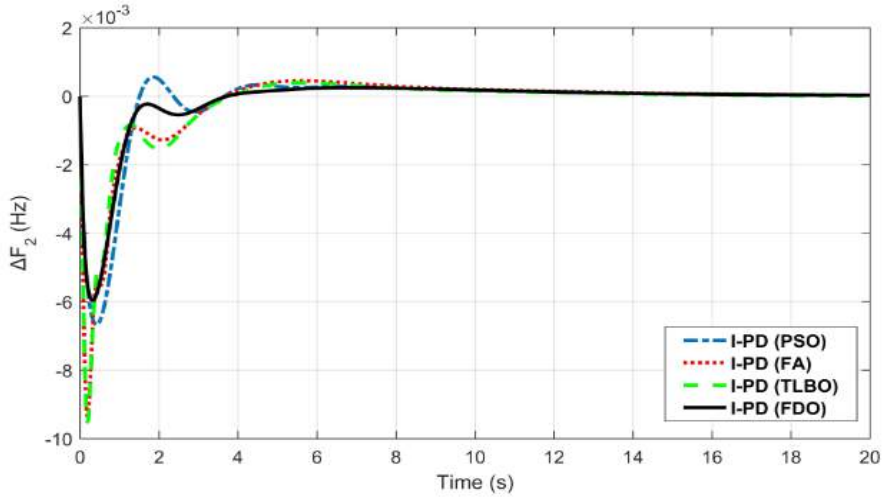

Figure 4.6 Results of multi-source with GDB and GRC for ΔF2 with I-PD controller.

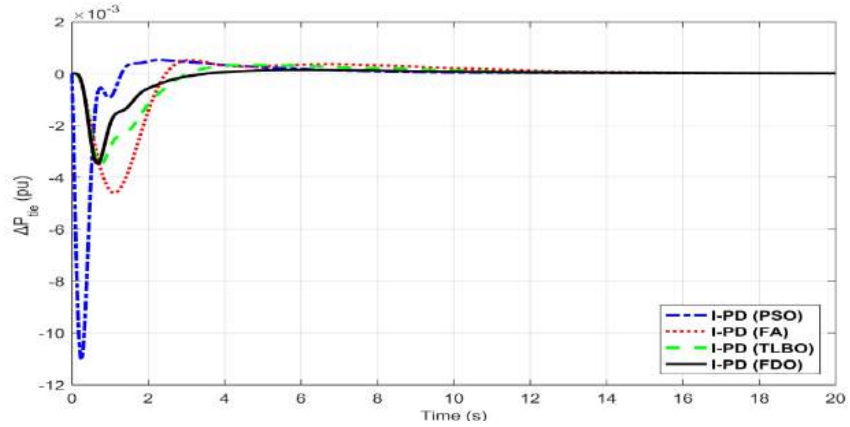

Figure 4.7 Results of multi-source with GDB and GRC for ΔPtie with I-PD controller.

Table 4.1 Performance of multi-source with two area including two non-linearities (GRC and GDB)

Techniques	**Settling time (Ts)**			**Overshoot (O_{sh})**			**Undershoot (U_{sh})**		
	ΔF_1	ΔF_2	ΔP_{tie}	ΔF_1	ΔF_2	ΔP_{tie}	ΔF_1	ΔF_2	ΔPt_{ie}
FDO-PID	**10.9**	**11.1**	**13.2**	**0.00115**	**0.000409**	**0.000554**	**-0.00968**	**-0.00972**	**-0.00682**
TLBO-PID	11.3	12.2	14.1	0.00224	0.000593	0.000660	-0.00968	-0.00673	-0.00686
FA-PID	11.9	11.1	16.2	0.00225	0.000823	0.00103	-0.00885	-0.00973	-0.00813
PSO-PID	11.1	12.9	17.1	0.00364	0.00107	0.00119	-0.0128	-0.00973	-0.00824
PSO-I-PD	13.3	12.8	7.9	0.000495	0.000559	0.000526	-0.00682	-0.00667	-0.01103
FA-I-PD	11.6	13.4	10.2	0.000393	0.000451	0.000518	-0.00891	-0.00934	-0.00460
TLBO-I-PD	13.1	11.4	9.3	0.000226	0.000391	0.000139	-0.00665	-0.00951	-0.00348

From Table 4.1 it can be observed that the FDO-PID controller outperforms in respect of settling time which shows the percentage improvement of 1.80%, 13.96%, and 22.80% for ΔF1, ΔF2, and ΔPtie respectively as compared to PSO-PID. Similarly, a significant percentage improvement can be seen as compared to PSO-PID in terms of overshoot by (68.40%, 61.77%, and 86.25%) and undershoot by (24.37%, 0.102%, and 16.11%) for ΔF1, ΔF2, and ΔPtie respectively. Furthermore, the results obtained from Fig 4.2- Fig 4.4 also reveal that the FDO-PID controller has the best performance in terms of Ts, Osh, and Ush as compared to FA-PID and TLBO-PID. The results are shown in Fig 4.5- Fig 4.7 disclose that FDO-IPD outperforms in terms of settling time and undershoot but, it also shows tremendous performance in term of overshoot as compared to other techniques such as PID/IPD-PSO, PID/I-PD-FA, and PID/I-PD -TLBO for an identical power system. FDO-I-PD controller shows percentage improvement in terms of Ts by (9.01%, 11.62%, and 45.61%), Osh by (93.79%, 96.55%, and 63.45%), and Ush by (48.04%, 2.26%, and 57.19%) as compared to PSO-PID for ΔF1, ΔF2, and ΔPtie respectively. Similarly, FDO-I-PD controller also shows best results as compared to PID-FA controller in respect of settling time by (15.70 %, 2.13%, and 42.59%), overshoot by (89.95%, 52.49%, and 95.64%) and undershoot by (24.85%, 2.26%, and 57.19%) for variation in Area 1, Area 2 and tie-line power respectively.

4.6 Case (b): System model with considering various non-linearities GRC, TD, BD and GDB.

In case (b) various nonlinearities like GRC, TD, BD, and GDB have been considered for the same generation sources to model the system more practical and evaluate

the effectiveness of the proposed approach. The TF model of multi-source IPS with various nonlinearities has been depicted in Fig 4.8 and their outcomes are given in Fig 4.9- Fig 4.14. The comparative performance between different techniques is quantified in Table 4.2

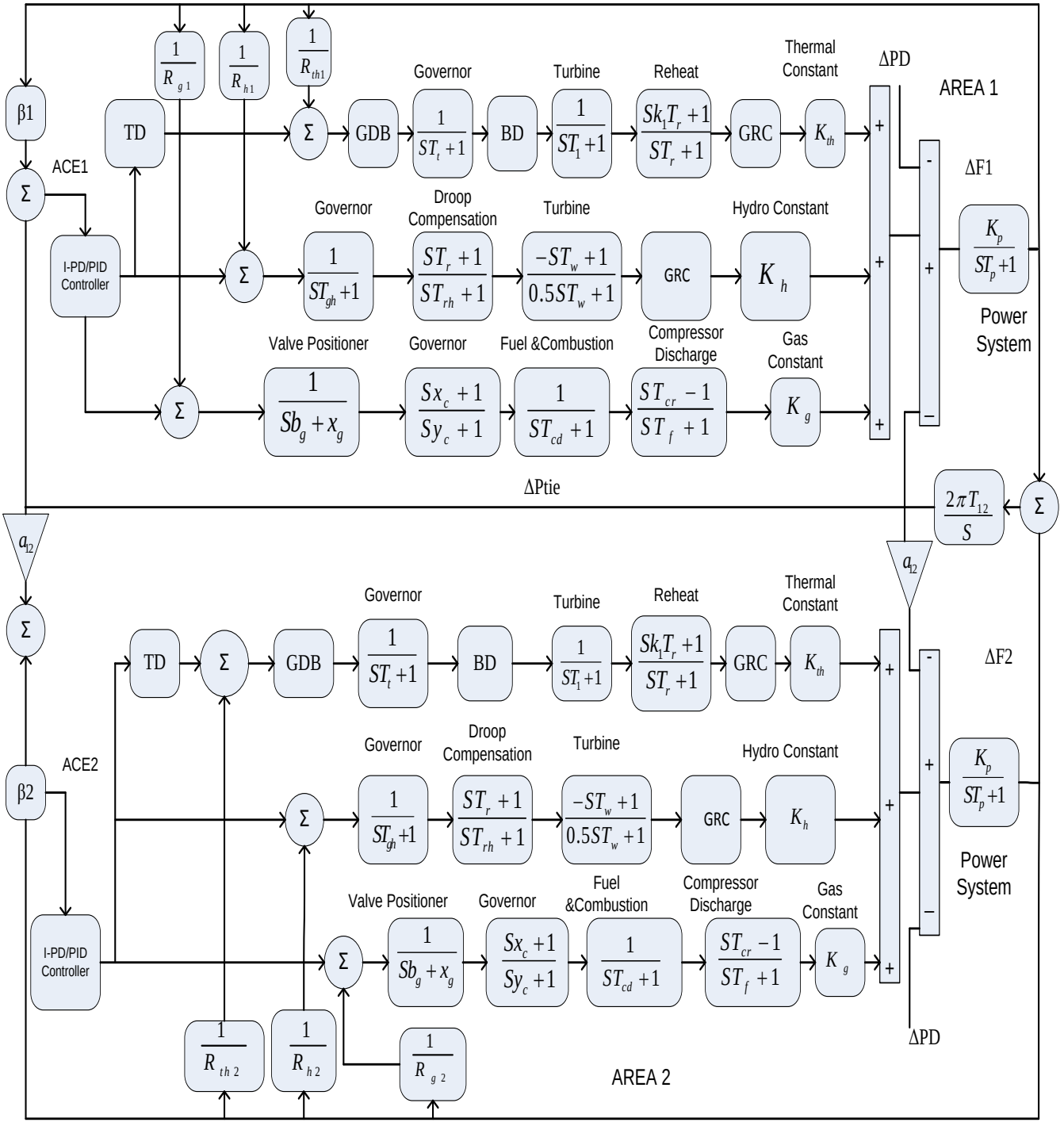

Figure 4.8 Multi-source interconnected power system with GRC, TD, BD and GDB.

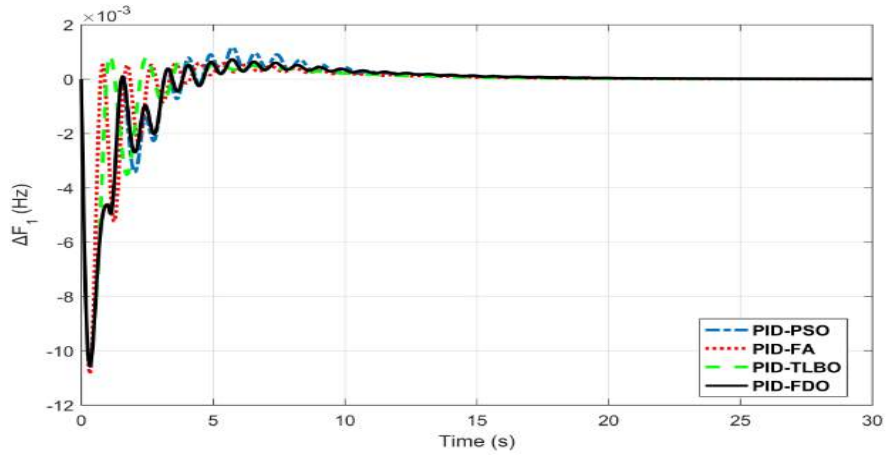

Figure 4.9 Results of a multi-source with GDB, TD, BD, and GRC for ΔF1 with PID controller.

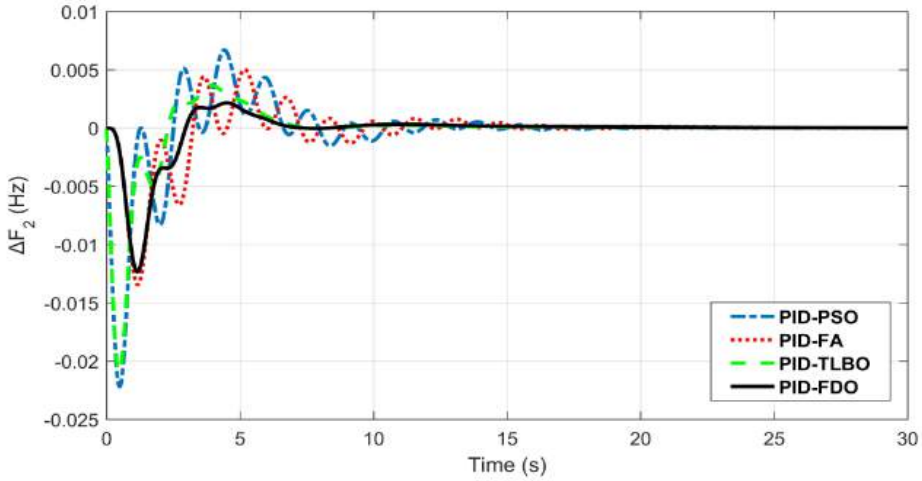

Figure 4.10 Results of a multi-source with GDB, TD, BD, and GRC for ΔF2 with PID controller.

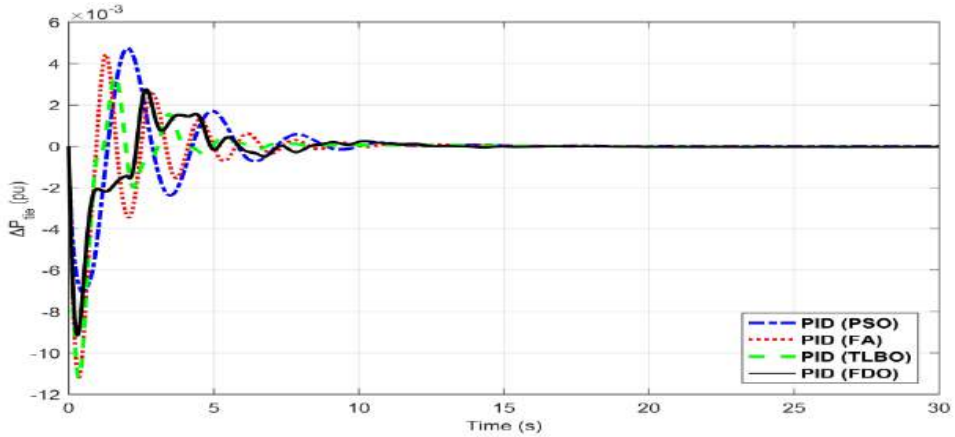

Figure 4.11 Results of multi-source with GDB, TD, BD, and GRC for ΔPtie with PID controller.

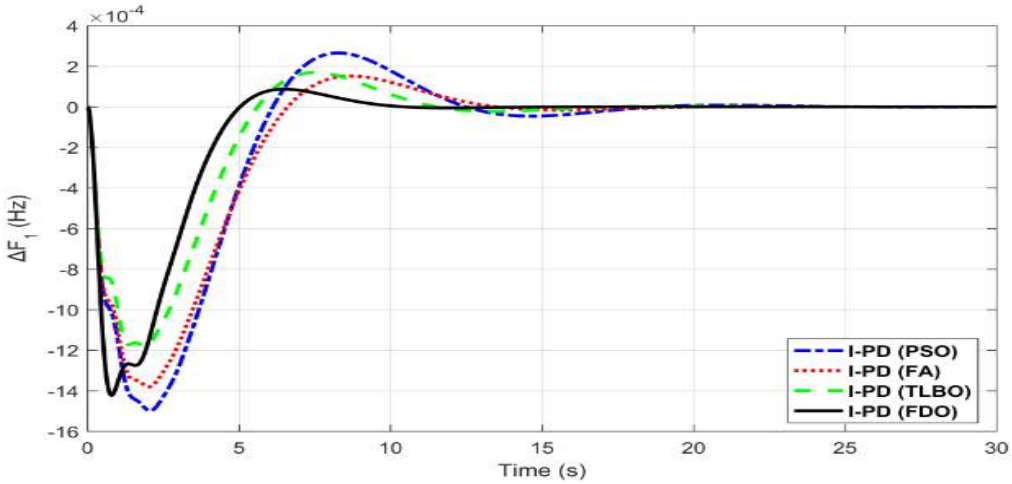

Figure 4.12 Results of multi-source with GDB, TD, BD, and GRC for ΔF1 with I-PD controller.

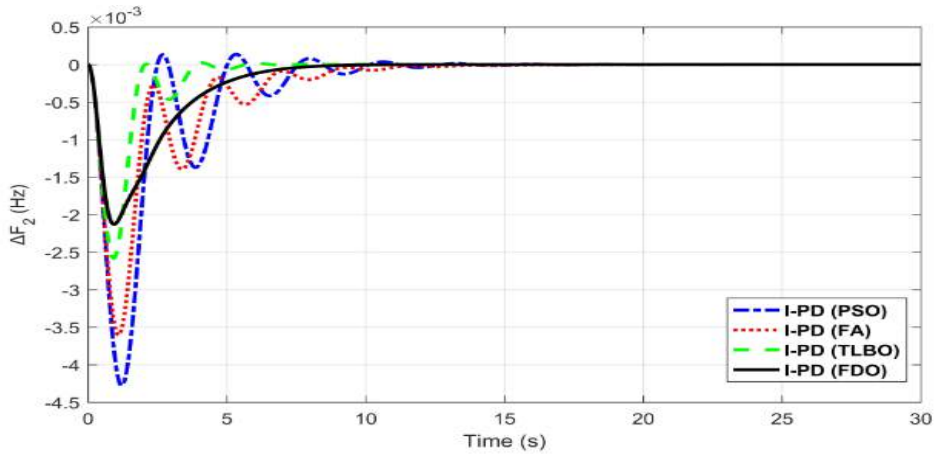

Figure 4.13 Results of a multi-source with GDB, TD, BD, and GRC for ΔF2 with I-PD controller.

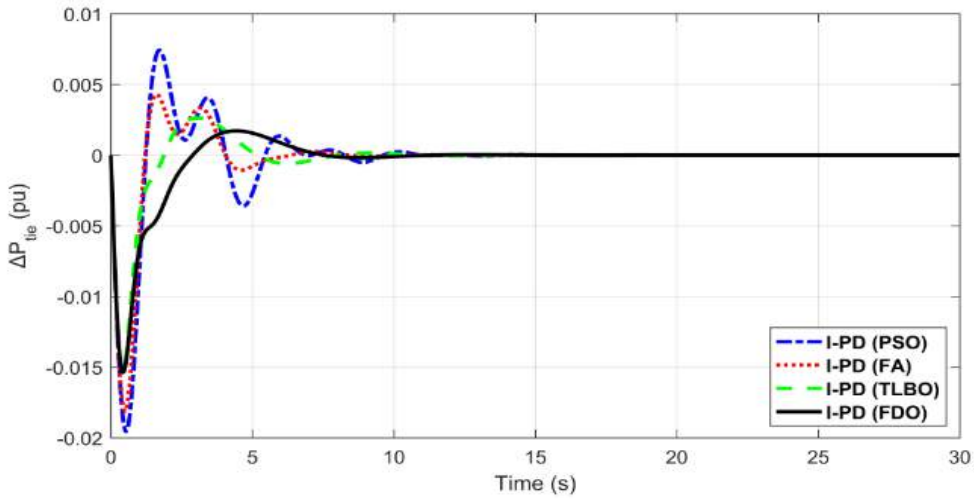

Figure 4.14 Results of multi-source with GDB, TD, BD, and GRC for ΔPtie with I-PD controller.

Table 4.2. Performance of multi-source with two areas including all non-linearities (GRC, BD TD, and GDB).

Techniques	Settling time (Ts)			Overshoot (O_{sh})			Undershoot (U_{sh})		
	ΔF_1	ΔF_2	ΔP_{tie}	ΔF_1	ΔF_2	ΔP_{tie}	ΔF_1	ΔF_2	ΔP_{tie}
FDO-PID	15.1	12.9	13.9	0.000588	0.000554	0.00274	-0.01056	-0.00682	-0.00916
TLBO-PID	14.8	12.7	15.4	0.000873	0.000660	0.00336	-0.01056	-0.00686	-0.0119
FA-PID	14.7	17.4	16.9	0.000721	0.00319	0.00444	-0.01085	-0.00813	-0.0119
PSO-PID	15.2	17.6	17.7	0.00117	0.00403	0.00474	-0.01056	-0.00824	-0.00707
PSO-I-PD	17.6	13.0	17.6	0.000226	0.000136	0.00742	-0.00150	-0.00428	-0.0196
FA-I-PD	15.1	12.9	15.1	0.000152	0.000000	0.00430	-0.00138	-0.00360	-0.0181
TLBO-I-PD	13.9	8.2	13.9	0.000169	0.000022	0.00263	-0.00118	-0.00258	-0.0152
FDO-I-PD	**12.6**	**7.6**	**12.6**	**0.000086**	**0.000003**	**0.00172**	**-0.00142**	**-0.00213**	**-0.0152**

To illustrate the effectiveness of the suggested techniques, the best-claimed outcome of FDO-PID/I-PD for two Area multi-source IPS with various nonlinearities is shown in Table 4.2. The results are depicted in Fig 4.9- Fig 4.14 reveals that the proposed FDO optimized PID/I-PD controllers perform better response as compared to FA/PSO/TLBO with PID/I-PD controller. The settling time (2.72%, 25.86%, and 17.75%), Overshoot (18.44%, 82.63% and 38.28%) and undershoot (2.67%, 16.11% and 23.02%) for ΔF1, ΔF2 and ΔPtie with FDO-PID controller are respectively improved compared to FA-PID. While FDO based I-PD controller shows a remarkable improvement in terms of settling time by (17.11%, 56.81%, and 28.81%), overshoot by (92.64%, 99.92%, and 63.71%) and undershoot by (86.55%, 74.15%, and 44.27%) for ΔF1, ΔF2, and ΔPtie respectively as compared to PSO-PID controller. Similarly, FDO based I-PD controller also show a percentage improvement in terms of settling time by (14.29%, 56.32%, and 25.44%), overshoot by (88.07%, 99.27%, and 61.26%) and undershoot (86.26%, 73.80, and 14.28%) for variation in the frequency of Area 1, Area 2 and tie-line respectively. FDO-I-PD

controller also shows a significant improvement in respect of settling time by (90.14%, 99.54%, and 48.80%), overshoot by (44%, 82.63%, and 38.22%) and undershoot by (86.55%, 68.95% and 14.28%) for ΔF1, ΔF2 and ΔPtie respectively as compared to TLBO with PID controller.

Chapter 5. Two Area Interconnected Power System in Deregulated Environment.

This chapter presents an Improved- Fitness Dependent Optimizer (I-FDO) algorithm for the optimization of a modified FOPID controller known as the FOI-PD algorithm for the AGC problem of two area multi-generation IPS considering the restructured environment. Two-area multi-source power unit comprised of thermal reheat, gas, wind hydro generation unit integrated with multiple non-linearities including GRC, GDZ, TD, and BD. Further, the performance of the system is improved by incorporating Redox Flow Battery (RBF) and Thyristor Controlled Series Capacitor (TCSC) with a tie-line.

5.1 System Investigated

A realistic model of two areas six-generation unit with several non-linearities including GDB, TD, BD and GRC in the restructured environment, is presented in Figure 5.1. Area-1 comprises of hydro, gas, thermal reheat, TCSC and RFB unit with two DISCOs (DISCO-1 and DISCO-2) and Area-2 consist of hydro, wind, thermal reheat and RFB unit with two DISCOs (DISCO-3 and DISCO-4). Thermal reheat generation unit composed of the turbine, governor and reheat with Transfer Function (TF) $\frac{1}{ST_1+1}$, $\frac{1}{ST_t+1}$ and $\frac{Sk_1T_r+1}{ST_r+1}$ respectively [2]. While gas power unit is composed of valve position TF ($\frac{1}{Sb_g+x_g}$), governor TF ($\frac{Sx_C+1}{Sy_C+1}$), fuel combustion reaction TF ($\frac{1}{ST_{cd}+1}$) and TF of compressor discharge ($\frac{ST_{cr}-1}{ST_f+1}$) [2]. TF of the hydro unit has consists of droop compensation ($\frac{ST_r+1}{ST_{rh}+1}$), governor ($\frac{1}{ST_{gh}+1}$)

and penstock turbine ($\frac{-ST_w+1}{0.5ST_w+1}$) [2]. Similarly, the wind power system is composed of a hydraulic pitch actuator and turbine blade pitch with transfer function $\frac{(ST_{p1}+1)K_{p1}}{(1+S)(ST_{p2}+1)}$ and $\frac{K_{p2}}{(S+1)}$ respectively [7].

5.2 AGC in Deregulated Power System.

In a deregulated environment, the GENCOs can exchange power to any DISCO while the DISCO has full autonomy to deal with the GENCOs in their region or any other area [4]. Such a transaction is known as "bilateral transactions" which is supervised by ISO. The idea of including DISCOs-GENCOs bilateral trading is articulated by DPM in which columns denote DISCOs and rows indicate GENCOs [8, 39]. Whereas, each entity in DPM shows Contract Participation Factor (cpf). Let us consider a two area IPS in a deregulated environment which is described by two DISCOs and three GENCOs in each control area and is expressed by Eq (5.1) [20].

$$DPM = \begin{bmatrix} cpf_{11} & cpf_{12} & cpf_{13} & cpf_{14} \\ cpf_{21} & cpf_{22} & cpf_{23} & cpf_{24} \\ cpf_{31} & cpf_{32} & cpf_{33} & cpf_{34} \\ cpf_{41} & cpf_{42} & cpf_{43} & cpf_{44} \\ cpf_{51} & cpf_{52} & cpf_{53} & cpf_{54} \\ cpf_{61} & cpf_{62} & cpf_{63} & cpf_{64} \end{bmatrix} \tag{5.1}$$

In Eq (5.1) DPM represent DISCO Participation Matrix and cpf shows contract participation factor. Cpf signifies the fraction of each GENCOs contribution to the entire load demand of DISCOs. Whereas the diagonal entity denotes the local demand and off-diagonal entities show the participation from other areas. The sum of all column elements of Eq (5.1) is equal to unity which can be expressed as below [8, 12].

$$\sum_{\mathrm{i}} \mathrm{cpf}_{\mathrm{ij}} = 1 \tag{5.2}$$

The scheduled tie line ($\Delta \mathrm{P}_{\mathrm{tie12}}^{\mathrm{Sch}}$) power may be expressed as [8].

$$\Delta \mathrm{P}_{tie12}^{Sch} = \sum_{m=1}^{2}\sum_{n=3}^{4} \mathrm{cpf}_{\mathrm{mn}} \Delta \mathrm{P}_{\mathrm{Ln}} - \sum_{m=3}^{4}\sum_{n=1}^{2} \mathrm{cpf}_{\mathrm{mn}} \Delta \mathrm{P}_{\mathrm{Ln}} \tag{5.3}$$

Where ΔP_{Ln} represents a change in DISCO load of n-th area. Error in tie-line power (ΔP_{tie12}^{Error}) from area-1 to area-2 is expressed as below [8].

$$\Delta \mathrm{P}_{\mathrm{tie12}}^{\mathrm{Error}} = \Delta \mathrm{P}_{\mathrm{tie12}}^{\mathrm{actual}} - \Delta \mathrm{P}_{\mathrm{tie12}}^{\mathrm{Sch}} \tag{5.4}$$

Whereas

$$\Delta \mathrm{P}_{\mathrm{tie12}}^{\mathrm{actual}} = \frac{2\Pi \mathrm{T}_{12}}{\mathrm{S}} \{\Delta \mathrm{f}_1 - \Delta \mathrm{f}_2\} \tag{5.5}$$

Where T_{12} shows synchronization constant of tie-line and Δf_1 , Δf_2 represent a change in the frequency of area-1 and area-2 respectively. The tie-line power error (ΔP_{tie12}^{Error}) from control area-1 to control area-2 is expressed as below:

(ΔP_{tie21}^{Error}) from area-2 to area-1 is expressed as follows [8].

$$\Delta \mathrm{P}_{\mathrm{tie21}}^{\mathrm{Error}} = a_{12} \Delta \mathrm{p}_{\mathrm{tie12}}^{\mathrm{error}} \therefore a_{12} = -1 \tag{5.6}$$

The Area Control Error (ACE) for area-1 and area-2 can be expressed as below [2].

$$\mathrm{ACE}_1 = \beta_1 \Delta \mathrm{f}_1 + \Delta \mathrm{P}_{\mathrm{tie12}}^{\mathrm{Error}} \tag{5.7}$$

$$\mathrm{ACE}_2 = \beta_2 \Delta \mathrm{f}_2 + a_{12} \Delta \mathrm{P}_{\mathrm{tie12}}^{\mathrm{Error}} \tag{5.8}$$

Where β_1 and β_2 represents the bias factor of area-1 and 2 respectively.

5.3 Thyristor Controlled Series Compensator (TCSC) Modeling

The flow of current for an interconnected area can be expressed as below [80]

$$\mathbf{I}_{12} = \frac{|\mathbf{V}_1| \angle \delta_1 - |\mathbf{V}_2| \angle \delta_2}{\mathbf{J}(\mathbf{X}_{12} - \mathbf{X}_{\mathrm{Tcsc}})} \tag{5.9}$$

Where V_1, V_2, δ_1, and δ_2 represent terminal voltages and respective phase angles. Complex tie-line power can be articulated as [80].

$$\mathrm{P_{tie}} - \mathrm{JQ_{tie12}} = \mathrm{V_1^* I_{12}} = |\mathrm{V_1}| \angle(-\delta_1) \left[\frac{|\mathrm{V_1}| \angle \delta_1 - |\mathrm{V_2}| \angle \delta_1}{\mathrm{J(X_{12} - X_{Tcsc})}} \right] \tag{5.10}$$

Where P and Q represent real and reactive power respectively. X_{Tcsc} shows the reactance of TCSC and X_{12} represents the reactance of the tie-line. The real part of Eq (5.10) can be written as below [86].

$$\mathrm{P_{tie12}} = \frac{|\mathrm{V_1}| . |\mathrm{V_2}|}{(\mathrm{X_{12} - X_{Tcsc}})} [\sin(\delta_1 - \delta_2)] \tag{5.11}$$

The above equation in respect of percentage compensation (K_c) can be expressed as [86]

$$\mathbf{P}_{\mathrm{tie12}} = \frac{|\mathbf{V}_1| . |\mathbf{V}_2|}{\mathbf{X}_{12}(\mathbf{1} - \mathbf{K}_c)} [\sin(\delta_1 - \delta_2)] \tag{5.12}$$

Where K_c denote the degree of compensation and can be written as:

$$\mathrm{K_c} = \frac{\mathrm{X_{Tcsc}}}{\mathrm{X_{12}}} \tag{5.13}$$

Equation (5. 13) can be written as

$$P_{tie12} = \frac{|V_1|.|V_2|}{(X_{12} - X_{Tcsc})}\left[\sin(\delta_1 - \delta_2\right] + \frac{K_c}{(1-K_c)}\frac{|V_1|.|V_2|}{(X_{12})}\left[\sin(\delta_1 - \delta_2\right] \quad (5.14)$$

The first term in Eq (5.14) represents tie-line power without TCSC while the second term denotes tie-line power with TCSC. The incremental change in the tie-line power can be attained as [86]

$$\Delta P_{tie12} = \frac{|V_1|.|V_2|}{(X_{12})}\left[\cos(\delta_1^\circ - \delta_2^\circ)\right]\left[\sin(\Delta\delta_1 - \Delta\delta_2)\right] + \frac{\Delta K_c}{(1-\Delta K_c)}\frac{|V_1|.|V_2|}{(X_{12})}\left[\sin(\delta_1^\circ - \delta_2^\circ\right] \quad (5.15)$$

The deviation of the bus voltage angle is practically smaller for minor variation in the actual power load.

$$\sin(\Delta\delta_1 - \Delta\delta_2) \approx \Delta\delta_1 - \Delta\delta_2 \quad (5.16)$$

$$\Delta P_{tie12} = \frac{|V_1|.|V_2|}{(X_{12})}\left[\cos(\delta_1^\circ - \delta_2^\circ)\right]\left[(\Delta\delta_1 - \Delta\delta_2)\right] + \frac{\Delta K_c}{(1-\Delta K_c)}\frac{|V_1|.|V_2|}{(X_{12})}\left[\sin(\delta_1^\circ - \delta_2^\circ\right] \quad (5.17)$$

Let us consider

$$T_{12} = \frac{|V_1|.|V_2|}{(X_{12})}\left[\cos(\delta_1^\circ - \delta_2^\circ)\right], \text{ and } K_{12} = \frac{|V_1|.|V_2|}{(X_{12})}\left[\sin(\delta_1^\circ - \delta_2^\circ\right] \quad (5.18)$$

$$\Delta P_{tie12} = \left[T_{12}(\Delta\delta_1 - \Delta\delta_2)\right] + \frac{\Delta K_c}{(1-\Delta K_c)}\left[K_{12}\right] \quad (5.19)$$

Hence

$$\Delta\delta_1 = 2\Pi\int \Delta f_1 dt \quad (5.20)$$

$$\Delta\delta_2 = 2\Pi\int \Delta f_2 dt \quad (5.21)$$

By substituting values of Eq (5.20) and (5.21) into Eq (5.19) and also taking Laplace Transform, Eq (5.20) can be written as:

$$\Delta P_{tie12}(s) = \frac{2\Pi T_{12}}{S}\left[\Delta f_1(s) - \Delta f_2(s)\right] + \frac{\Delta K_c}{(1-\Delta K_c)}\left[K_{12}\right] \quad (5.\ 22)$$

In Eq (5. 22) the tie-line power can be controlled by ΔK_c and can be written as [80]

$$K_c = \frac{K_{Tcsc}}{1+ST_{Tcsc}} \quad (5.\ 23)$$

Where T_{Tcsc} and K_{Tcsc} indicate the time constant and gain of TCSC. If the input signal is considered to be the change in error and TF of the signal conditioning circuit as [86].

$$\Delta K_c(s) = \frac{K_{Tcsc}}{1+ST_{Tcsc}}\left[\Delta \text{Error}(s)\right] \quad (5.\ 24)$$

$$\Delta K_c(s) = \frac{K_{Tcsc}}{1+ST_{Tcsc}}\left[\Delta f_1(s)\right] \quad (5.25)$$

5.4 Redox Flow Battery (RFB) Modeling

Redox flow batteries (RFBs) are made of electrolytes comprising the dynamic redox species enclosed in exterior tanks. Cells are normally arranged in bipolar mounts where electrolytes flow during charge and discharge. Subsequently, the storage bulk is then calculated concerning electrolyte tank size and the reactant concentration, while the energy is determined by the quantity, configuration, and choice of the component of cell stacks. The soluble flow batteries gained attention over other devices to work efficiently without a cell separation membrane. RFBs are power devices that can be used as a frequency fluctuations stabilizer besides a fast energy compensation source. RFB can be considered as an energy storage device to reduce fluctuation in the tie-line power and frequency of an

IPS [21, 22, and 39]. RFB is used more frequently as compared to other storage devices like SMES owing to its simple operation under normal temperature, low losses, and long lifespan and maintenance. During abrupt changes in load, the RFB device delivers energy to the system and is also charged constantly during system operation. RFB model of the system output versus frequency variation is expressed as follows [87].

$$\Delta P_{RFB} = \frac{K_{RFB}}{1+T_{RFB}}\left[\Delta f\right] \tag{5. 26}$$

Where T_{RFB} shows time constant and K_{RFB} denote gain of RFBs.

5.5 Controller Structure and Fitness Function

Various controllers have been designed and implemented for AGC in literature. However, fractional-order controllers attained considerable attention in the last few decays as compared to traditional controllers due to better disturbance rejection ratio, low noise effect, and reduction of calculation time [28, 42]. In this section, a modified FOPID controller known as the FOI-PD controller is designed and developed for the AGC problem in a restructured environment to handle the complexity of the system. The structure of FOPID and FOI-PD controllers are shown in Figures 5.1 and 5.2 respectively, which consist of five parameters including derivative gain (K_d), integral gain (K_i), proportional gain (K_p), fractional integrator order (λ) and fractional derivative order (μ). In the FOPID controller, all the parameters are put in feedforward direction while, in the FOI-PD controller, the integral parameter (K_i) with integrator order (λ) is put in a forward direction and the remaining parameters are put in feedback The output of FOPID and FOI-PD

controllers in terms of a differential equation are specified by Eq (5. 27) and Eq (5. 28) respectively [127], [128].

$$u(t) = K_p e(t) + K_i D^{-\lambda} e(t) + K_d D^{\mu} e(t) \tag{5.27}$$

$$u\left(t\right) = K_i D^{-\lambda} e(t) - [K_p y(t) + K_d D^{\mu} y(t)] \tag{5.28}$$

Where u(t) represents control signal, e(t) denotes error signal, which is ACE in this case and y(t) is the output of the system. A step-change in FOPID controller reference input R(s) can cause an instant spike change in control signal output U(s). This spike is called a proportional or derivative kick which quickly changes the control signal to the actuator and can trigger a major problem in the Gp(s) plant. To overcome these drawbacks the modified structure of the FOPID controller is introduced. In this arrangement, an instant variation in R(s) will not affect the derivative and proportional gains, since these two gains work on the output process Y(s) [44, 45].

The Transfer Function (TF) of the closed-loop system by considering a plant $G_p(s)$ with FOPID and FOI-PD controllers is given by Eq (5. 29) and (5. 30) respectively [127, 128].

$$\frac{Y(s)}{R(s)} = \frac{G_p(s)[K_p S^{\lambda} + K_i + S^{\lambda} K_d S^{\mu}]}{S^{\lambda} + G_p(s)[K_p S^{\lambda} + K_i + S^{\lambda} K_d S^{\mu}]} \tag{5.29}$$

$$\frac{Y(s)}{R(s)} = \frac{G_p(s) K_i}{S^{\lambda} + G_p(s) K_i + K_p S^{\lambda} + S^{\mu} K_d S^{\lambda}} \tag{5.30}$$

Eq (5. 29) shows that there are two zeros with the FOPID controller which is tough to adjust the response of the system with these zeros. Their impact takes place as a higher overshoot or an earlier peak. The proposed modified FOPID controller known as the FOI-

PD controller gets over these effects of zeros as shown in Eq (5.30) and enhances the response of the system by adding derivative and proportional terms of FOPID on feedback path instead of feedforward. The system's profile with the FOI-PD controller is thus better than the FOPID controller that is evident in the results and discussion section.

To assess the performance of the proposed I-FDO method ITSE is used as a cost function to optimize AGC problem [23, 29, 30 and 45]. ITSE expression can be written as:

$$J_1 = \text{ITSE} = \int_0^t \left[\Delta f_1^{\,2} + \Delta f_2^{\,2} + \Delta P_{tie12}^{\,2} \right] t \, dt \tag{5.31}$$

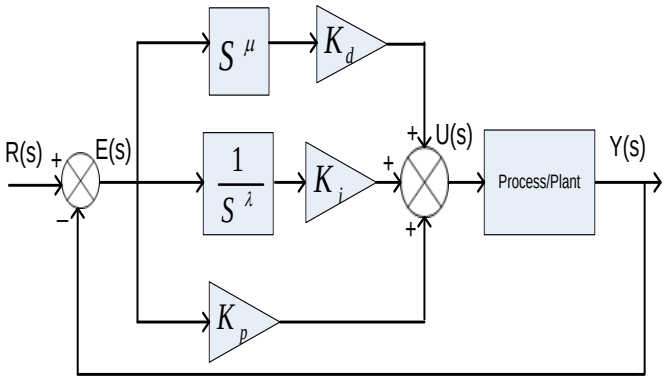

Figure 5.1 Structure of FOPID controller.

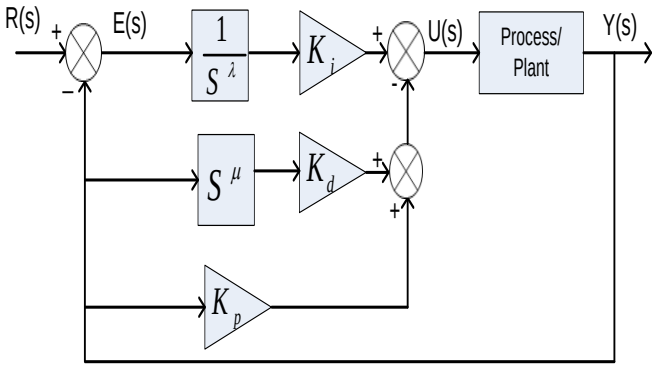

Figure 5.2 Structure of FOI-PD controller.

5.6 Improved- Fitness Dependent Optimizer (I-FDO)

I-FDO is the improved form of FDO which was recently developed by Danial *et al.* [129] and has been tested on 19 classical benchmark functions and shows its superiority from FDO and other recent metaheuristic algorithms. The concept of algorithm is based on the collective decision-making and generative process used by bees. Our proposed I-FDO algorithm differs from FDO algorithms which consist of two phases including position updates of scout bees and randomization of weight factor (Υ).

1) UPDATING THE SOUT BEE POSITION

In the I-FDO algorithm, the position of the scout's bee is updated by adding two parameters that are Cohesion (*C*) and Alignment (*A*) to the original FDO. These two parameters are important signifiers of group motion; alignment (*A*) shows pace matching of individuals in the neighborhood or group to that of other individuals whereas, cohesion (*C*) is the tendency of scouts towards the center of mass of the neighborhood. The new position of artificial scout's bee can be articulated as follows [129].

$$X_k^{t+1} = X_k^t + P + (A \times \frac{1}{C}) \tag{5.32}$$

Where x_k^{t+1} represents the next position, x_k^t denotes the current position, *P* represents the moment of scout bees, *A* represent alignment and *C* represents the cohesion of scouts bee. Whereas alignment and cohesion are expressed in Eq (5.33) and (5.34) respectively [129].

$$A_i = \sum_{i=1}^{N} \frac{P_i}{N} \tag{5.33}$$

$$A_i = \sum_{i=1}^{N} \frac{X_i}{N} - X \tag{5.34}$$

Where P_i represents the pace of i-th neighboring scout's bee, N represents the neighborhood number, X is the location of current individuals and x_i is the position of i-th neighboring scout.

2) RANDOMIZATION of WEIGHT FACTOR

In the I-FDO algorithm weight factor (γ) is generated in the range of [0, 1] by using random phenomenon to control the fitness weight (F_W) instead of original FDO in which weight factor is considered to be 0 or 1. However in FDO, for most cases, the weight factor is used to be 0. In I-FDO algorithm improvement in terms of fitness weight can be written as below [129].

$$F_w = \left| \frac{f(X^*_{k,t})}{f(X^t_k)} \right| \tag{5.35}$$

In Eq (5.35) if the value of Fitness weight (F_W) is equal to or less than generated weight factor (γ) then weight factor can be ignored otherwise, compared to the previous one. The flow chart for the I-FDO algorithm is depicted in Figure 5.3.

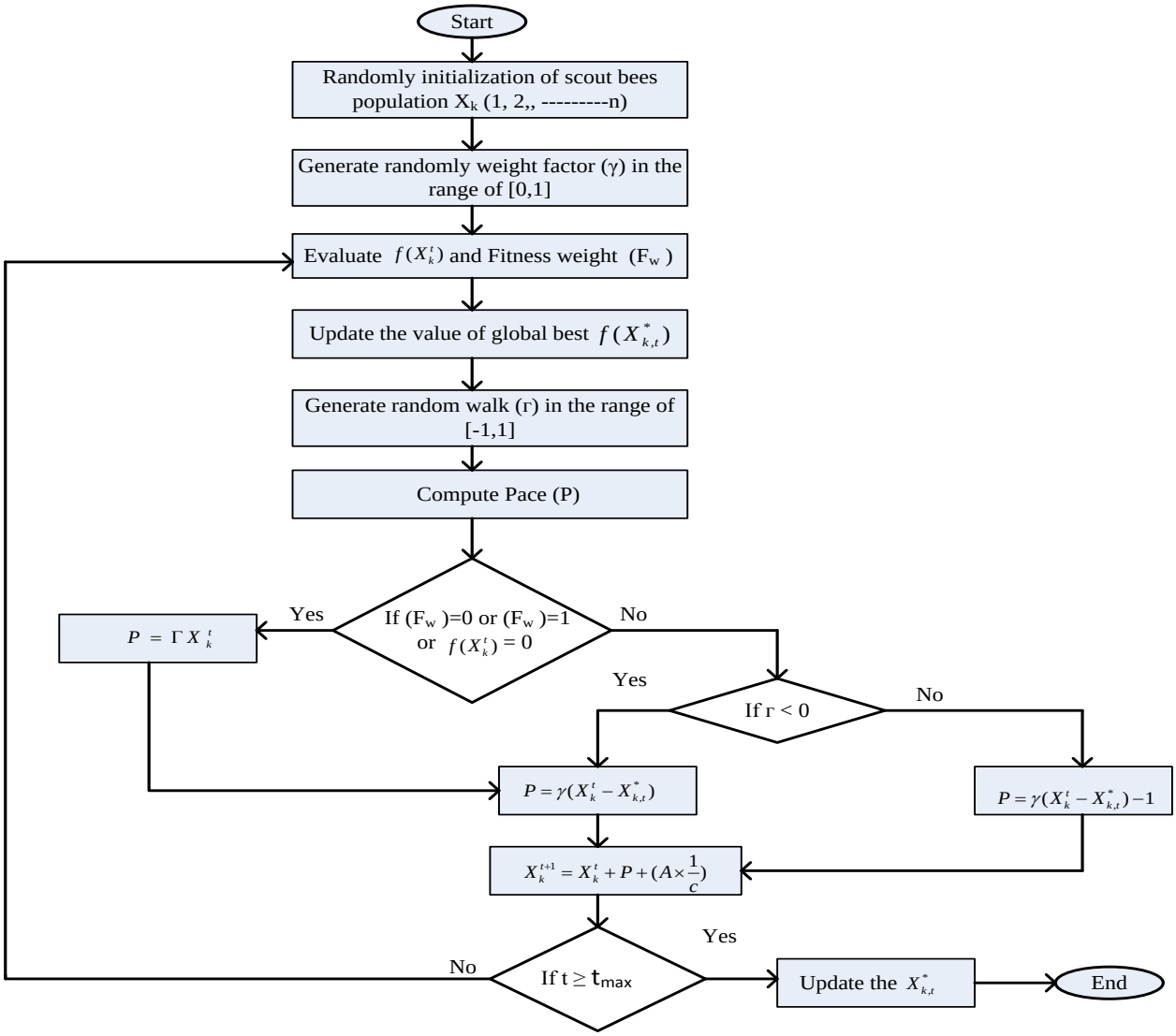

Figure 5.3 Flow chart of the I-FDO Algorithm [129].

5.7 Implementation and Results

In this section, the model as shown in Figure 5.4 is developed in Matlab/Simulink using the values from Appendix (Table 1) and the I-FDO algorithm is written in m. file. ITSE criteria are used as an objective function to tune the gains of the proposed controller. For the optimization of controller gains, the values of I-FDO parameters were taken from the Appendix (Table 3). The optimization process has been performed 20 times for each algorithm, and the best optimal values among the 20 iterations are chosen as the controller's

final gains. The optimal values for two areas six-generation unit in the deregulated environment under the Poolco Based Transaction (PBT) considering different cases are provided in Table 5.1. While the optimum values under Contract Violation Based Transaction (CVBT) and Bilateral Based Transaction (BBT) is presented in Table 5.2. The results attained from the proposed approach are associated with other algorithms such as FDO, FA and TLBO based FOI-PD algorithm. ITSE based convergence diagram of different algorithm is depicted in Figure 5.5.

Table 5.1 Parameters setting for controller under Poolco Based Transaction (PBT) considering different cases.

Gains	Case-1				Case -2				Case-3			
	FOI-PD (I-FDO)	FOI-PD (FDO)	FOI-PD (TLBO)	FOI-PD (FA)	I-FDO (FOI-PD)	I-FDO (FOPID)	I-FDO (I-PD)	I-FDO (PID)	With RFB& TCSC	TCSC	RFB	Without RFB & TCSC
K_{p1}	1.176	1.010	1.091	1.130	1.290	1.405	1.032	0.998	1.678	1.340	1.458	1.009
K_{i1}	1.232	0.305	1.012	0.200	0.232	1.012	1.024	1.010	1.989	1.543	1.120	1.101
K_{d1}	1.190	0.011	-1.023	1.030	0.010	1.890	0.110	1.900	0.110	-0.22	1.456	1.988
λ_1	0.230	0.991	0.789	0.765	0.090	0.786	-	-	0.671	0.223	0.101	0.989
μ_1	0.002	0.910	0.675	0.003	0.002	0.344	-	-	0.678	0.972	0.234	0.760
K_{P2}	1.064	1.098	1.011	0.303	1.009	0.120	0.300	2.810	1.600	0.011	1.030	0.010
K_{i2}	1.040	1.023	1.304	1.109	-1.199	0.160	0.340	1.020	2.000	0.991	0.165	0.090
K_{d2}	1.200	1.100	1.008	1.001	1.560	0.305	1.090	1.200	1.078	-0.91	0.003	0.002
λ_2	0.090	0.786	0.165	0.090	0.099	0.001	-	-	0.899	0.165	0.671	0.213
μ_2	0.002	0.344	0.003	0.002	0.564	0.988	-	-	0.006	0.013	0.678	0.992
K_{p3}	0.948	2.000	1.903	0.789	1.230	1.200	1.234	1.876	1.124	0.898	1.234	1.678
K_{i3}	1.786	0.148	1.234	1.020	-1.11	1.456	1.987	1.002	1.001		1.298	1.200
K_{d3}	1.056	-1.001	1.678	0.789	1.098	1.011	0.303	1.009	1.064	1.098	1.011	1.004
λ_3	0.015	0.890	0.006	0.765	0.671	0.213	-	-	1.090	0.165	0.090	0.786
μ_3	0.013	0.102	0.124	0.013	0.678	0.992	-	-	1.898	0.003	0.002	0.344

Table 5.2 Parameters setting for the controller with Bilateral Based Transaction (BBT) and Contract Violation Based Transaction (CVBT).

	Bilateral Based Transaction				Contract Violation Based Transaction			
Controller Gains	**FOI-PD (I-FDO)**	**FOI-PD (FDO)**	**FOI-PD (TLBO)**	**FOI-PD (FA)**	**FOI-PD (I-FDO)**	**FOI-PD (FDO)**	**FOI-PD (TLBO)**	**FOI-PD (FA)**
K_{p1}	1.678	1.989	1.543	1.120	1.101	1.064	1.032	0.998
K_{i1}	1.989	1.078	0.910	0.003	0.002	1.040	1.024	1.010
K_{d1}	0.110	-1.760	1.023	1.030	0.010	1.200	-0.110	1.900
λ_1	0.671	0.010	0.789	0.765	-0.090	0.190	0.189	0.100
μ_1	0.678	0.090	0.675	0.003	0.002	0.102	0.786	0.165
K_{P2}	1.290	0.450	0.032	0.303	1.009	0.420	0.300	2.810
K_{i2}	0.203	0.112	0.024	1.109	1.199	0.360	0.340	1.020
K_{d2}	-1.101	0.189	0.100	1.001	-1.560	0.005	1.090	1.200
λ_2	0.009	0.786	0.165	0.090	0.059	0.101	0.671	0.010
μ_2	0.767	0.344	0.003	0.002	0.564	0.188	0.678	0.090
K_{p3}	0.948	2.000	1.903	0.789	1.230	1.100	1.234	1.876
K_{i3}	1.786	0.148	1.234	1.020	1.111	-1.056	1.987	1.002
K_{d3}	1.064	-1.098	1.011	1.054	0.064	1.001	0.303	1.009
λ_3	0.899	0.165	0.671	0.165	0.601	0.003	0.110	0.330
μ_3	0.006	0.013	0.678	0.01s3	0.608	0.902	0.671	0.504

5.7.1 Poolco Based Transaction (PBT)

In PBT, Discos have a power contract with Gencos in their same control area. It is presumed that the two discos demands of 0.05 p.u.MW ($\Delta P_{L1} = \Delta P_{L2}$ =0.05 p.u.MW) power in control area1 from the Gencos of a similar control area. In the control area, 2 Discos have not any contract with Gencos i.e ($\Delta P_{L3} = \Delta P_{L4}$ =0.00 p.u.MW). Hence, the total load disturbance in area 1 is (ΔP_{d1} =0.1 p.u.MW) and in area 2 is (ΔP_{d2} =0.0 p.u.MW). A specific case of PBT between Gencos and Discos is simulated by considering below DPM.

$$\text{DPM} = \begin{bmatrix} 0.5 & 0.5 & 0.0 & 0.0 \\ 0.3 & 0.3 & 0.0 & 0.0 \\ 0.2 & 0.2 & 0.0 & 0.0 \\ 0.0 & 0.0 & 0.0 & 0.0 \\ 0.0 & 0.0 & 0.0 & 0.0 \\ 0.0 & 0.0 & 0.0 & 0.0 \end{bmatrix} \tag{5.36}$$

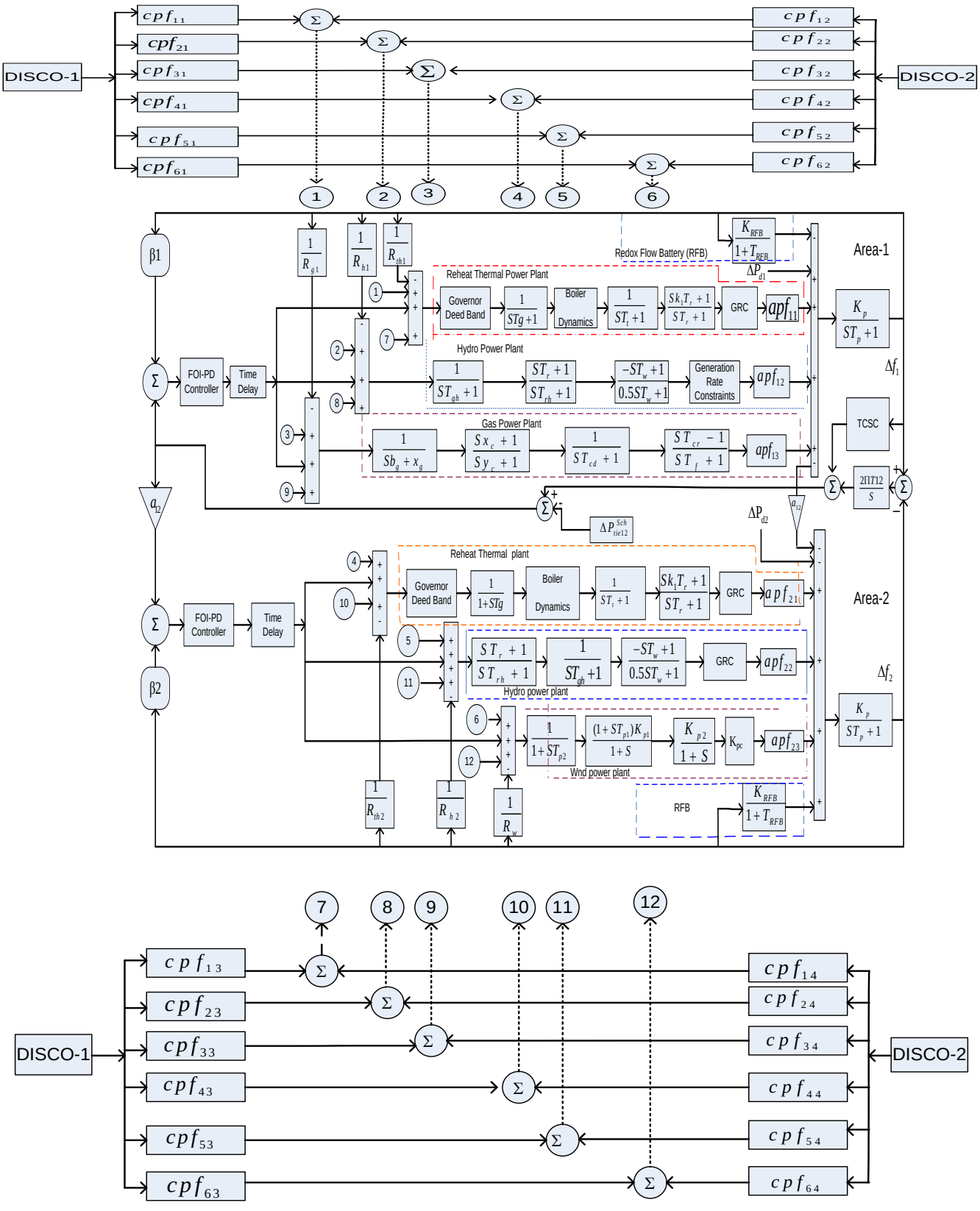

Figure 5.4 Two areas multi-generation deregulated power system with TD, GRC, BD and GDB.

Three cases have been considered under PBT. The first case is the validation of the proposed I-FDO technique, which is compared with other optimized techniques such as FDO, TLBO and FA. In the second case, the performances of the novel proposed controller have been compared with the performance of other conventional controllers like FOPID, I-PD and PID. In the third case, the performance of the system has been evaluated with and without RFB and TCSC with proposed methods.

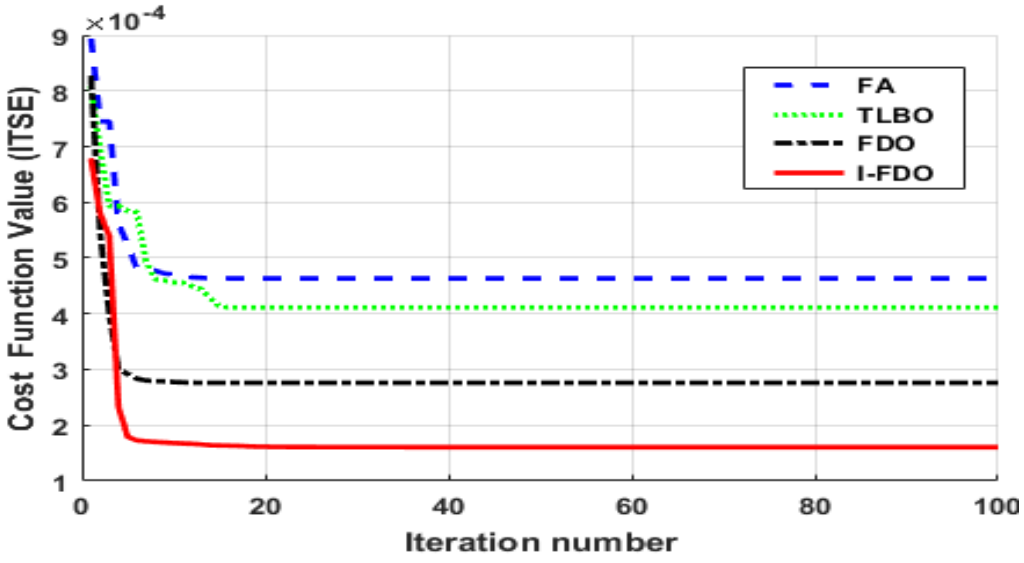

Figure 5.5 Convergence diagram for different algorithms.

1) CASE-1

In case-1 the superiority of the proposed I-FDO technique has been validated by comparing the result with other optimization techniques including FDO, TLBO and FA. The dynamic response profile of the system with proposed techniques for 1% step load in area 1 under PBT is presented in Figure 5. 6- Fig 5.8. It can be observed from Fig 5. 6- Fig 5.8 that I-FDO based optimization method quickly suppressed oscillation for frequency variation in area 1 (Δf_1), area 2 (Δf_2), and variation in tie-line power (ΔP_{tie}). Comprehensive comparative results for various algorithms in terms of Settling time (T_s), Overshoot (O_s),

and Undershoot (U_S) for Δf_1, Δf_2 and ΔP_{tie} are given in Table 5.3. From Fig 5. 6- Fig 5.8 it can be observed that the FOI-PD controller tuned with the I-FDO algorithm has nearly the same peak overshoot as compared with FOI-PD tuned with FDO techniques but improved settling time by 11.95% for change in area-1 and 16.63% for change in area-2. Similarly, FOI-PD controller tuned with I-FDO improved settling time by (47.56%, 10.88% and 0.20%) and effectively reduced overshoot by (97.10%, 56.20%, and 69.41%) for Δf_1, Δf_2 and ΔP_{tie} respectively as compared to FOI-PD controller tuned with FA. From Table 5.3, it can be observed that I-FDO based tuned FOI-PD controller as compared to hDE-PS based MID controller provides a significant improvement of 76.85%, 26.42% and 21.43% for both areas and in tie-line power, while effectively reduced peak overshoot of 97.80%, 85.88%, and 37.00% and undershoot of 6.00%, 70.13% and 75.00% for Δf_1, Δf_2 and ΔP_{tie} respectively. Similarly, I-FDO based FOI-PD controller also provides an improvement of 53.62%, 4.96%, and 6.37% in T_s for load frequency of Δf_1, Δf_2 and ΔP_{tie} respectively as compared hTLBO-PS based TID controller. From Fig 5.5 it can be seen that I-FDO algorithm converge rapidly by using ITSE criteria and obtained the value of (ITSE= 0.000168) as compared to FDO (ITSE=0.000290), TLBO (ITSE=0.000410) and FA (ITSE= 0.000513).

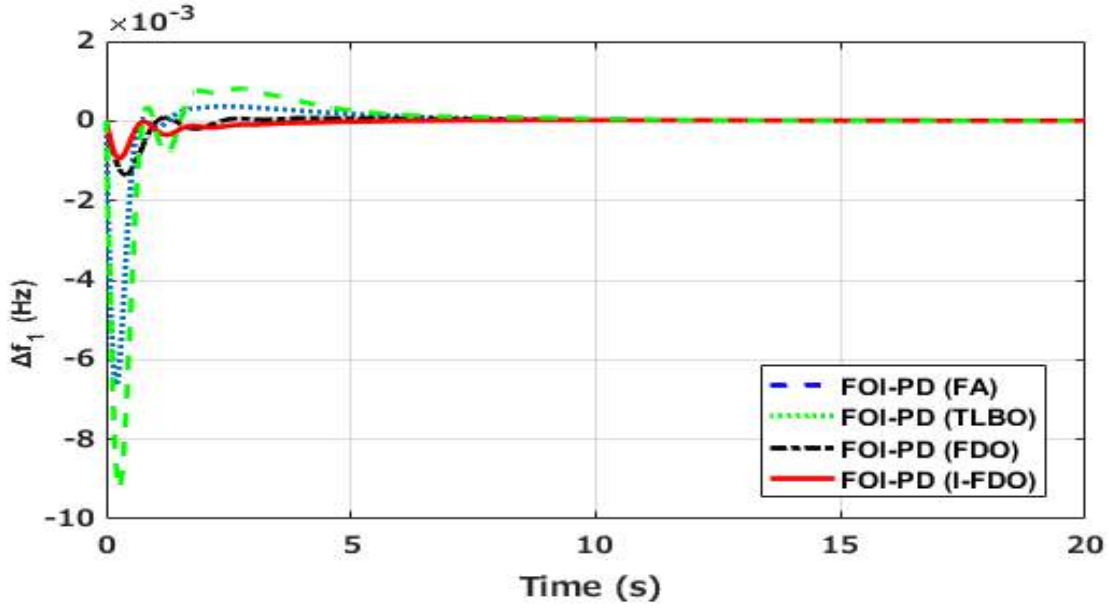

Figure 5.6 Results under poolco based transaction for ΔF1 considering case-1.

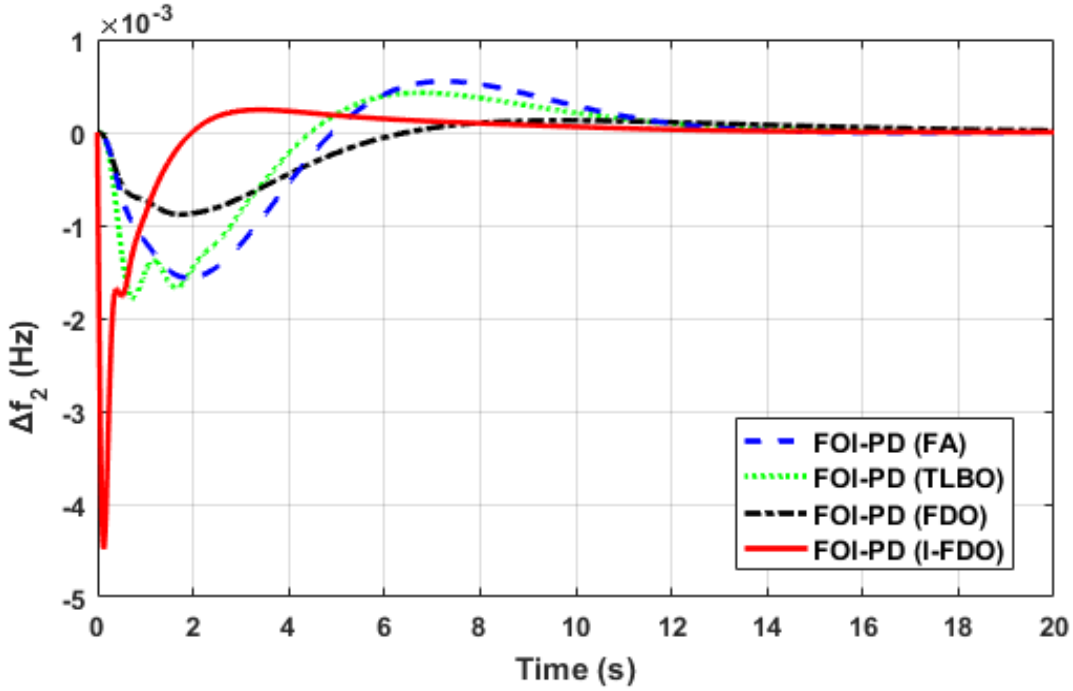

Figure 5.7 Results under poolco based transaction for ΔF2 considering case-1.

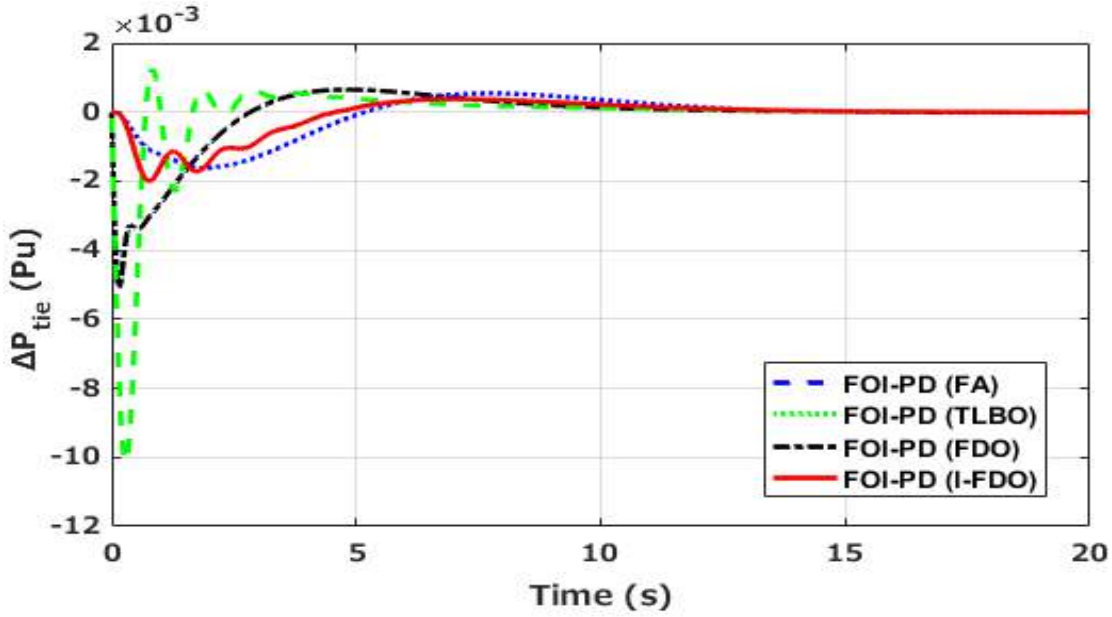

Figure 5.8 Results under poolco based transaction for ΔPtie considering case-1.

CASE-2

In this case, the performance of FOI-PD controller optimized with I-FDO algorithms have been compared with FO-PID, I-PD, and PID controllers tuned with the same algorithm for two area multi-source IPS under poolco based transaction. The results obtained from the proposed techniques are shown in Fig 5.9 – Fig 5.11 and Table 5.4. From Table 5.4 it can be seen that FOI-PD controller with I-FDO tuned method superiorly performs in respect of settling time by (2.80%, 16.56%, and 23.87%), overshoot by (69.36%, 62.55%, and 88.35%) for Δf_1 , Δf_2 and ΔP_{tie} respectively as compared to FOPID controller tuned with I-FDO techniques. From Fig 5.9- Fig 5.11 and Table 5.3 it can be observed that FOI-PD controller improved settling time by (42.84%, 10.65%, and 20.86%), effectively reduced peak overshoot by (49.56%, 89.24%, and 95.40%) and reduced undershoot by (31.88%, 41.90%, and 87.0%) for Δf_1 , Δf_2 and ΔP_{tie} respectively, when compared with PID controller optimized with similar algorithms. Hence, it can be inferred that our proposed

controller outperforms in respect of T_s, O_s, and U_s as compared to PID and I-PD controllers optimized with a similar algorithm i.e. I-FDO.

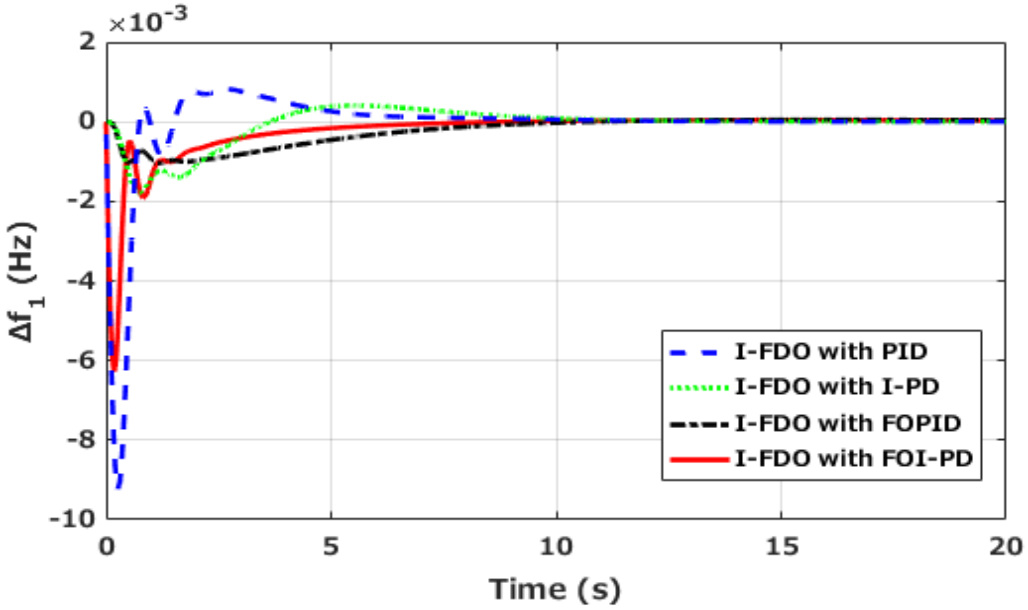

Figure 5.9 Results under poolco based transaction for ΔF1 considering case-2.

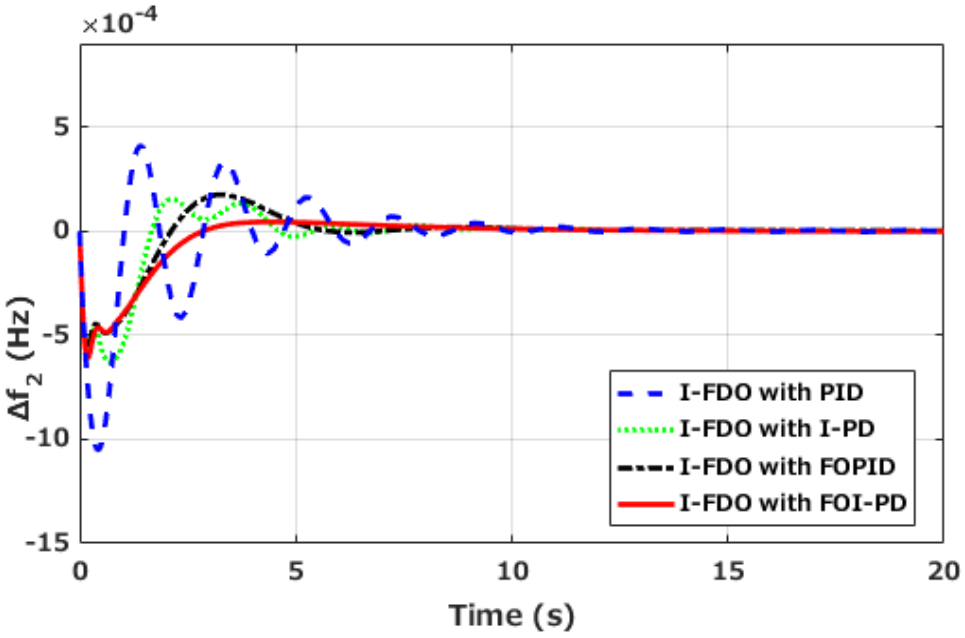

Figure 5.10 Results under poolco based transaction for ΔF2 considering case-2.

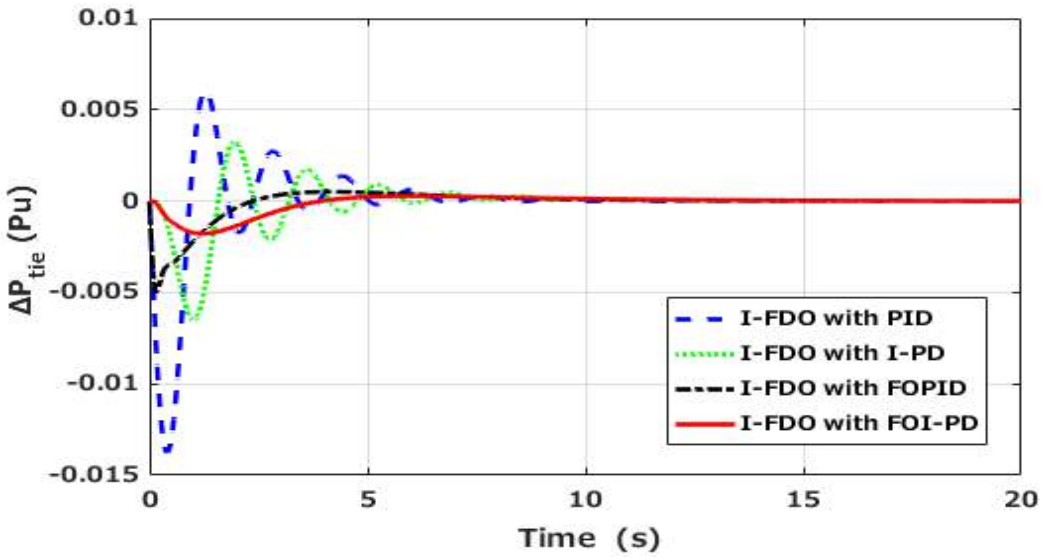

Figure 5.11 Results under poolco based transaction for ΔPtie considering case-2.

CASE-3

In case 3, the effect of introducing RFB and TCSC units on AGC is investigated. RFB unit is incorporated in each area and TCSC is considered in the tie-line of the system. The performance of the system is evaluated with I-FDO based FOI-PD controller considering the effect of RFB, TCSC, both RFB and TCSC and without RFB and TCSC. The results attained for Δf_1 , Δf_2 and ΔP_{tie} are shown in Fig 5.12- Fig 5.14. From Fig 5.12- Fig 5.14 it can be observed that the performance of the proposed techniques including TCSC and RFB unit is superior as compared to without considering TCSC and RFB for Δf_1 , Δf_2 and ΔP_{tie} in terms of T_s, O_s, and U_s. The dynamic response of the system incorporated with TCSC and RFB unit is improved in respect of settling time by (11.30%, 12.96%, and 23.56%), reduced overshoot by (55.67%, 47.78%, and 34.89 %) and undershoot by (14.50%, 11.08%, and 2.09%) for Δf_1 , Δf_2 and ΔP_{tie} respectively as compared to a system without considering the effect of RFB and TCSC unit. From Fig 12- Fig 14 and Table 5.5 it can be perceived that the response of the system considering the individual effect of TCSC and

RFB is improved in respect of T_s, O_s and U_s as compared to without including the effect of TCSC and RFB unit for Δf_1 , Δf_2 and ΔP_{tie} . Hence, it can be concluded from Table 5.5 that our proposed techniques perform outstanding incorporating with RFB and TCSC.

Table 5.3. Comparison performance of various algorithms under PBT for case-1 in terms of T_s, Os, and Us.

Controller with Algorithms	**T_s (Settling time)**			**O_s (Overshoot)**			**U_s (Undershoot)**		
	ΔF_1	**ΔF_2**	**ΔP_{tie}**	**ΔF_1**	**ΔF_2**	**ΔP_{tie}**	**ΔF_1**	**ΔF_2**	**ΔP_{tie}**
FOI-PD (I-FDO)	**4.42**	**13.1**	9.97	**0.000017**	0.000240	**0.000378**	**-0.00094**	-0.00448	**-0.00199**
FOI-PD (FDO)	5.02	15.9	**9.81**	0.000082	**0.000126**	0.000651	-0.00135	**-0.00088**	-0.00507
FOI-PD (TLBO)	6.53	14.8	12.7	0.000363	0.000424	0.000542	-0.00664	-0.00178	-0.00162
FOI-PD (FA)	8.43	14.7	9.99	0.000813	0.000548	0.001236	-0.00922	-0.00156	-0.01012
TID (hTLBO-PS) [89]	9.53	13.75	10.36	0.007222	0.070400	0.003500	-0.18888	-0.24010	-0.06330
MID(hDE-PS) [87]	19.0	18.09	12.69	0.00080	0.001700	0.000600	-0.00100	-0.01500	-0.00800

Table 5.4. Comparison performance of various algorithms under PBT for case-2 in terms of T_s, Os, and Us.

Controller with Algorithms	**T_s (Settling time)**			**O_s (Overshoot)**			**U_s (Undershoot)**		
	ΔF_1	ΔF_2	ΔP_{tie}	ΔF_1	ΔF_2	ΔP_{tie}	ΔF_1	ΔF_2	ΔP_{tie}
I-FDO with FOI-PD	**6.23**	**10.9**	**8.23**	**0.000041**	**0.000044**	**0.000272**	-0.00628	-0.00061	**-0.00178**
I-FDO with FOPID	7.93	11.1	8.46	0.000048	0.000174	0.000509	**-0.00104**	**-0.00056**	-0.00500
I-FDO with I-PD	8.61	11.0	9.02	0.000406	0.000153	0.003254	-0.00179	-0.00062	-0.00651
I-FDO with PID	10.9	12.2	10.4	0.000813	0.000409	0.006035	-0.00922	-0.00105	-0.01376

Table 5.5 Comparison performance of various algorithms under PBT for case-3 in terms of T_s, Os and Us.

Controller with Algorithms	**T_s (Settling time)**			**O_s (Overshoot)**			**U_s (Undershoot)**		
	ΔF_1	ΔF_2	ΔP_{tie}	ΔF_1	ΔF_2	ΔP_{tie}	ΔF_1	ΔF_2	ΔP_{tie}
I-FDO with RFB& TCSC	**8.10**	**6.23**	**10.8**	**0.00011**	**0.00003**	**0.00116**	**-0.00446**	-0.00527	**-0.00681**
I-FDO with TCSC	9.80	7.80	11.2	0.00050	0.00031	0.00223	-0.00912	**-0.00441**	-0.00685
I-FDO with RFB	9.90	8.20	11.8	0.00055	0.00031	0.00224	-0.00691	-0.00568	-0.00812
Without RFB&TCSC	11.8	12.4	12.1	0.00141	0.00161	0.00363	-0.01023	-0.00695	-0.00823

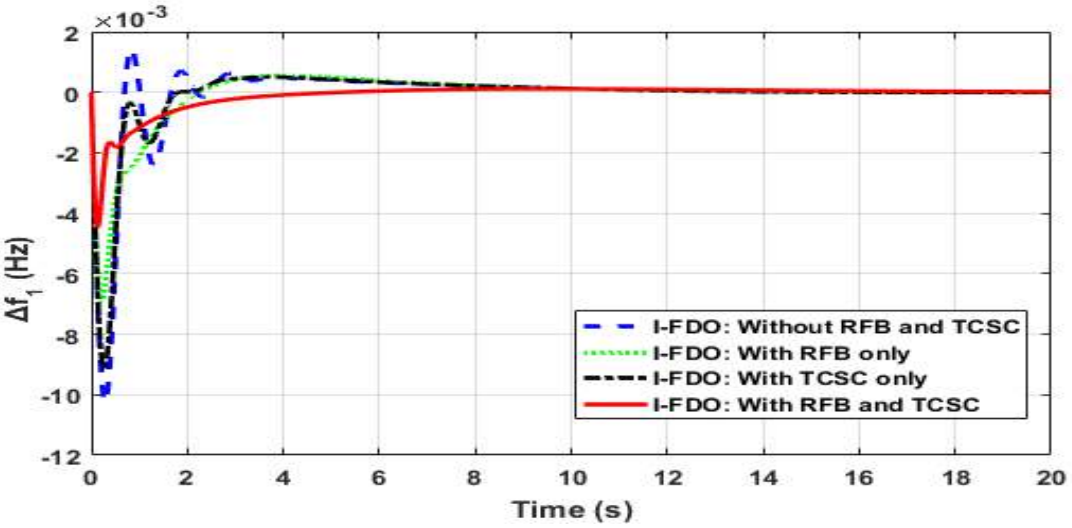

Figure 5.12 Results under poolco based transaction for ΔF1 considering case-3.

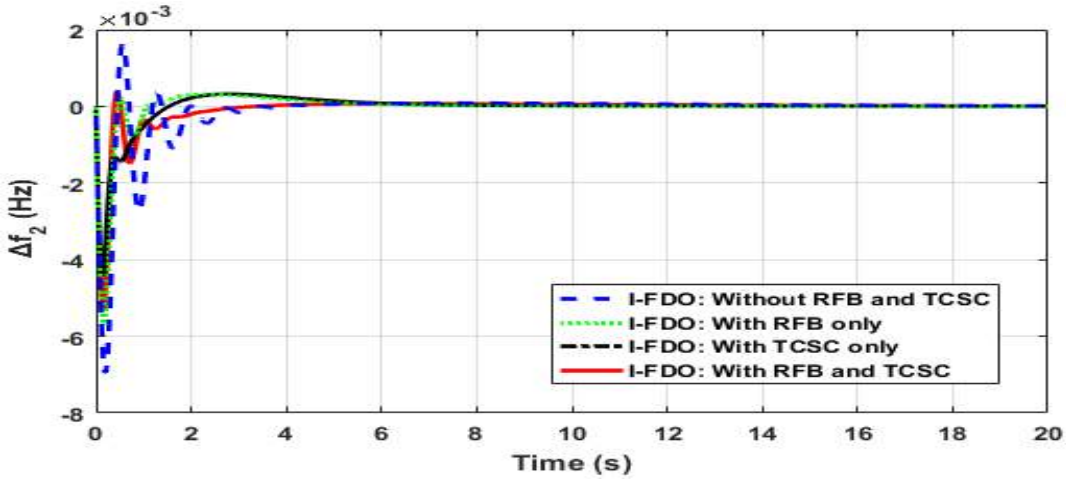

Figure 5.13 Results under poolco based transaction for ΔF2 considering case-3.

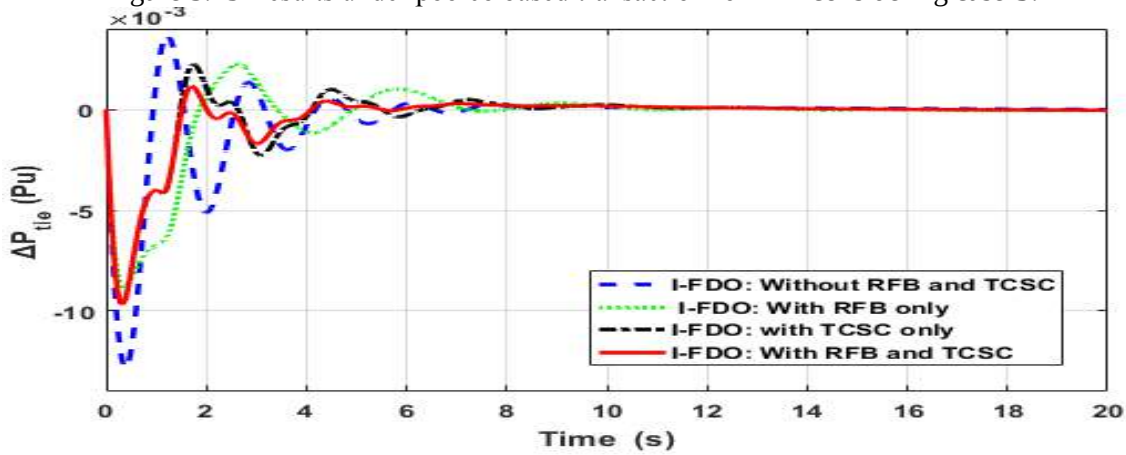

Figure 5.14 Results under poolco based transaction for ΔPtie considering case-3.

5.7.2 Bilateral Base Transaction (BBT)

In BBT, Discos have a power contract with Gencos in their same or different control area. It is presumed that each Discos demand of 0.05 p.u.MW ($\Delta P_{L1} = \Delta P_{L2} = \Delta P_{L3} = \Delta P_{L4}$ =0.05 p.u.MW) power in both areas and hence, the entire load disturbance in area 1 is (ΔP_{d1} =0.1 p.u.MW) and in area 2 is (ΔP_{d2} =0.1 p.u.MW). All Gencos that participated in the AGC task can be represented by below DPM.

$$DPM = \begin{bmatrix} 0.2 & 0.10 & 0.3 & 0.00 \\ 0.2 & 0.25 & 0.1 & 0.16 \\ 0.1 & 0.25 & 0.2 & 0.16 \\ 0.2 & 0.10 & 0.2 & 0.36 \\ 0.1 & 0.20 & 0.1 & 0.16 \\ 0.1 & 0.10 & 0.1 & 0.16 \end{bmatrix} \tag{5.37}$$

The response of the system under BBT is given in Fig 5.15- Fig 5.17 and the overall comparison of mentioned techniques in terms of T_s, O_s and U_s for Δf_1 , Δf_2 and ΔP_{tie} respectively is shown in Table 5.6. When comparing the settling time (T_s) of Fig 5.15- Fig 5.17, the proposed I-FDO tuned FOI-PD controller has quickly reached the T_s at 12.63%, 34.56%, and 23.67% is compared to FOI-PD controller tuned with FA algorithm. When comparing the undershoot (U_s) of FA tuned FOI-PD controller, the proposed FOI-PD controller optimized with I-FDO techniques has efficiently reduced the U_S as 78.30%, 45.67%, and & 49.30% as compared to FA tuned FOI-PD controller. When comparing the overshoot (O_s) of Fig 5.15- Fig 5.17, the proposed I-FDO optimized FOI-PD controller has efficiently reduced the overshoot as 56.03%, 78.06%, and 48.69% is compared to FOI-PD controller tuned with FA algorithm. Hence, it can be inferred, that I-FDO based FOI-PD controller has better performance in terms of T_s, O_s and U_s for Δf_1 , Δf_2 and ΔP_{tie} respectively as compared to FOPID controller optimized with FDO/TLBO/FA.

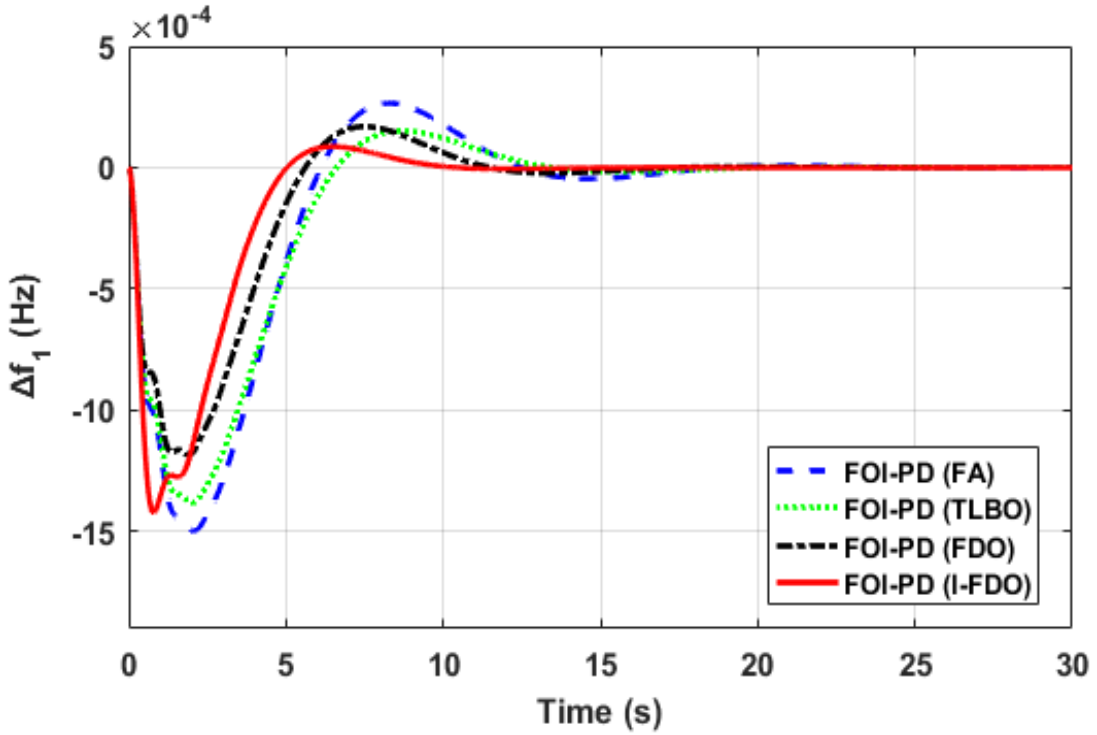

Figure 5.15 Results under bilateral based transaction for ΔF1.

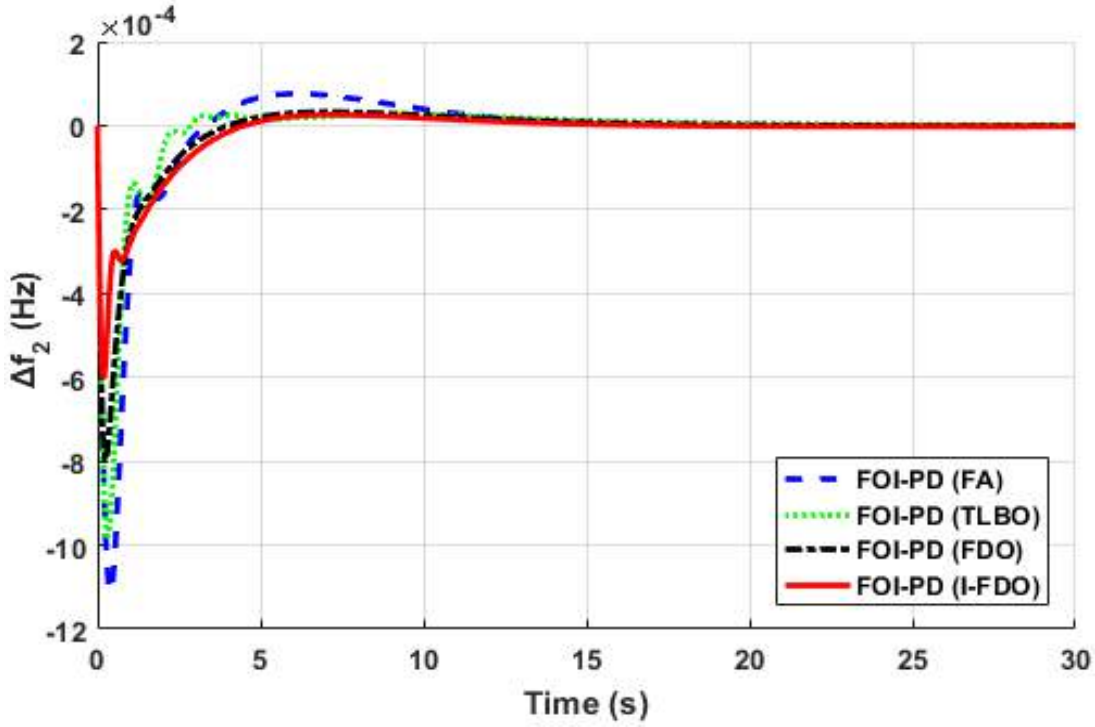

Figure 5.16 Results under bilateral based transaction for ΔF2.

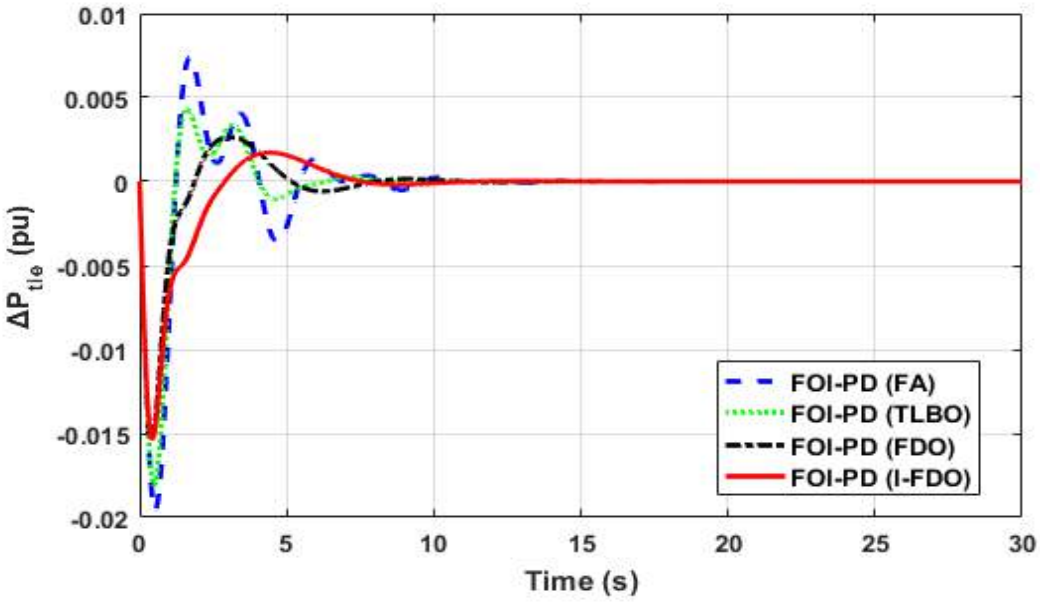

Figure 5.17 Results under bilateral based transaction for ΔPtie.

5.7.3 Contract Violation Based Transaction (CVBT)

In contract violation, Discos need more power than a specified contract which is not contracted out to any Gencos. This uncontracted power must be provided by Gencos to Discos in a similar area. In this scenario, a poolco based transaction is again considered with modification of 10% excess uncontracted power i.e (ΔP_{uc1} =0.1pu.MW) demanded by Disco-1 from area-1 and (ΔP_{uc2} =0.0 pu.MW) from area 2. So, the total load demand (ΔP_{d1}) in Area -1= $\Delta P_{L1} + \Delta P_{L2} + \Delta P_{uc1}$ =0.1+0.1+0.1= 0.3 p.u.MW. Whereas $\Delta P_{d2} = \Delta P_{L3} + \Delta P_{L4} + \Delta P_{uc2}$ =0.1+0.1+0=0.2 p.u.MW. Under contract violation, the dynamic profile of the system is shown in Fig 5.18- Fig 5.20. From Table 5.7 it can be seen that FOI-PD controller with I-FDO tuned method superiorly performs in respect of T_s by (10.34%, 09.54%, and 31.76%), O_s by (78.77%, 57.76%, and 89.36%) and U_s by (14.56%, 3.09%, and 19.56%) for Δf_1, Δf_2 and ΔP_{tie} respectively as compared to FOI-PD controller tuned with FDO

optimization techniques. Similarly, when comparing the overshoot (O_s) of Fig Fig 5.18-Fig 5.20, the proposed I-FDO optimized FOI-PD controller has efficiently reduced the overshoot as 76.22%, 28.16%, and 83.32% is compared to FOI-PD controller tuned with FA algorithm. The settling time of the I-FDO optimized FOI-PD controller is improved by (39.12%, 12.08%, and 41.63%) Δf_1 , Δf_2 and ΔP_{tie} respectively as compared to the FOI-PD controller tuned with the FA algorithm.

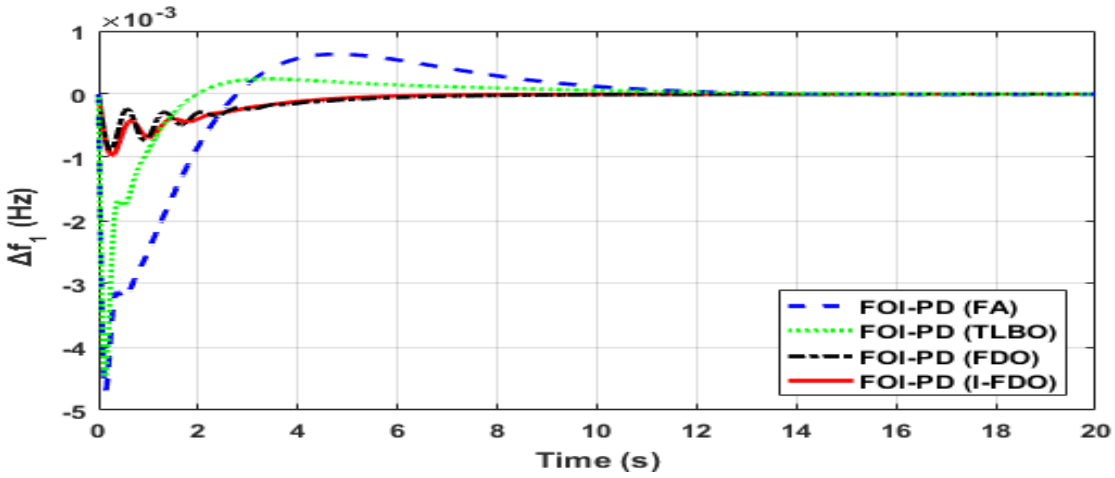

Figure 5.18 Results under contract violation based transaction for ΔF1.

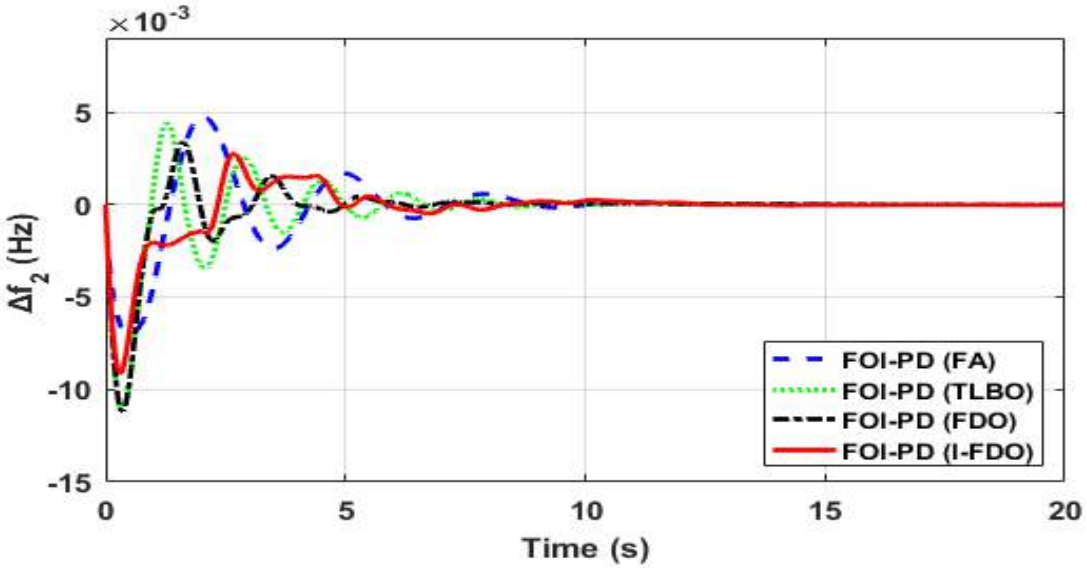

Figure 5.19 Results under contract violation based transaction for ΔF2.

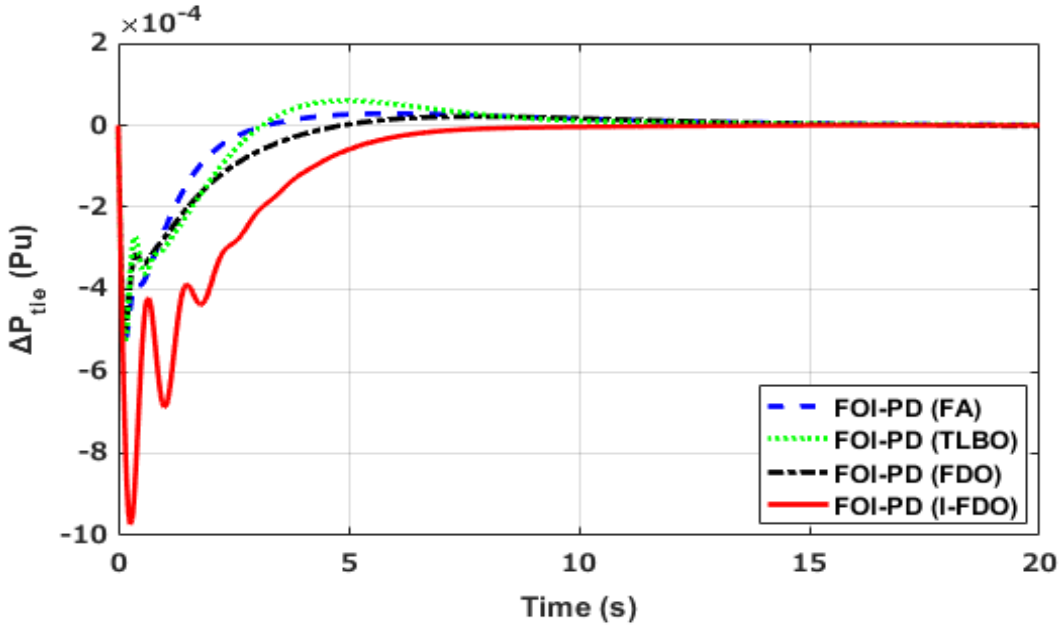

Figure 5.20 Results under contract violation based transaction for ΔPtie.

5.7.4 Sensitivity Analysis/ Robustness

Sensitivity analysis is performed to examine the uncertainty of the power system in dynamic behavior under a nominal condition concerning a certain change in a few of the essential parameters of the system. The purpose of this analysis is to study the robust performance of the controller by varying system parameters. This paper has carried out a sensitivity analysis of some of the system parameters with nominal value by varying the turbine time constant (T_g), synchronizing coefficient (T_{12}), droop constant (R), and governor time constant (T_t) in the range of ± (25%). The results obtained by varying system parameters in the range of ± (25) % are shown in Fig 21- Fig 26. The comparison of various parameters in respect of settling time, undershoot, and overshoot with a change of ± (25) % from their nominal values are specified in Table 5.8. From Fig 5.21- Fig 5. 26, it can be observed that the response of the system plotted for various parameters are almost similar to the nominal values which show that the proposed I-FDO based FOI-PD controller

provides a robust performance within a range of ± (25) % of the system parameters. Furthermore, the optimized values of the proposed controller don't need to be re-tuned for wide-ranging parameters attained at a nominal load with nominal parameters.

Table 5. 6 Comparison performance under BBT in terms of T_s, O_s and U_s.

Controller with Algorithms	**T_s (Settling time)**			**O_s (Overshoot)**			**U_s (Undershoot)**		
	ΔF_1	ΔF_2	ΔP_{tie}	ΔF_1	ΔF_2	ΔP_{tie}	ΔF_1	ΔF_2	ΔP_{tie}
FOI-PD (I-FDO)	**17.6**	18.3	**11.7**	**0.000085**	**0.0000257**	0.00171	-0.00410	**-0.00060**	-0.0151
FOI-PD (FDO)	18.2	19.4	12.8	0.000168	0.0000326	0.00262	-0.00117	-0.00080	-0.0151
FOI-PD (TLBO)	21.1	19.9	13.2	0.000151	0.0000276	0.00429	-0.00137	-0.00098	-0.0180
FOI-PD (FA)	23.2	**12.1**	14.1	0.000225	0.0000765	0.00741	-0.00149	-0.00111	-0.0195
TID(hTBO-PS) [89]	27.9	26.1	12.3	0.05990	0.0591000	0.00116	-0.39500	-0.42160	**-0.0123**
MID(hDE-PS) [87]	20.1	18.5	14.2	0.00100	0.0016000	**0.00090**	**-0.00100**	-0.00150	-0.0800

Table 5.7 Comparison performance under contract violation in terms of T_s, O_s and U_s.

Controller techniques	**T_s (Settling time)**			**O_s (Overshoot)**			**U_s (Undershoot)**		
	ΔF_1	ΔF_2	ΔP_{tie}	ΔF_1	ΔF_2	ΔP_{tie}	ΔF_1	ΔF_2	ΔP_{tie}
FOI-PD (I-FDO)	**11.0**	**13.8**	**12.8**	**0.00000**	0.00273	**0.00000**	-0.00097	**-0.0068**	**-0.0009**
FOI-PD (FDO)	11.0	13.9	13.3	0.00000	0.00335	0.00002	**-0.00088**	-0.0068	-0.00049
FOI-PD (TLBO)	16.4	17.3	14.4	0.00063	0.00442	0.00002	-0.00468	-0.0081	-0.00052
FOI-PD (FA)	16.9	17.7	15.3	0.00024	0.00473	0.00006	-0.00448	-0.0082	-0.00053
TID (hTBO-PS) [89]	24.5	24.6	18.7	0.02310	0.03520	0.03900	-0.54960	-0.6898	-0.07590
MID (hDE-PS) [87]	24.3	22.7	19.0	0.00160	**0.00210**	0.00100	-0.00234	-0.0095	-0.01890

Table 5.8 Results of Sensitivity analysis for the proposed I-FDO based FOI-PD controller considering PBT.

Parameter	% Change	T_s (Settling time)			O_s (overshoot)			U_s (Undershoot)		
		ΔF_1	ΔF_2	ΔP_{tie}	ΔF_1	ΔF_2	ΔP_{tie}	ΔF_1	ΔF_2	ΔP_{tie}
R	+25	6.78	6.38	12.72	0.0006	0.00068	0.000323	-0.00610	-0.00240	-0.00315
	-25	7.90	8.01	12.73	0.0005	0.00047	0.000276	-0.00600	-0.00236	-0.00313
Tg	+25	6.74	6.38	13.01	0.0009	0.00037	0.000296	-0.00693	-0.00713	-0.00489
	-25	7.91	8.03	13.03	0.0009	0.00030	0.000289	-0.00678	-0.00913	-0.00482
Tt	+25	6.14	6.10	12.80	0.0008	0.00014	0.000310	-0.00731	-0.00780	-0.00361
	-25	8.10	7.80	12.79	0.0007	0.00017	0.000311	-0.00725	-0.00740	-0.00361
T_{12}	+25	6.17	6.09	13.10	0.0006	0.00032	0.000315	-0.00623	-0.00830	-0.00251
	-25	8.10	7.82	13.08	0.0006	0.00031	0.000316	-0.00618	-0.00840	-0.00257

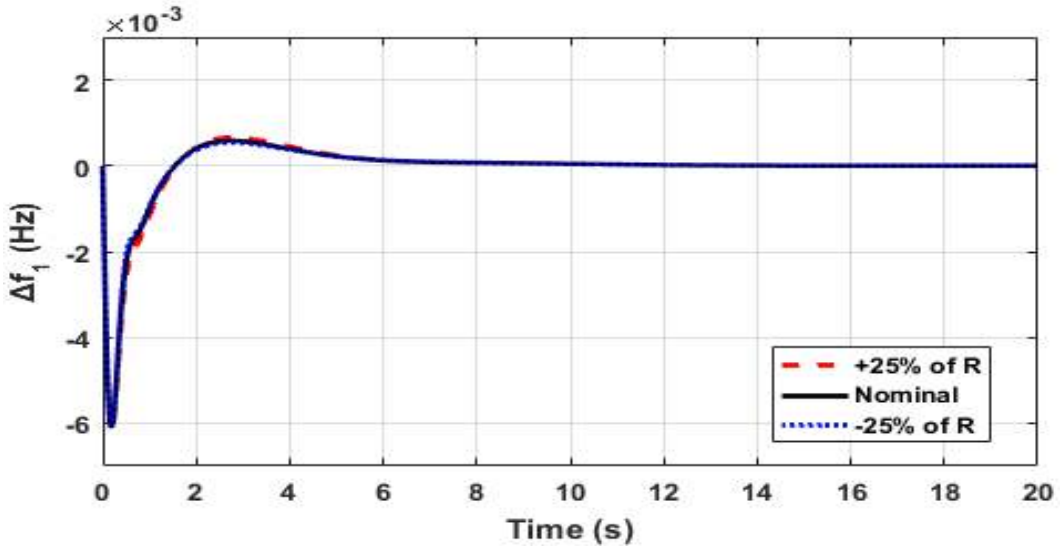

Figure 5.21 System response with variation of R for ΔF1.

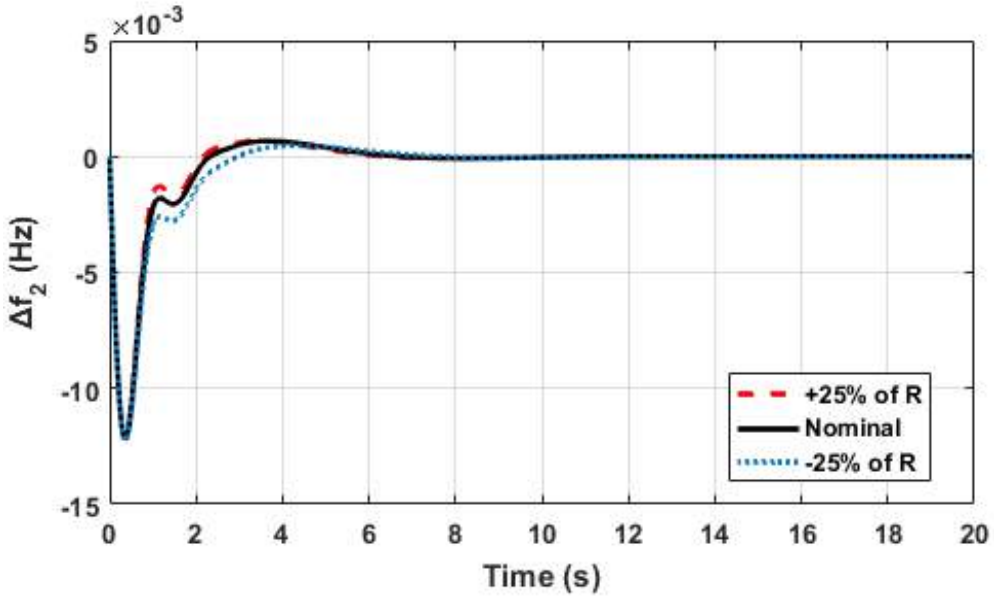

Figure 5.22 System response with variation of R for ΔF2.

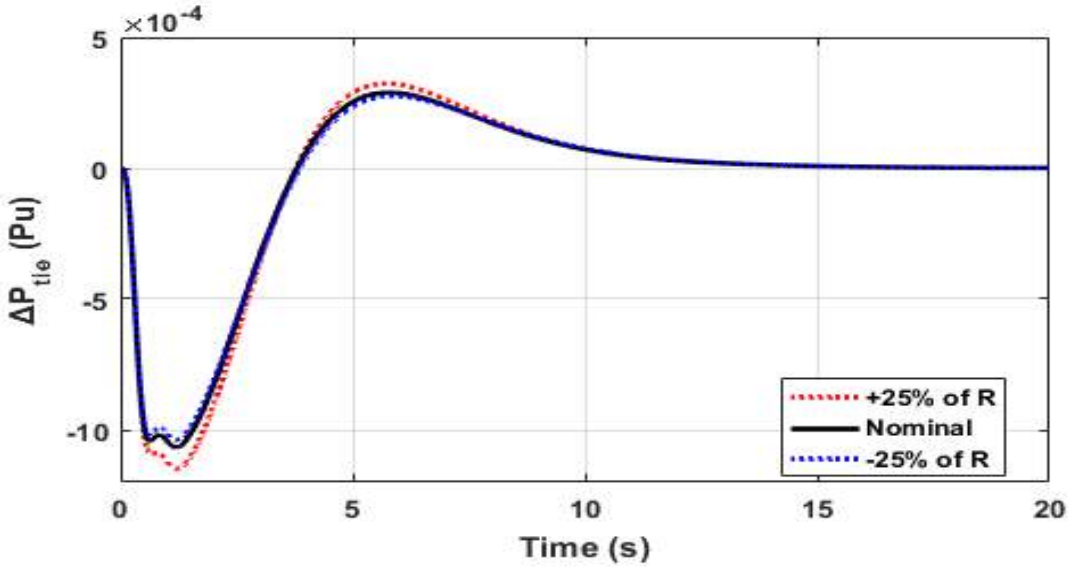

Figure 5.23 System response with variation of R for ΔPtie.

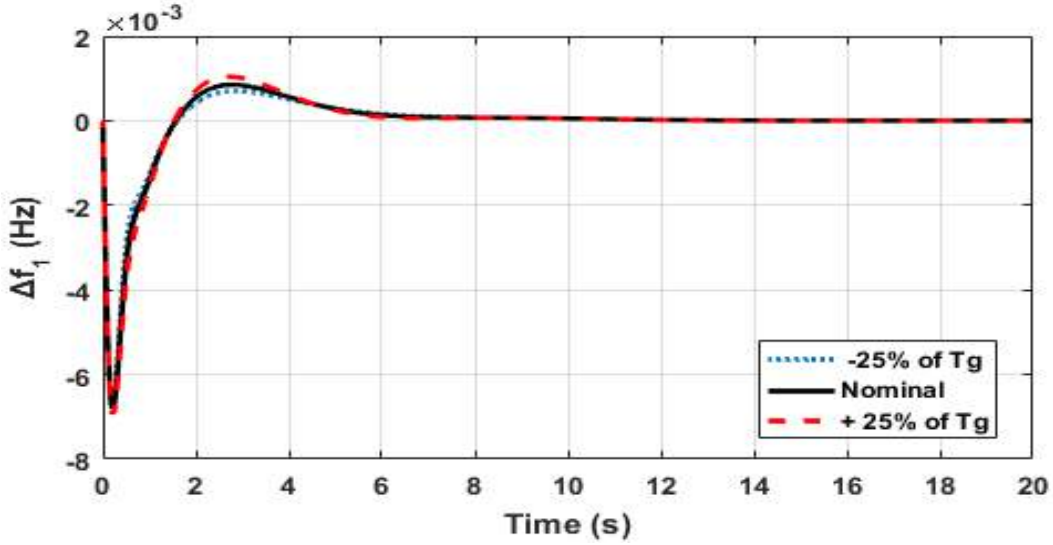

Figure 5.24 System response with variation of Tg for ΔF1.

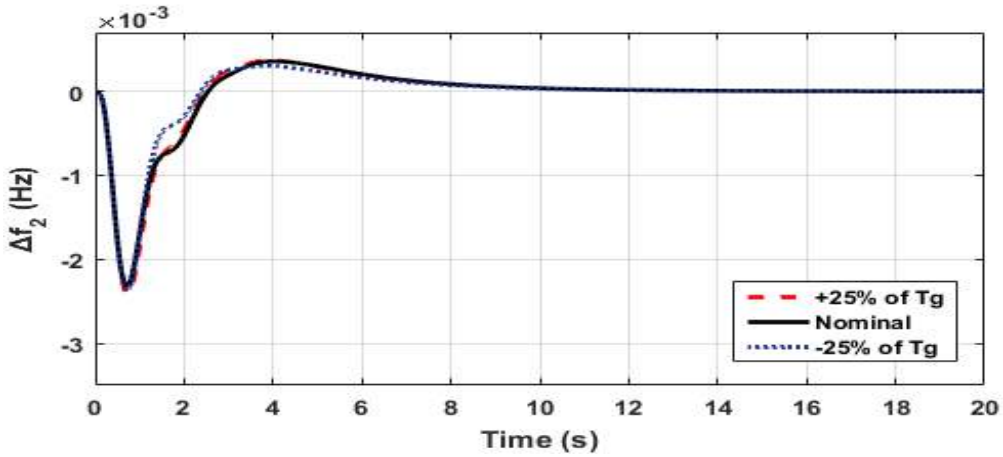

Figure 5.25 System response with variation of Tg for ΔF2.

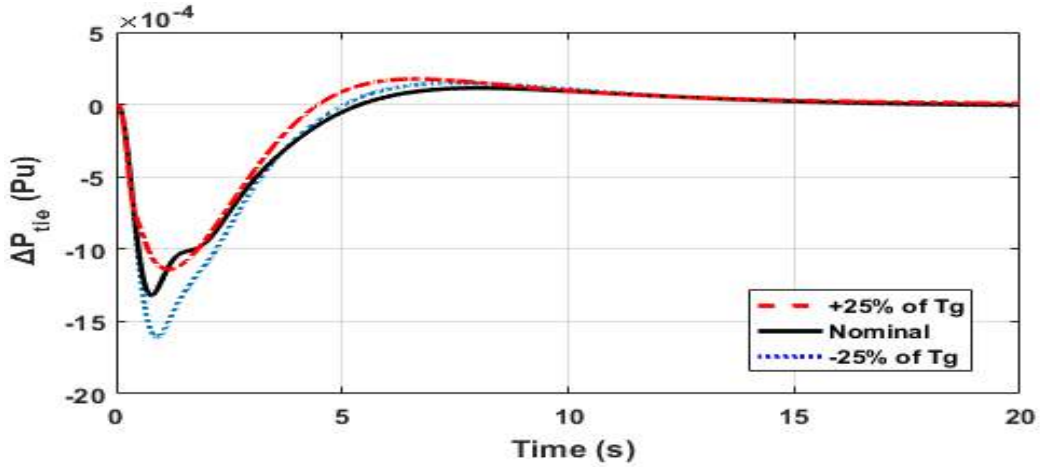

Figure 5.26 System response with variation of Tg for ΔPtie.

Chapter 6. Conclusion and Future Work

This chapter includes a brief survey of the main contributions made from the analysis work discussed in the dissertation. In this dissertation, various strategies on multi-area multi-generation restructured and conventional power systems are discussed. In this study, to solve AGC issues in deregulated and conventional power network systems, some new control methods were proposed. To compare the outcomes of the proposed controllers, the analysis is conducted on various conventional and restructured multi-area power systems available in the literature. The outcome of the study, carried out in this dissertation are as follows:

6.1.1 AGC of Two Area Interconnected Linear Power System

PID and modified form of PID controller known as I-PD controllers have been designed and successfully implemented to handle Automatic Generation Control (AGC) of multi-source with multi-area Interconnected Power System (IPS). Fitness Dependent Optimizer (FDO) algorithm has been used to attain the gains of these controllers. The effectiveness of FDO based controllers i.e. FDO-PID and FDO-I-PD are evaluated on two-area with reheat thermal, gas, and hydropower system individually and then collectively with all three generation units present in the system. The transient response performance achieved by the designed controllers with 1% step load perturbation is presented and quantified in detail via simulations and compared with several other controller techniques. The comparison of outcomes indicates that FDO-PID and FDO-I-PD controllers provide superior results in respect of Settling time (T_s), overshoot (O_{sh}), and undershoot (U_{sh}).

- It is observed that FDO-I-PD as compared to DE-PID eliminates O_{sh} in load frequency of both areas and tie-line power, while 83.38%, 80.24%, and 77.54% improvement in T_s in area-1 and area-2 load frequency, and tie-line power are achieved respectively.

- Similarly, FDO-I-PD also provides an improvement of 83.1%, 77.4%, and 87.8% in U_{sh} as compared to DE-PID. The results further show that FDO- I-PD as compared to LUS-PID provides a significant improvement of 75.24%,64.28%, and 66.98% in T_s of load frequency for ΔF_1, ΔF_2, and ΔP_{tie} respectively, while an improvement in U_{sh} of 63.23%,49.43%, and 57.58% are achieved for load frequency of ΔF_1, ΔF_2, and ΔP_{tie} respectively.

- The supremacy of FDO based PID and I-PD controllers proposed in this work demonstrate the capability of these controllers to tackle the automatic generation control problem effectively with oscillation-free and quick response.

6.1.2 AGC of Two Area Multi-Source Interconnected Power System with Non-Linearities.

The two areas of multi-source power systems with diverse generation sources such as reheat thermal, gas, and hydropower system with various constraints including GDB, GRC, TD, and BD have been considered. The gains of PID/I-PD controllers are tuned by a recently developed meta-heuristic technique known as Fitness Dependent Optimizer (FDO). The transient response performance attained by the proposed controller provides a significant improvement in respect of Overshoot (Osh), Undershoot (Ush), and Settling Time (Ts) as compared to other techniques such as FA, TLBO and PSO.

- It is perceived that the FDO-PID controller improved results as compared to FA/TLBO/PSO-PID in terms of Ts, Osh and Ush for ΔF_1, ΔF_2, and ΔP_{tie} respectively.
- Similarly, FDO based I-PD controller shows a remarkable improvement in terms of T_S, Osh and Ush compared to PSO/FA/TLBO-PID controller for ΔF_1, ΔF_2, and ΔP_{tie} respectively.
- The efficacy of FDO based PID /I-PD controllers demonstrate the competency of these controllers to tackle the AGC problem effectively with sustained oscillation and quick response.

6.1.3 AGC of Two Area Multi-Source Deregulated Power System.

The modified form of FOPID controller known as the FOI-PD controller is designed and developed for AGC of two areas, six-generation units under the deregulated environment with the inclusion of various non-linearities including GDB, BD, TD, and GRC. Improved–Fitness Dependent Optimizer (I-FDO) meta-heuristic algorithm is used to optimize the parameters of the proposed controller. Besides, the dynamic response of the system is improved by incorporating RFB in each area and TCSC in series with the tie-lines.

- From simulation results, it can be observed that I-FDO based tuned FOI-PD controller as compared to hDE-PS based MID controller provides a significant improvement of 76.85%, 26.42%, and 21.43% for both areas and in tie-line power, while effectively reduced peak overshoot of 97.80%, 85.88%, and 37.00% and undershoot of 6.00%, 70.13%, 75.00% for Δf_1, Δf_2 and ΔP_{tie} respectively.

- Similarly, I-FDO based FOI-PD controller also provides an improvement of 53.62%, 4.96%, and 6.37% in T_s for load frequency of Δf_1, Δf_2 and ΔP_{tie} respectively as compared hTLBO-PS based TID controller.
- Finally, the robustness of the FOI-PD controller is evaluated by varying the system parameters from nominal values and the results show that the gains of the FOI-PD controller have not been reset when the system parameters or load conditions changed.

6.2 Future Work

In this study, some good designs of AGC controllers for AGC power systems interconnected in conventional and restructured modes were proposed. Suggested controllers showed very good results. However, numerous areas require more study to develop AGC controller designs for different types of power system structures which are given as below:

1. The current research is limited to two area conventional and deregulated power systems, but this analysis can be expanded to three/four / five areas of power systems at the cost of increasing complexity.
2. In this work, I-PD and PID controllers are developed and optimized by employing the FDO algorithm. Similarly, FOPID and FOI-PD controllers are optimized with the I-FDO algorithm. However, some fruitful outcomes may be obtained by employing some new meta-heuristic algorithms.
3. Any other types of additional controllers, such as neural-fuzzy, two degrees of freedom (2-DOF)-FOPID, fuzzy tilt integral derivative (FTID), (2-DOF-

FOFPID), etc., may be used in future studies on restructured and conventional power systems in combination with some modern tuning techniques.

4. In the future, one may can use the power system with other types of source generation like diesel, nuclear, and geothermal, etc.
5. The effect of various energy storage and FACTS devices can be studied to solve AGC multi-area multi-generation restructured power systems.
6. The current study is conducted only on LFC of two area network system but, in future the combined effect of LFC and AVR can be implemented for conventional and restructured power system.
7. AGC controllers are designed in continuous mode, but discrete mode AGC controllers can be studied in the future.
8. The present work can be implemented practically for regulated and deregulated power system by incorporating all non-linearities in the AGC system.

BIBLIOGRAPHY

[1] Y. Arya, “Impact of hydrogen aqua electrolyzer-fuel cell units on automatic generation control of power systems with a new optimal fuzzy TIDF-II controller,” *Renew. Energy.*, vol. 139, pp. 468–482, 2019.

[2] Y. Arya, P. Dahiya, E. Çelik, G. Sharma, H. Gözde, and I. Nasiruddin, “AGC performance amelioration in multi-area interconnected thermal and thermal-hydro-gas power systems using a novel controller,” *Eng. Sci. Technol. an Int. J.*, vol. 24 no. 2, pp. 384-396, 2020.

[3] A. Daraz, S. Abdullah, M. Ihsan, and U. Haq, "Modified PID Controller forAutomatic Generation Control of Multi-Source Interconnected Power System Using Fitness De pendent Optimizer," *Plos one.*, vol. 8, no.5, pp.1-31, 2020.

[4] W. Tasnin and L. C. Saikia, “Impact of renewables and FACT device on deregulated thermal system having sine cosine algorithm optimised fractional order cascade controller,” *IET Renew. Power Gener.*, vol. 13, no. 9, pp. 1420–1430, 2019.

[5] Y. Arya, “Effect of electric vehicles on load frequency control in interconnected thermal and hydrothermal power systems utilising CF- FOIDF controller,” *IET Generation, Transmission & Distribution.*, vol. 14, no. 14, pp. 1420–1430, 2020.

[6] K. P. S. Parmar, “Load Frequency Control of Multi-Source Power System with Redox Flow Batteries: An Analysis,” *Int. J. Comput. Appl.*, vol.88, no.8, 2014.

[7] N. Hakimuddin, I. Nasiruddin, T. S. Bhatti, and Y. Arya, “Optimal Automatic Generation Control with Hydro , Thermal , Gas , and Wind Power Plants in 2- Area

Interconnected Power System Optimal Automatic Generation Control with Hydro , Thermal , Gas , and Wind Power Plants in," *Electr. Power Components Syst.*, vol. 58, no. 6, pp. 558–571, 2020.

[8] Y. Arya, "incorporating energy storage units via optimal fractional-order fuzzy PID AGC of restructured multi-area multi-source hydrothermal power systems incorporating energy storage units via optimal fractional-order fuzzy PID controller," *Neural Comput. Appl.*, vol. 31, no. 3, pp. 851–872, 2019.

[9] A. Daraz, S. A. Malik, and A. Haq, "Review of Automatic Generation Control For Multi- Source Interconnected Power System Under Deregulated Environment," *4th Int. Conf. Power Gener. Syst. Renew. Energy Technol.*, vol. 4, pp. 1–5, 2018.

[10] Y. Arya, "AGC of restructured multi-area multi-source hydrothermal power systems incorporating energy storage units via optimal fractional-order fuzzy PID controller," *Neural Comput. Appl.*, vol. 31, no. 3, pp. 851–872, 2019.

[11] Y. Arya, "Impact of ultra - capacitor on automatic generation control of electric energy systems using an optimal FFOID controller," *Int J Energy Res.*, vol.43, no.12 pp. 8765–8778, 2019.

[12] Y. Arya, "Effect of energy storage systems on automatic generation control of interconnected traditional and restructured energy systems," *Int J Energy Res.*, vol.43,no.13, pp. 6475-6493, 2019.

[13] A. Fathy and A. M. Kassem, "Antlion optimizer-ANFIS load frequency control for multi-interconnected plants comprising photovoltaic and wind turbine," *ISA Trans.*, vol. 87, pp. 282–296, 2019.

[14] Y. Arya, "AGC of PV-thermal and hydro-thermal energy systems using CES and a new multi- stage FPIDF-(1+PI) controller," *Renew. Energy.*, vol. 134, pp.796-806, 2018.

[15] Y. Arya, "Impact of ultra capacitor on automatic generation control of electric energy systems using an optimal FFOID controller," *Int J Energy Res.*, vol.43, no.12 pp. 8765–8778, 2019.

[16] U. Raj, and R.shankar, "Deregulated Automatic Generation Control using Novel Opposition- based Interactive Search Algorithm Cascade Controller Including Distributed Generation and Electric Vehicle," *Iran. J. Sci. Technol. Trans. Electr. Eng.*, vol. 44, no. 3, pp. 1233–1251, 2020.

[17] N. Patel, A. Jadav, P. Modi, and S. Choubey, "Literature Review on Automatic Generation Control," *Int. Res. J. Eng. Technol.*, vol. 4, no. 3, pp. 719–721, 2017.

[18] Y. Arya, "A new optimized fuzzy FOPI-FOPD controller for automatic generation control of electric power systems," *J. Franklin Inst.*, vol. 356, no. 11, pp. 5611–5629, 2019.

[19] B. A. Sutterfield, G. Caprez and J. Hanelineand, "Automatic generation control for hydro System," *IEEE Trans. Energy Convers.*, vol. 18, no.6, 1988.

[20] C.T. Pan; C.M. Liaw, "An adaptive controller for power system load-frequency control," *JIEEE Trans. Power Syst.*, vol. 4, no. 1, pp. 122–128, 1989.

[21] K. S. S. Ramakrishna and T. S. Bhatti, "Automatic generation control of single area power system with multi-source power generation," *Proc. Inst. Mech. Eng. Part A*

J. Power Energy, vol. 222, no 1, 2008.

[22] Y. L. Abdel-Magid and M. M. Dawoud, "Optimal AGC tuning with genetic algorithms," *Electr. Power Syst. Res19*, vol. 38, no. 3, pp. 231–235, 1996.

[23] G. Kusic, J. Sutterfield, A. Caprez, J. Haneline, B. Bergman, "Automatic generation control for hydro systems.," *IEEE Trans. Energy Convers.*,vol.12, no. 3, pp. 33–39, 1988.

[24] K. P. S. Parmar, S. Majhi, and D. P. Kothari, "Load frequency control of a realistic power system with multi-source power generation," *Int. J. Electr. Power Energy Syst.*, vol. 42, no. 1, pp. 426–433, 2012.

[25] D. Guha, P. Kumar, and S. Banerjee, "Load frequency control of large scale power system using quasi-oppositional grey wolf optimization algorithm," *Eng. Sci. Technol. an Int. J.*, vol. 19, no. 4, pp. 1693–1713, 2016.

[26] B. K. Sahu and M. K. Debnath, "A novel application of ALO-based fractional order fuzzy PID controller for AGC of power system with diverse sources of generation," *International Journal of Electrical Engineering & Education.*, vol.1, no. 1,pp. 1-23, 2019.

[27] B. Mohanty, S. Panda, and P. K. Hota, "Controller parameters tuning of differential evolution algorithm and its application to load frequency control of multi-source power system," *Int. J. Electr. Power Energy Syst.*, vol. 54, pp. 77–85, 2014.

[28] B. Kumar, T. Kumar, J. Ranjan, S. Panda, and S. Kumar, "A novel hybrid LUS – TLBO optimized fuzzy-PID controller for load frequency control of multi-source

power system," *Int. J. Electr. Power Energy Syst.*, vol. 74, pp. 58–69, 2016.

[29] S. Debbarma, L. C. Saikia, and N. Sinha, "Automatic generation control using two degree of freedom fractional order PID controller," *Int. J. Electr. Power Energy Syst.*, vol. 58, pp. 120–129, 2014.

[30] V. Veerasamy et al., "A Hankel Matrix Based Reduced Order Model for Stability Analysis of Hybrid Power System Using PSO-GSA Optimized Cascade PI-PD Controller for Automatic Load Frequency Control," *IEEE Access.*, vol. 8, 2020.

[31] P. Dash, L. Chandra, and N. Sinha, "Flower Pollination Algorithm Optimized PI-PD Cascade Controller in Automatic Generation Control of a Multi-area Power System," *Int. J. Electr. Power Energy Syst.*, vol. 82, pp. 19–28, 2016.

[32] E. Sahin, "Design of an optimized fractional high order differential feedback controller for load frequency control of a multi-area multi-source power system with nonlinearity," *IEEE Access*, vol. 8, pp. 12327-12342, 2020.

[33] G. Chen, "An Improved ACO Algorithm Optimized Fuzzy PID Controller for Load Frequency Control in Multi Area Interconnected Power Systems," *IEEE Access*, vol. 8, pp. 6429–6447, 2020.

[34] C. K. Shiva and V. Mukherjee, "Automatic generation control of interconnected power system for robust decentralized random load disturbances using a novel quasi-oppositional harmony search algorithm," *Int. J. Electr. Power Energy Syst.*, vol. 73, pp. 991–1001, 2015.

[35] Y. Arya, "A novel CFFOPI-FOPID controller for AGC performance enhancement

of single and multi-area electric power systems," *ISA Trans.*, vol. 100, pp. 126–135, 2020.

[36] B. . K. Sahoo. P. C. Sahoo, R C Prusty, "Modified sine cosine algorithm-based fuzzy-aided PID controller for automatic generation control of multiarea power systems," *Soft Comput.*, vol. 12, no. 2, 2020.

[37] D. Guha, P. Kumar, and S. Banerjee, "Application of backtracking search algorithm in load frequency control of multi-area interconnected power system," *Ain Shams Eng. J.*, vol. 9, no. 2, pp. 257–276, 2018.

[38] Y. Arya, "Improvement in automatic generation control of two-area electric power systems via a new fuzzy aided optimal PIDN-FOI controller," *ISA Trans.*, vol. 80, no. 4, pp. 475–490, 2018.

[39] K. S. Rajesh, S. S. Dash, and R. Rajagopal, "Hybrid improved firefly-pattern search optimized fuzzy aided PID controller for automatic generation control of power systems with multi-type generations," *Swarm Evol. Comput.*, vol. 44, no. March 2018, pp. 200–211, 2019.

[40] R. K. Sahu, T. S. Gorripotu, and S. Panda, "Automatic generation control of multi-area power systems with diverse energy sources using Teaching Learning Based Optimization algorithm," *Eng. Sci. Technol. an Int. J.*, vol. 19, no. 1, pp. 113–134, 2016.

[41] H. H. Ali, A. M. Kassem, M. Al-dhaifallah, and A. Fathy, "Multi-verse Optimizer for Model Predictive Load Frequency Control of Hybrid Multi- Interconnected Plants Comprising Renewable Energy," *IEEE Acess.*, vol. 08, 2020.

[42] P. Dash, L. C. Saikia, and N. Sinha, “Comparison of performances of several Cuckoo search algorithm based 2DOF controllers in AGC of multi-area thermal system,” *Int. J. Electr. Power Energy Syst.*, vol. 55, pp. 429–436, 2014.

[43] R. K. Sahu, S. Panda, and U. K. Rout, “DE optimized parallel 2-DOF PID controller for load frequency control of power system with governor dead-band nonlinearity,” *Int. J. Electr. Power Energy Syst.*, vol. 49, no. 1, pp. 19–33, 2013.

[44] B. Mohanty and P. K. Hota, “A hybrid chemical reaction-particle swarm optimisation technique for automatic generation control,” *J. Electr. Syst. Inf. Technol.*, vol. 08, pp. 1–16, 2017.

[45] R. Kumar *et al.*, “Design and analysis of tilt integral derivative controller with filter for load frequency control of multi-area interconnected power systems,” *ISA Trans.*, vol. 61, pp. 251–264, 2016.

[46] M. R. Sathya and M. Mohamed Thameem Ansari, “Design of biogeography optimization based dual mode gain scheduling of fractional order PI load frequency controllers for multi source interconnected power systems,” *Int. J. Electr. Power Energy Syst.*, vol. 83, pp. 364–381, 2016.

[47] M. H. Khooban and T. Niknam, “Electrical Power and Energy Systems A new intelligent online fuzzy tuning approach for multi-area load frequency control : Self Adaptive Modified Bat Algorithm,” *Int. J. Electr. Power Energy Syst.*, vol. 71, pp. 254–261, 2015.

[48] M. Raju, L. C. Saikia, and N. Sinha, “ Automatic generation control of a multi-area system using ant lion optimizer algorithm based PID plus second order derivative

controller," *Int. J. Electr. Power Energy Syst.*, vol. 80, pp. 52–63, 2016.

[49] A. Delassi, S. Arif, and L. Mokrani, "Load frequency control problem in interconnected power systems using robust fractional PIλD controller," *Ain Shams Eng. J.*, vol. 12, no. 2, 2015.

[50] M. K. Debnath, T. Jena, and R. K. Mallick, "Optimal design of PD-Fuzzy-PID cascaded controller for automatic generation control," *Cogent Eng.*, vol. 91, no. 1, pp. 1–27, 2017.

[51] H. M. Hasanien and A. A. El-fergany, "Salp swarm algorithm-based optimal load frequency control of hybrid renewable power systems with communication delay and excitation cross- coupling effect," *Electr. Power Syst. Res.*, vol. 176, no. July, p. 105938, 2019.

[52] A. K. Barisal, T. K. Panigrahi, and S. Mishra, "A Hybrid PSO-LEVY Flight Algorithm Based Fuzzy PID Controller for Automatic Generation Control of Multi Area Power Systems," *Int. J. Energy Optim. Eng.*, vol. 6, no. 2, pp. 42–63, 2017.

[53] M. G. M. Alizadeh, and S. Farahani, "PID controller adjustment using chaotic optimisation algorithm for multi-area load frequency control," *IET Ccntrol Theory & Applications.*, vol. 6, no. 13, pp. 1984–1992, 2012.

[54] S. Gupta, G. Shankar, K. Kumari and S. Kumari, "Load Frequency Control using BAT Algorithm," 1st International Conference on Power Electronics, Intelligent Control and Energy Systems (ICPEICES)., pp. 1–5, 2016.

[55] A. Behera, T. K. Panigrahi, S. Member, P. K. Ray, S. Member, and A. K. Sahoo, "A

Novel Cascaded PID Controller for Automatic Generation Control Analysis With Renewable Sources," *IEEE/CAA Journal of Automatica Sinica.*, vol. 6, no. 6, pp. 1438–1451, 2019.

[56] S. Debbarma, L. C. Saikia, and N. Sinha, "Automatic generation control using two degree of freedom fractional order PID controller," *Int. J. Electr. Power Energy Syst.*, vol. 58, no. 1, pp. 120–129, 2014.

[57] K. Naidu, H. Mokhlis, A. H. A. Bakar, V. Terzija, and H. A. Illias, "Application of firefly algorithm with online wavelet filter in automatic generation control of an interconnected reheat thermal power system," *Int. J. Electr. Power Energy Syst.*, vol. 63, no. 3, pp. 401–413, 2014.

[58] D. Guha, P. Kumar, and S. Banerjee, "Symbiotic organism search algorithm applied to load frequency control of multi-area power system," *Energy Syst.*, vol. 9, no. 2, pp. 439–468, 2018.

[59] A. Mishra and G. V. Nagesh, "Congestion management of deregulated power systems by optimal setting of Interline Power Flow Controller using Gravitational Search algorithm," *J. Electr. Syst. Inf. Technol.*, vol. 4, no. 1, pp. 198–212, 2017.

[60] S. A. P. Melba and M. M. Willjuice, "Automatic generation control of a multi-area power system with renewable energy source under deregulated environment : adaptive fuzzy logic-based differential evolution (DE) algorithm," *Soft Comput.*, vol. 23, no. 22, pp. 12087–12101, 2019.

[61] J. Morsali, K. Zare, and M. T. Hagh, "Comparative performance evaluation of fractional order controllers in LFC of two-area diverse-unit power system with

considering GDB and GRC effects," *J. Electr. Syst. Inf. Technol.*, vol.13, no.6, 2017.

[62] A. A. El-fergany and M. A. El-hameed, "Efficient frequency controllers for autonomous two-area hybrid microgrid system using social-spider optimiser," *IET, Gen, Tran, and Distribution.,* vol. 11, pp. 637–648, 2017.

[63] S. K. Pandey, S. R. Mohanty, and N. Kishor, "A literature survey on load – frequency control for conventional and distribution generation power systems," *Renew. Sustain. Energy Rev.*, vol. 25, pp. 318–334, 2013.

[64] D. Rerkpreedapong, "Novel Control Design and Strategy for Load Frequency Control in Restructured Power Systems," PhD thesis,*West Virginia University*, 2003.

[65] M. Bhavani, K. Selvi, and R. Durga, "A Novel Approach for a Two Area Load Frequency Control in a Competitive Electricity Market Adopting Unscheduled Interchange Price," no. May, pp. 1155–1166, 2016.

[66] T. S. Gorripotu, R. K. Sahu, and S. Panda, "AGC of a multi-area power system under deregulated environment using redox flow batteries and interline power flow controller," *Eng. Sci. Technol. an Int. J.*, vol. 18, no. 4, pp. 555–578, 2015.

[67] A. Prakash, S. Murali, R. Shankar, and R. Bhushan, "HVDC tie-link modeling for restructured AGC using a novel fractional order cascade controller," *Electr. Power Syst. Res.*, vol. 170, no. 18, pp. 244–258, 2019.

[68] K. P. S. Parmar, S. Majhi, and D. P. Kothari, "LFC of an interconnected power system with multi-source power generation in deregulated power environment," *Int.*

J. Electr. Power Energy Syst., vol. 57, pp. 277–286, 2014.

[69] P. Sharma *et al.*, "A Novel Hybrid Salp Swarm Differential Evolution Algorithm Based 2DOF Tilted-Integral-Derivative Controller for Restructured AGC A Novel Hybrid Salp Swarm Differential Evolution Algorithm Based 2DOF Tilted-Integral-De," *Electr. Power Components Syst.*, vol. 47, no. 19, pp. 1775–1790, 2020.

[70] S. B. Shree and N. Kamaraj, "Hybrid Neuro Fuzzy approach for automatic generation control in restructured power system," *Int. J. Electr. Power Energy Syst.*, vol. 74, pp. 274–285, 2016.

[71] A. Prakash, K. Kumar, and S. K. Parida, "PIDF (1 + FOD) controller for load frequency control with SSSC and AC – DC tie-line in deregulated environment," *IET Generation, Transmission & Distribution.*, vol.14, no.14, pp. 2751–2762, 2020.

[72] S. Muthuraman, A. S. Priyadarsin, and S. Arumugom, "PSO Optimized Load Frequency Control of Two Area Power System in Deregulated Environment," *Electrical & Electronic Systems.*, vol. 5, no. 4, 2016.

[73] A. G. D. Kumar and N. V Ramana, "A Wavelet based Multi Resolution Controller for Load frequency Control of Multi Area Deregulated Power System," *3rd International Conference on Electrical, Electronics, Engineering Trends, Communication, Optimization and Sciences (EEECOS 2016).*, pp. 617–621, 2016.

[74] I. J. Electron, C. Aeü, S. Hamid, and D. Farsi, "Analysis of Load Frequency Control in a restructured multi-area power system with the Kalman filter and the LQR controller," *Int. J. Electron. Commun.*, vol. 86, no.4, pp. 25–46, 2018.

[75] G. T. C. Sekhar, R. Kumar, A. K. Baliarsingh, and S. Panda, “Load frequency control of power system under deregulated environment using optimal firefly algorithm,” *Int. J. Electr. Power Energy Syst.*, vol. 74, pp. 195–211, 2016.

[76] M. Ma, C. Zhang, X. Liu, and H. Chen, “Distributed Model Predictive Load Frequency Control of the Multi-Area Power System after Deregulation,” *IEEE Trans. Ind. Electron.*, vol. 64, no. 6, pp. 5129–5139, 2017.

[77] P. K. Hota and B. Mohanty, “Automatic generation control of multi source power generation under deregulated environment,” *Int. J. Electr. Power Energy Syst.*, vol. 75, pp. 205–214, 2016.

[78] A. Ghasemi-marzbali, “Multi-area multi-source automatic generation control in deregulated power system,” *Energy.*, vol. 201, pp. 117667, 2020.

[79] A. Pappachen and A. P. Fathima, “NERC’s control performance standards based load frequency controller for a multi area deregulated power system with ANFIS approach,” *Ain Shams Eng. J.*, vol. 9, no. 4, pp. 2399-2414, 2017.

[80] M. Nandi, C. K. Shiva, and V. Mukherjee, “TCSC based automatic generation control of deregulated power system using quasi-oppositional harmony search algorithm,” *Eng. Sci. Technol. an Int. J.*, vol. 20, no. 4, pp. 1380–1395, 2017.

[81] A. Pappachen and A. P. Fathima, “Load frequency control in deregulated power system integrated with SMES – TCPS combination using ANFIS controller,” *Int. J. Electr. Power Energy Syst.*, vol. 82, pp. 519–534, 2016.

[82] M. Ponnusamy, B. Banakara, S. Sekhar, and M. Veerasamy, “Design of integral

controller for Load Frequency Control of Static Synchronous Series Compensator and Capacitive Energy Source based multi area system consisting of diverse sources of generation employing Imperialistic ," *Int. J. Electr. Power Energy Syst.*, vol. 73, pp. 863–871, 2015.

[83] D. K. Sahoo, R. K. Sahu, G. T. C. Sekhar, and S. Panda, "A novel modified differential evolution algorithm optimized fuzzy proportional integral derivative controller for load frequency control with thyristor controlled series compensator," *J. Electr. Syst. Inf. Technol.*, vol. 5, no. 3, pp. 944-963, 2016.

[84] M. Deepak and R. J. Abraham, "Load following in a deregulated power system with Thyristor Controlled Series Compensator," *Int. J. Electr. Power Energy Syst.*, vol. 65, pp. 136–145, 2015.

[85] P. C. Pradhan, R. K. Sahu, and S. Panda, "Firefly algorithm optimized fuzzy PID controller for AGC of multi-area multi-source power systems with UPFC and SMES," *Eng. Sci. Technol. an Int. J.*, vol. 19, no. 1, pp. 338–354, 2016.

[86] J. Morsali, K. Zare, and M. T. Hagh, "Performance comparison of TCSC with TCPS and SSSC controllers in AGC of realistic interconnected multi-source power system," *Ain Shams Eng. J.*, vol. 7, no. 1, pp. 143–158, 2016.

[87] R. K. Sahu, T. S. Gorripotu, and S. Panda, "A hybrid DE – PS algorithm for load frequency control under deregulated power system with UPFC and RFB," *Ain Shams Eng. J.*, vol. 6, no. 3, pp. 893–911, 2015.

[88] S. Mostafa, M. Bornapour, and M. Abbasi, "Control Engineering Practice Grasshopper optimization algorithm for optimal load frequency control considering

Predictive Functional Modified PID controller in restructured multi-resource multi-area power system with Redox Flow Battery units," *Control Eng. Pract.*, vol. 89, no. 3, pp. 204–227, 2019.

[89] D. Khamari, R. K. Sahu, T. S. Gorripotu, and S. Panda, "Automatic generation control of power system in deregulated environment using hybrid TLBO and pattern search technique," *Ain Shams Eng. J.*, vol. 11, no. 3, pp. 553-573, 2019.

[90] J. Morsali, K. Zare, and M. Tarafdar Hagh, "A novel dynamic model and control approach for SSSC to contribute effectively in AGC of a deregulated power system," *Int. J. Electr. Power Energy Syst.*, vol. 95, pp. 239–253, 2018.

[91] J. Morsali, K. Zare, and M. Tarafdar Hagh, "Applying fractional order PID to design TCSC-based damping controller in coordination with automatic generation control of interconnected multi-source power system," *Eng. Sci. Technol. an Int. J.*, vol. 20, no. 1, pp. 1–17, 2017.

[92] Y. Arya and N. Kumar, "Optimal AGC with redox flow batteries in multi-area restructured power systems," *Eng. Sci. Technol. an Int. J.*, vol. 19, no. 3, pp. 1145–1159, 2016.

[93] M. Tarafdar Hagh, J. Morsali, K. Zare, and K. M. Muttaqi, "Introducing FOPLC based TCSC in coordination with AGC to improve frequency stability of interconnected multi-source power system," *Australas. Univ. Power Eng. Conf. Challenges Futur. Grids, AUPEC*, pp. 1-6, 2015.

[94] N. Hakimuddina, A. Khoslab, J. K. Garg "Centralized and decentralized AGC schemes in 2-area interconnected power system considering multi source power

plants in each area," *J. King Saud Univ. - Eng. Sci.*, vol. 32, no. 2, pp. 123-132, 2020.

[95] S. H. Rouhani, A. Sheikholeslami, R. Ahmadi, and H. Hosseini "Using optimal fuzzy logic controller to improve transient fluctuations in deregulated power system with random variable load," *J. Intell. Fuzzy Syst. Appl. Eng. Tech.*, vol. 27, no. 6, pp. 3145–3157, 2014.

[96] Y. K. Bhateshvar, H. D. Mathur, and H. Siguerdidjani. "Impact of wind power generating system integration on frequency stabilization in multi-area power system with fuzzy logic controller in deregulated environment," *Front. Energy*, vol. 9, no. 1, pp. 7–21, 2015.

[97] Y. K. Bhateshvar, H. D. Mathur, H. Siguerdidjane and S. Bhanot, "Frequency stabilization for multi-area thermal-hydro power system using genetic algorithm optimized fuzzy logic controller in deregulated environment," *Elect. Power Compon. Syst.*, vol. 43, no. 2, pp. 146–155, 2015.

[98] H. Shayeghi, and A. Ghasemi, "Market based LFC design using artificial bee colony," *Int. J. Tech. Phys. Prob. Eng.*, vol. 3, no. 6, pp. 1–10, 2011.

[99] A. O. Aluko, D. G. Dorrell, R. P. Carpanen, and E. E. Ojo, "Heuristic optimization of virtual inertia control in grid-connected wind energy conversion systems for frequency support in a restructured environment," *Energies*, vol. 13, no. 3, 2020.

[100] R. Thirunavukarasu, B. Paramasivam, and I. A. Chidambaram, "Power system restoration assessment indices computation for a restructured power system with bacterial foraging optimized load-frequency controller," *Int. J. Comput. Appl*, vol.

78, no. 16, pp. 41–54, 2013.

[101] R. Thirunavukarasu. and I. A. Chidambaram, "PI^2 controller based coordinated control with redox flow battery and unified power flow controller for improved restoration indices in a deregulated power system," *Ain Shams Eng. J*, vol. 7, no. 4, pp. 1011–1027, 2016.

[102] P. C. Nayak, R. C. Prusty, and S. Panda, "Grasshopper optimisation algorithm of multistage PDF+ (1 + PI) controller for AGC with GDB and GRC nonlinearity of dispersed type power system," *Int. J. Ambient Energy*, vol. 2, no. 1, pp. 1–13, 2020.

[103] D. Tripathy, N. B. Dev Choudhury, S. Behera, and B. K. Sahu, "Grasshopper Optimization Algorithm based Fuzzy PD-PI Cascade Controller for LFC of Interconnected Power System Coordinate with Renewable sources," *IEEE Calcutta Conf. CALCON 2020 - Proc.*, pp. 111–116, 2020.

[104] K. Jagatheesan, B. Anand, K. N. Dey, A. S. Ashour, and S. C. Satapathy, "Performance evaluation of objective functions in automatic generation control of thermal power system using ant colony optimization technique-designed proportional–integral–derivative controller," *Electr. Eng.*, vol. 3, no. 2, 2018.

[105] Y. K. Bhateshvar, H. T. Mathur, H. Siguerdidjane, and R. C. Bansal "Ant Colony Optimized Fuzzy Control Solution for Frequency Oscillation Suppression.," *Electr. Power Components Syst. Taylor Fr.*, vol. 45, no. 14, pp. 1573–1584, 2017.

[106] S. J. Sujiprasad , S. Varghese, and P. A. Balakrishnan "Optimization of I-PD Controller for a FOLIPD Model using Particle Swarm Intelligence," *International Journal of Computer Applications.*, vol. 43, no. 9, pp. 23–26, 2012.

[107] S. A. Bhatti, S. A. Malik, and A. Daraz, "Comparison of P-I and I-P controller by using Ziegler-Nichols tuning method for speed control of DC motor," *International Conference on Intelligent Systems Engineering, ICISE.*, pp. 1-6, 2016.

[108] S. Chakraborty, S. Ghosh, and A. K. Naskar, "I-PD controller for integrating plus time-delay Processes," *IET Control Theory Appl.*, vol. 11, no. 17, pp. 3137–3145, 2017.

[109] D. Sain, S. K. Swain, and S. K. Mishra, "Real Time Implementation of Optimized I-PD Controller for the Magnetic Levitation System using Jaya Algorithm," *IFAC-PapersOnLine*, vol. 51, no. 1, pp. 106–111, 2018.

[110] J. Abdullah and T. A. Rashid, "Fitness Dependent Optimizer : Inspired by the Bee Swarming Reproductive Process," *IEEE Access.*, vol. 07, pp. 43473-43486, 2019.

[111] D. S. Abdul-minaam, W. Mohammed, E. Saqar, M. A. Awad, and W. H. El-ashmawi, "An Adaptive Fitness-Dependent Optimizer for the One-Dimensional Bin Packing Problem," vol. 8, pp. 97959–97974, 2020.

[112] G. Hou, L. Qin, X. Zheng, and J. Zhang, "Application of PSO-based fuzzy PI controller in multi-area AGC system after deregulation," in *Proceedings of the 7th IEEE Conference on Industrial Electronics and Applications (ICIEA).*, pp. 1417–1422., 2012.

[113] J. Morsali, K. Zare, and M. T. Hagh, "MGSO optimised TID-based GCSC damping controller in coordination with AGC for diverse-GENCOs multi-DISCOs power system with considering GDB and GRC non-linearity effects," *IET Gener. Transm. Distrib.*, vol. 11, no. 1, pp. 193–208, 2017.

[114] A. Kumar, O. Malik, and G. Hope, "Variable-structure-system control applied to AGC of an interconnected power system," *IEE Proc. Gener. Transm. Distrib.,* vol. 132, pp. 123–129, 1985.

[115] A. Demiroren and E. Yesil, "Automatic generation control with fuzzy logic controllers in the power system including SMES units," *Int. J. Elect. Power Energy Syst*, vol. 26, no. 4, pp. 291–305, 2004.

[116] B. Hassan, Y. Mithani, and K. Tsuji "Robust decentralized load-frequency control using an iterative linear matrix inequalities algorithm," *IET, Gener. Transm. Distrib.,* vol. 151, no.3,pp. 347, 354 2004.

[117] V. S. Vakula and K. R. Sudha, "Differential evolutionary algorithm based structure preserving controller in three area deregulated environment," *J. Intell. Fuzzy Syst. Appl. Eng. Tech.,* vol. 28, no. 1, pp. 85–105, 2015.

[118] D. K. Lal and A. K. Barisal, "Comparative performances evaluation of FACTS devices on AGC with diverse sources of energy generation and SMES," *Cogent Eng.*, vol. 4, no. 1, pp. 1–29, 2017.

[119] O. Singh and I. Nasiruddin, "Hybrid evolutionary algorithm based fuzzy logic controller for automatic generation control of power systems with governor dead band non-linearity," *Cogent Eng.*, vol. 3, no. 1, pp. 1–16, 2016.

[120] B. Anand and A. E. Jeyakumar, "Load frequency control with fuzzy logic controller considering non-linearities and boiler dynamics," *ICGST-ACSE J*, vol. 8, no. 3, pp. 15–20, 2009.

[121] K. Jagatheesan, B. Anand, S. Samanta, N. Dey, A. S. Ashour, and V. E. Balas, "Particle swarm optimisation-based parameters optimisation of PID controller for load frequency control of multi-area reheat thermal power systems," *Int. J. Adv. Intell. Paradig.*, vol. 9, no. 5, 2017.

[122] K. Jagatheesan, B. Anand, V. Santhi, N. Dey, A. S. Ashour, and V. E. Balas, "Dynamic performance analysis of AGC of multi-area power system considering Proportional-Integral-Derivative controller with different cost functions," *International Conference on Electrical, Electronics, and Optimization Techniques, ICEEOT*, pp. 1-5, 2016.

[123] S. Pothiya and I. Ngamroo, "Optimal fuzzy logic-based PID controller for loadfrequency control including superconducting magnetic energy storage units,"," *Energy Convers. Manag.*, vol. 149, no. 10, pp. 2833–2838, 2008.

[124] H. Golpira, H. Bevrani, H. Golpira "Application of GA optimization for automatic generation control design in an interconnected power system," *Energy Convers. Manag.*, vol. 52, no. 5, pp. 2247–2255, 2011.

[125] S. Debbarma. and A. Dutta, "Utilizing electric vehicles for LFC in restructured power systems using fractional order controller," *IEEE Trans. Smart Grid*, vol. 8, no. 6, pp. 2554–2564, 2017.

[126] F. M. Miavagh, E. A. A. Miavaghi, A. R. Ghiasi, and M. Asadollahi, "Applying of PID, FPID, TID and ITID controllers on AVR system using particle swarm optimization (PSO)," *2nd Int. Conf. Knowledge-Based Eng. Innov. KBEI*, pp. 866–871, 2016.

[127] I. Pan and S. Das, “Chaotic multi-objective optimization based design of fractional order PI λD μ controller in AVR system,” *Int. J. Electr. Power Energy Syst.*, vol. 43, no. 1, pp. 393–407, 2012.

[128] D. Sain, S. K. Swain, A. Saha, S. K. Mishra, and S. Chakraborty, “Real-Time Performance Analysis of FOI-PD Controller for Twin Rotor MIMO System,” *IETE Tech. Rev. (Institution Electron. Telecommun. Eng. India)*, vol. 36, no. 6, pp. 547–567, 2019.

[129] D. A. Muhammed, S. A. M. Saeed, T. A. Rashid, and I. Member, “Improved Algorithm Fitness - Dependent Optimizer,” *IEEE Access.*, vol. 8, pp. 19074-19088, 2020.

Appendix

Table 1: Parameters setting of two area interconnected power system.

Parameters	Values	Parameters	Values	Parameters	Values
β_1, β_2	0.431 MW/Hz	$R_{th}1, R_{th}2, R_{hy}1, R_{hy}2, R_g1, R_g2$	2.40 Hz/p.u	T_{gh}	0.080 s
T_t	0.30 s	K_1	0.30	T_r	10 s
K_P	68.95	T_p	11.490 s	$T12$	0.0430
$a12$	-1	T_w, y_c	1 s	Trs	5 s
T_{rh}	28.70 s	Tgh, Tcd, TDC	0.20 s	x_c	0.60 s
K_g	0.1304	K_{DC} , x_g	1	b_g	0.050 s
K_t	0.5434	Tcr	0.010 s	T_F	0.230 s
K_h	0.3268	R_{w1}	2.40 Hz/p.u	R_{w2}	2.40 Hz/p.u

Table 2: Values of Fitness Dependent Optimizer (FDO) parameters.

Parameters	Values	Parameters	Values	Parameter	Value	Parameter	Value
Number of Population (Np)	30	Number generations (Ng)	100	Lower bound	-2	Upper bound	2
Number dimension	9	random number (α)	[1 -1]	Weight factor (ϒ)	0.0		

Table 3: Values of Improved -Fitness Dependent Optimizer (FDO) parameters.

Parameters	Values	Parameters	Values	Parameters	Values	Parameters	Values
Number of Population (Np)	30	Numbe of generatio (Ng)	100	Lower bound	-2	Upper bound	2
Number dimension	15	random number (α)	[1 -1]	Weight factor (ϒ)	[1, 0]		